Université du Québec à Rimouski
Institut des sciences de la mer de Rimouski

Contamination au mercure et aux absorbants UV chez le sébaste (*Sebastes mentella*) de l'estuaire et du golfe du Saint-Laurent : Variation spatiale et implications de l'exposition

Mémoire présenté

dans le cadre du programme de maîtrise en océanographie

en vue de l'obtention du grade de maître ès sciences (M.Sc.)

PAR

© FELLA MOUALEK

[novembre 2023]

Composition du jury :

Youssouf Djibril Soubaneh, président du jury, UQAR

Zhe Lu, directeur de recherche, UQAR-ISMER

Dominique Robert, codirecteur de recherche, UQAR-ISMER

Magali Houde, examinatrice externe, Environnement et Changement Climatique

Canada, ECCC

Dépôt initial le [07 aout 2023]   Dépôt final le [23 novembre 2023]

UNIVERSITÉ DU QUÉBEC À RIMOUSKI
Service de la bibliothèque

Avertissement

La diffusion de ce mémoire ou de cette thèse se fait dans le respect des droits de son auteur, qui a signé le formulaire « *Autorisation de reproduire et de diffuser un rapport, un mémoire ou une thèse* ». En signant ce formulaire, l'auteur concède à l'Université du Québec à Rimouski une licence non exclusive d'utilisation et de publication de la totalité ou d'une partie importante de son travail de recherche pour des fins pédagogiques et non commerciales. Plus précisément, l'auteur autorise l'Université du Québec à Rimouski à reproduire, diffuser, prêter, distribuer ou vendre des copies de son travail de recherche à des fins non commerciales sur quelque support que ce soit, y compris Internet. Cette licence et cette autorisation n'entraînent pas une renonciation de la part de l'auteur à ses droits moraux ni à ses droits de propriété intellectuelle. Sauf entente contraire, l'auteur conserve la liberté de diffuser et de commercialiser ou non ce travail dont il possède un exemplaire.

« L'océan est une force puissante qui nécessite de la persévérance pour être compris, tout comme les femmes en science doivent persévérer pour être reconnues dans leur champ. » - Sylvia Earle

REMERCIEMENTS

x

RÉSUMÉ

Le milieu marin profond (>200m) est considéré comme un réservoir final pour les contaminants persistants dans l'océan, y compris le mercure et les contaminants émergents tels que les agents absorbant les rayons ultraviolets (UV). Alors que la population de sébastes (*Sebastes mentella*) dans l'estuaire et le golfe du Saint-Laurent (EGSL) se rétablit rapidement d'un effondrement dans les années 1990, la possibilité d'une future pêche à grande échelle de cette espèce pourrait conduire à une exposition humaine aux contaminants persistants par le biais de leur consommation. L'étude vise à examiner les schémas spatiaux du mercure (Hg), du méthylmercure (MeHg) et des composés absorbants les UV dans le muscle du sébaste de l'EGSL et à explorer les corrélations entre les niveaux de ces contaminants dans le sébaste et les variables environnementales/biologiques. L'étude a révélé que le sébaste de l'estuaire avait des niveaux de mercure Hg et MeHg plus élevés que celui du chenal Laurentien et du nord-est du golfe. Les indicateurs significatifs des concentrations de MeHg dans le muscle du sébaste étaient la taille du poisson, la teneur en eau du muscle, le δ^{15}N et le pourcentage d'azote N%. L'étude a également identifié le filtre UV 2-hydroxy-4-méthoxybenzophénone (BP-3) comme le contaminant le plus fréquemment détecté dans le muscle de sébaste, avec des concentrations plus élevées chez les petits poissons (< 30 cm). Toutefois, le quotient de risque estimé suggère qu'il est peu probable que les contaminants détectés présentent des risques pour la santé humaine en cas de consommation de sébaste. L'étude constitue un point de départ pour la surveillance future du mercure dans les eaux profondes de cette région, mais des recherches supplémentaires sont nécessaires pour comprendre les relations de cause à effet entre divers facteurs environnementaux et biologiques (tels que la température de l'eau, la profondeur, le régime alimentaire, l'âge des poissons, les mécanismes de détoxification, les courants océaniques, les caractéristiques géologiques, la présence de prédateurs, les conditions de reproduction, et les pratiques de pêche) et l'accumulation et la toxicité des polluants chez les poissons d'eau profonde.

Mots clés : Mercure, méthylmercure, absorbants UV, sébaste, eaux profondes, Estuaire et Golfe du Saint-Laurent, Évaluation du risque.

ABSTRACT

The deep marine environment (>200m) is considered a final reservoir for persistent contaminants in the ocean, including mercury and emerging contaminants such as UV absorbants. While the deepwater redfish (*Sebastes mentella*) population in the St. Lawrence the Estuary and Gulf (SLEG) is rapidly recovering from collapse in the 1990s, the possibility of future large-scale fishing of this species could lead to human exposure to persistent contaminants through redfish consumption. The study aimed to to examine the spatial patterns of mercury (Hg), methylmercury (MeHg), and UV absorbants in SLEG redfish muscle and explore correlations between levels of these contaminants and environmental/biological variables. The study revealed that redfish from the estuary had higher levels of Hg and MeHg than those from the Laurentian Channel and northeast Gulf. Significant indicators of MeHg concentrations in redfish muscle were fish size, muscle water content, $\delta^{15}N$, and percentage of nitrogen N%. The study also identified the UV filter 2-hydroxy-4-methoxybenzophenone (BP-3) as the most frequently detected contaminant in redfish muscle, with higher concentrations in smaller fish (< 30 cm). However, the estimated hazard quotient suggests that the detected contaminants are unlikely to pose a risk to human health from redfish consumption. The study provides a starting point for future monitoring of mercury in deepwater environments in this region, but more research is needed to understand the cause-and-effect relationships between various environmental and biological factors (such as water temperature, depth, diet, fish age, detoxification mechanisms, ocean currents, geological features, predator presence, reproduction conditions, and fishing practices) and the accumulation and toxicity of pollutants in deepwater fish.

Keywords: Mercury, methylmercury, UV absorbants, redfish, deep water, St. Lawrence Estuary and Gulf, Risk assessment.

TABLE DES MATIÈRES

.

LISTE DES TABLEAUX

LISTE DES FIGURES

LISTE DES ABRÉVIATIONS, DES SIGLES ET DES ACRONYMES

Abréviations	Définitions
Hg	Mercury / Mercure
MeHg	Methylmercury / Méthylmercure
THg	Total Mercury / Mercure totaux
UV	Ultraviolet
UVAs	Ultraviolet Absorbants / Absorbants Ultraviolet /
BZT-UVs	Ultraviolet stabilizers - Benzotriazoles / Stabilisateurs Ultraviolets – Benzotriazoles
UVFs	Ultraviolet filters / Filtres Ultraviolets
MDL	Method Detection Limit / Limite de détection de la méthode
EGSL	The Estuary and Gulf of St. Lawrence / L'Estuaire et le Golfe du Saint-Laurent
EWI	Estimated Weekly Intake/ Estimation de l'apport hebdomadaire
EDI	Estimated Daily Intake/ Estimation de l'apport journalier
HQ	Hazard Quotient / Quotient de risque

Acronymes	Composés	Numéros CAS
UVFs		
BP-3	2-Hydroxy-4-methoxybenzophenone	131-57-7
EHMC	2-Ethylhexyl methoxycinnamate	5466-77-3
EHS	2-éthylhexyl salicylate	118-60-5
4MBC	4-Methylbenzylidene camphor	36861-47-9
OC	2-Ethylhexyl 2-cyano-3,3-diphenylacrylate	6197-30-4
BZT-UVs		
UVP	2-(2H-benzotriazol-2-yl)-p-cresol	2440-22-4
UV090	2-[3-(2H-benzotriazol-2-yl)-4-hydroxyphenyl]ethyl methacrylate	96478-09-0
UV9	2-(2H-benzotriazol-2-yl)-4-methyl-6-(2-propenyl)phenol	2170-39-0
UV234	2-(2H-benzotriazol-2-yl)-4,6-bis(1-methyl-1-phenylethyl)phenol	70321-86-7
UV320	2-Benzotriazole-2-yl-4,6-di-*tert*-butylphenol	3846-71-7
UV326	2-*tert*-Butyl-6-(5-chloro-2H-benzotriazol-2-yl)-4-methylphenol	3896-11-05
UV327	2,4-Di-*tert*-butyl-6-(5-chloro-2H-benzotriazol-2-yl) phenol	3864-99-1
UV328	2-(2H-benzotriazol-2-yl)-4,6-di-*tert*-pentylphenol	25973-55-1
UV329	2-(2H-benzotriazol-2-yl)-4-(1,1,3,3-tetramethyl butyl)phenol	3147-75-9
UV350	2-(2H-benzotriazol-2-yl)-4-(*tert*-butyl)-6-(*sec*-butyl)phenol	36437-37-3

INTRODUCTION GÉNÉRALE

1.1 SÉBASTE (*SEBASTES MENTELLA*) DU SAINT-LAURENT

Le sébaste (*Sebastes* spp.) est un poisson marin que l'on trouve dans l'Atlantique Nord-Ouest. Il vit dans les eaux froides, près du fond, à des profondeurs comprises entre 40 à 500 m (Senay et al., 2019). On le reconnaît à sa coloration rouge distincte, qui devient plus prononcée chez les spécimens matures. Il s'agit d'une espèce à croissance lente et à longue durée de vie (espérance de vie moyenne de 40 ans), certains individus pouvant dépasser 75 ans (Senay et al., 2019). Ce poisson se nourrit généralement de crustacés et son régime alimentaire se diversifie au fur et à mesure qu'il grandit. Les sébastes migrent verticalement pendant la journée et quittent le fond de la mer la nuit pour suivre leurs proies au cours de leur migration (Senay et al., 2019).

Ils sont ovovivipares et libèrent leurs larves d'avril à juillet, avec une fécondité absolue allant de 3 330 à 107 000 larves par femelle et augmentant selon la taille (Gascon, 2023a). Le succès du recrutement de cette espèce est très variable, avec des classes d'âge importantes produites à intervalles irréguliers (Senay et al., 2019). Il est considéré comme une espèce en voie de disparition par le Comité sur la situation des espèces en péril au Canada (COSEPAC) en 2010 (COSEPAC, 2010).

Un fort recrutement dans la population de sébaste atlantique (*Sebastes* spp.) a été observé en 1980-1981, suivi de périodes de pêche intensive dans l'estuaire et le golfe du Saint-Laurent (SLEG). Les taux élevés d'exploitation, le faible recensements et l'absence de recrutement significatif suite aux années 1981 ont conduit à l'instauration d'un moratoire en 1995 (Savenkoff et al., 2006). Depuis 1998, une pêche sentinelle est autorisée (i.e pêche contrôlé pour évaluer l'abondance et la biomasse du sébaste) et les indices d'abondance et de biomasse du sébaste ont été stables et faibles (15 % de la biomasse total) jusqu'en 2011, année marquée par un fort recrutement. Depuis 2014, une forte présence (estimée à

3,2 millions de tonnes en 2022) de jeunes sébastes a été enregistrée dans les relevés du MPO (Figure 1).
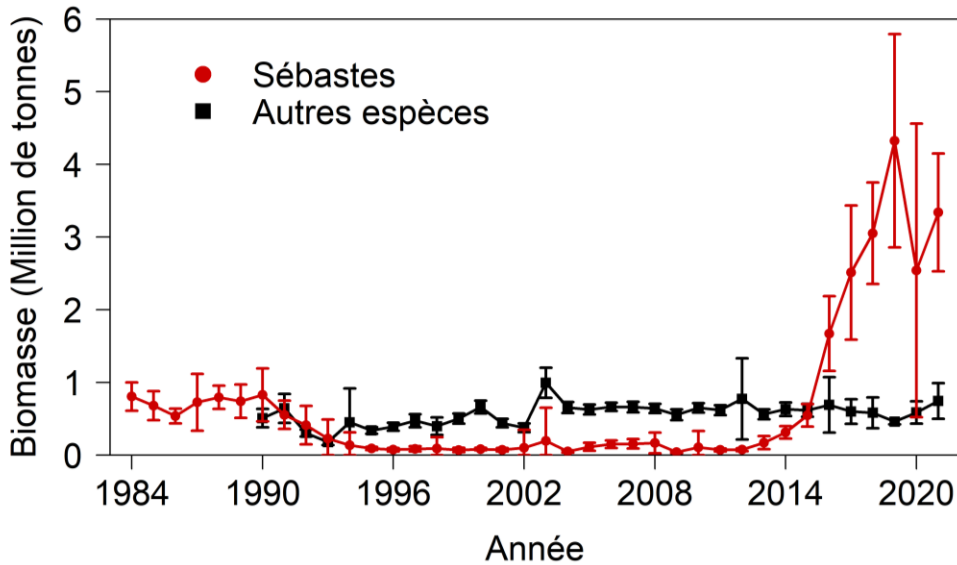
Figure 1: Biomasse chalutable (millions de tonnes) des sébastes (cercles rouges) et de toutes les autres espèces (rectangles noirs) collectée dans le cadre du relevé du MPO sur l'unité 1 de 1984 à 2021 (MPO, 2022).

Les perspectives récentes de pêche pour le recensement de sébastes sont très prometteuses (Senay et al., 2019) étant donné que le sébaste représente 82 % des captures lors d'une étude scientifique de Pêches et Océans Canada (MPO) en 2021, contre seulement 15 % dans les années précédentes (DFO, 2022). Une telle augmentation marquée de la population de sébastes peut affecter de manière significative la structure du réseau trophique, ainsi que la dynamique des nutriments et des contaminants dans ce même réseau.

L'éventuelle consommation de sébastes par l'Homme pourrait représenter une source d'exposition à différents contaminants, qui n'a pas été étudiée. Il a été rapporté que le sébaste des eaux profondes de l'est de l'Arctique accumule des polluants organiques persistants dans les tissus, entre autres les composés organiques fluorés (Tomy et al., 2004). Le facteur de bioamplification du perfluorooctanesulfonate (PFOS) entre le béluga et le sébaste a été estimé à 4, ce qui indique que le sébaste peut transmettre ce contaminant dans le réseau trophique de l'est de l'Arctique aux mammifères marins. Les polybromodiphényléthers

(PBDEs ; 11 congénères) ont aussi été détectés dans le muscle sébaste du SLEG (Ferchiou, 2019). Cependant, l'occurrence, les concentrations et la répartition de plusieurs autres contaminants dans le sébaste du Saint-Laurent sont encore largement inconnues. Dans notre étude, nous nous concentrons particulièrement sur deux groupes de contaminants : le mercure et les absorbants UV.

1.2 ZONE D'ÉTUDE « L'ESTUAIRE ET LE GOLFE DU SAINT-LAURENT »

L'estuaire du Saint-Laurent figure parmi les plus vastes estuaires du monde. Il s'étend de la ville de Québec au golfe du Saint-Laurent, dans l'est du Canada. Il est situé à l'embouchure du fleuve Saint-Laurent, où celui-ci rencontre l'océan Atlantique. Le mélange de ces deux masses d'eau crée un environnement unique qui abrite un large éventail d'espèces végétales et animales. La profondeur moyenne de l'estuaire est d'environ 50 m, mais elle peut atteindre 300 m à certains endroits, notamment dans le chenal laurentien. Avec des profondeurs moyennes de plus de 200 (MPO, 2020). Il constitue un habitat essentiel pour une grande variété d'espèces marines, dont plusieurs espèces de baleines (baleine bleue, rorqual commun, rorqual à museau pointu, baleine noire de l'Atlantique Nord), de phoques (phoque commun et phoque gris) et de poissons (morue : *Gadus morhus*, flétan de l'Atlantique : *Hippoglossus hippoglossus*, hareng : *Clupea harengus*, crevette nordique : *Pandalus borealis*, plusieurs espèces de plies, sébaste : *Sebastes mentella*). Il constitue un habitat pour de nombreuses espèces rares et menacées (marsouin commun, requin-pèlerin, béluga). L'estuaire abrite une population de bélugas estimée à moins de 2 000 individus (MPO, 2020).

1.3 MERCURE ET MÉTHYLMERCURE

1.3.1 Sources et spéciation

Le mercure est un élément de la croûte terrestre et un polluant réparti mondialement et qui constitue un problème pour l'environnement et la santé humaine. Il peut être émis dans l'environnement à partir de sources naturelles telles que des éruptions volcaniques et l'altération des roches. Il peut aussi provenir de sources anthropiques comme l'exploitation minière, l'incinération des déchets et la combustion de combustibles fossiles (Fitzgerald et

al., 1998 ; Ramirez-Llodra et al., 2011). Le mercure émis peut pénétrer dans l'atmosphère sous forme élémentaire (Hg (II)) et inorganique (Hg (0)) ; le Hg (0) peut résider et se déplacer dans l'atmosphère pendant six mois à deux ans avant d'être oxydé en Hg (II) et déposé dans les écosystèmes aquatiques et terrestres (Fitzgerald et al., 1998). Dans les milieux aquatiques, le Hg se combine avec le méthyle pour former le méthylmercure (MeHg) (transformation chimique), qui constitue la forme la plus toxique et qui peut facilement se bioaccumuler et se bioamplifier dans les chaînes alimentaires, entraînant des concentrations élevées et toxiques de mercure chez les poissons et les mammifères (Al-Sulaiti et al., 2022 ; Selin, 2009 ; Wolfe et al., 1998).

Les principales sources de Hg dans l'estuaire et le golfe du Saint-Laurent seraient les dépôts atmosphériques provenant du transport sur de longues distances (Miller et al., 2005), les apports fluviaux et les apports provenant des processus d'érosion côtière (Cossa and Gobeil, 2000a). Diverses activités humaines qui ont lieu le long du fleuve Saint-Laurent sont également responsables de la pollution par le Hg. Par exemple, l'usine de production de chlore et de soude caustique qui opère depuis plusieurs décennies dans différentes régions du Saint-Laurent, la dernière (à Cornwall, entre l'embouchure du lac Ontario et Montréal) a fermé en 1995 (Cossa and Gobeil, 2000a). La quantité de mercure déposée dans le bassin du Saint-Laurent depuis l'ère industrielle a été estimée à 170×10^3 kg (Cossa and Gobeil, 2000b). Après sa libération dans l'environnement, le mercure peut se retrouver dans diverses matrices. À titre d'exemple, des niveaux de mercure élémentaire allant de 31 à 22 ng/L ont été détectés dans un échantillon d'eau du Haut-Saint-Laurent collecté en 1998, (en amont de l'estuaire, entre la ville de Québec et le lac Ontario) (Amyot et al., 2000), alors que les teneurs en mercure dans les sédiments du corridor fluvial du Saint-Laurent varient de 34 à 2 790 ng/g poids sec en 1998 (Désy et al., 2011). De plus, le niveau de THg dans différents organismes marins du SLEG, tels que les crustacés (12,6± 0,6 - 231±19 ng/g poids sec), les mollusques (42,0±3,6 - 127±8 ng/g poids sec) et les vertébrés (28,1±2,2 - 1789±98 ng/g poids sec), variait entre 12,6 ± 0,6 et 1789 ± 98 ng/g poids sec (Lavoie et al., 2010).

1.3.2 Bioaccumulation chez les poissons et les humains

L'activité microbienne est un facteur déterminant de la concentration de mercure dans les poissons, car le Hg (II) inorganique est méthylé dans l'environnement par des bactéries hétérotrophes telles que Desulfovibrio spp. (*Desulfovibrio desulfuricans*) et Geobacter spp. (*Geobacter sulfurreducens*), ce qui entraîne la formation de MeHg (Al-Sulaiti et al., 2022 ; Gworek et al., 2016). Les poissons assimilent entre 65 % et 80 % du MeHg par le biais de leur nourriture. Le MeHg est alors transporté par le système circulatoire vers tous les organes et tissus après s'être lié aux globules rouges. Il traverse facilement les membranes internes et s'accumule principalement dans les muscles (Kidd et al., 2011). Le MeHg est l'un des rares métaux connus pour s'accumuler le long de la chaîne alimentaire, avec une concentration plus élevée dans les niveaux trophiques supérieurs que dans les niveaux inférieurs (Kidd et al., 2011). Cette accumulation est connue sous le nom de bioamplification et se produit en raison de son absorption et de son accumulation rapide du MeHg dans les tissus et de sa lente élimination (Braune et al., 2015). Les organismes marins peuvent également accumuler le MeHg provenant des sédiments. Une corrélation étroite a été observée entre les concentrations de MeHg chez les gastéropodes prosobranches *Bithynia tentaculata* et les concentrations de MeHg dans les sédiments de la rivière du Saint-Laurent (Désy et al., 2011).

Bien qu'il y ait peu d'informations sur les niveaux de mercure dans les poissons de la région du SLEG, les travaux réalisés jusqu'à présent suggèrent que les différentes espèces de poissons ont des concentrations de mercure variables. Par exemple, la concentration moyenne de THg était de 1,3 ng/g poids sec (ps) pour le capelan, de 20,1 ng/g ps pour le hareng de l'Atlantique, de 18,8 ng/g ps pour le lançon et de 100 ng/g ps pour la plie grise (Lavoie et al., 2010). Ces résultats impliquent qu'en fonction de variables telles que la taille de l'organisme et la zone de collecte des échantillons, il peut y avoir des fluctuations substantielles dans les concentrations de THg au sein d'une espèce. Pour bien comprendre le niveau de pollution par le mercure des poissons dans la région du SLEG, il est nécessaire de mener des recherches plus approfondies.

La principale voie d'accumulation du Hg chez l'Homme est la consommation de poisson et fruits de mer contaminés (Bradley et al., 2017; Ha et al., 2017). Une fois dans le corps humain, le Hg peut être absorbé par le canal digestif et transporté dans les différents organes via la circulation sanguine (Bradley et al., 2017). Il peut traverser facilement la barrière entéro-encéphalique et son accumulation dans le cerveau peut causer des dommages neurologiques dangereux (Al-Sulaiti et al., 2022 ; Aschner and Aschner, 1990).

Dans l'enquête canadienne sur les mesures de la santé 2007-2009, la concentration moyenne de mercure total (THg) dans le sang était de 0,69 µg/L chez la population canadienne, 0,72 µg/L chez les femmes âgées de 16 à 49 ans (incluant les femmes enceintes) (Lye et al., 2013). En outre, la teneur en THg chez la population canadienne (1.14 µg/L) et chez la population asiatique (1.41 µg/L) était plus élevée que chez les Caucasiens (0.62 µg/L). En revanche, il n'y avait pas de différence significative dans la concentration de THg entre ceux qui s'identifiaient comme Autochtones (0.56 µg/L) et ceux qui s'identifiaient comme Caucasiens (0.62 g/L) (Lye et al., 2013). En outre, Wong et Lye (2008) ont trouvé des concentrations de Hg dans le sang de la population canadienne de 0,91 µg/L. Par conséquent, la plupart des Canadiens ont des niveaux de mercure dans leur sang qui sont nettement inférieurs aux normes de Santé Canada concernant les niveaux de mercure dans le sang pour les hommes de plus de 18 ans (20 µg/L) et pour les enfants de 18 ans et moins, les femmes en âge de procréer (19 à 49 ans) et les femmes enceintes (8 µg/L) (Legrand et al., 2010). Cependant, les femmes enceintes de certains groupes de la population, comme le peuple autochtone inuit au Nunavik pour qui les produits de la mer (poissons et mammifères) constituent la base du régime alimentaire — ont une concentration moyenne de Hg dans le sang de 5,08µg/L, où 37 % d'entre eux dépassaient la valeur guide provisoire pour le sang de 8 µg/L de la ligne directrice de Santé Canada (Adamou et al., 2018).

1.3.3 Effet chez les poissons et les humains

L'exposition à des concentrations sublétales de MeHg peut entraîner des effets neurotoxiques chez les poissons en perturbant leur capacité à nager, à se nourrir et à éviter les prédateurs (Fjeld et al., 1998). Par exemple, la Dorade Blanche (*Diplodus sargus)*

exposés à des concentrations de mercure de 8.7 µg/g avait une capacité de nage réduite (Puga et al., 2016).

L'exposition au THg peut aussi entraîner des perturbations endocriniennes et des effets néfastes sur la reproduction (Pinheiro et al., 2020). Une corrélation négative entre le THg dans les tissus et les niveaux plasmatiques de testostérone et de 17β-estradiol chez les poissons femelles suggère un impact potentiel sur la reproduction des barbottes brunes du fleuve Saint-Laurent (Pinheiro et al., 2020). Le MeHg peut perturber les mécanismes de reproduction de Tête-de-boule (*Pimephales promelas*) in vivo poissons en altérant le développement des gonades, en réduisant le succès reproductif des adultes (Hammerschmidt et al., 2002). Des études ont montré que le MeHg peut affecter la santé et la survie des stades larvaires embryonnaires (Hammerschmidt et al., 2002), réduire le succès d'éclosion des œufs (Fjeld et al., 1998) et même provoquer une apoptose des cellules gonadiques, entraînant une diminution de la fertilité chez les poissons exposés *in situ,* tel que le brochet (*Esox lucius*) (Drevnick et al., 2008).

En outre, il a été rapporté que l'exposition au Hg peut provoquer des changements histologiques dans le foie des poissons, tel qu'une variation de couleur du foie du brochet (*Esox lucius*), liée à la concentration du THg dans les tissus musculaires. Cette variation de couleur est due à la présence de pigments formés par des lipides oxydés et des protéines oxydées résultant d'un stress oxydatif (Drevnick et al., 2008).

Des effets synergiques, qui varient en fonction de l'espèce et du composé considéré, ont également été signalés. Par exemple, dans le cas de la moule *Mytilus edulis*, certains cofacteurs peuvent augmenter la bioaccumulation de certaines toxines comme le sélénium, tandis que d'autres peuvent réduire l'absorption du cadmium lorsque l'espèce est exposée simultanément au mercure et au cadmium (Breittmayer et al., 1980).

Chez l'Homme, la neurotoxicité est l'un des effets du Hg le plus répandu et néfaste. Le MeHg peut nuire au développement du cerveau du fœtus, du nouveau-né et du jeune enfant, entraînant des troubles du comportement et des retards de développement (Jackson, 2018). Les adultes peuvent souffrir de retard cognitif et comportemental, puis des caractéristiques

psychiatriques, des tremblements et des pertes auditives et déséquilibres peuvent survenir (Jackson, 2018). En Irak, 11 % des patients intoxiqués au MeHg ont développé une démence (Rustam and Hamdi, 1974). Les symptômes psychiatriques sont associés à la tristesse et l'irritabilité chez 74 % et 44 % des patients (Maghazaji, 1974). Il a été estimé que la déficience auditive affectait 29 % des habitants de Minamata au Japon (Yorifuji et al., 2008) et 19 % des patients contaminés au MeHg en Irak (Rustam and Hamdi, 1974). De plus, des tremblements et statiques ont été observés chez 13 % des patients contaminés au MeHg en Irak (Rustam and Hamdi, 1974) et chez 2 % des patients atteints de la maladie de Minamata (Yamanaga, 1983).

Une exposition à de faibles quantités de mercure chez l'humain peut perturber le système endocrinien en diminuant la fonction de l'hypophyse, de la thyroïde, des glandes surrénales et du pancréas (Bakir et al., 1973) et en altérant la fonction, hormones telles que l'insuline, l'œstrogène, la testostérone et l'adrénaline (Rice et al., 2014). En empêchant la dégradation des catécholamines, le mercure peut provoquer une tachycardie, une hypertension ou une hyperhidrose (Bakir et al., 1973). L'accumulation de mercure dans l'hypophyse et la thyroïde peut provoquer une dépression, des idées suicidaires, une hypothyroïdie et une diminution du contrôle de la température corporelle (McGregor and Mason, 1991; Wada et al., 2009).

1.4 ABSORBANT ORGANIQUE ULTRAVIOLET

Les absorbants organiques UV (UVA) comprennent deux groupes de contaminants, les filtres UVs (UVF) et les stabilisateurs benzothiazole UV (BZT-UV).

1.4.1 UVF

1.4.1.1 Propriétés

Les filtres UV (UVF) sont utilisés dans divers produits de soins personnels tels que les écrans solaires, les dentifrices, les shampooings, les savons, les gommages, les teintures capillaires, les crèmes hydratantes, les formules de maquillage et les lotions après-rasage (Gaspar and Campos, 2010; Nakata et al., 2009a; Zhang et al., 2011). Ils sont considérés comme des agents de protection solaire pour protéger la peau et les matériaux contre les

rayons UV (Kameda et al., 2011). Les UVF ont une variété de propriétés, mais ils ont généralement tous la capacité d'absorber et de bloquer les rayons UV tout en restant transparents (Egambaram et al., 2020). Les structures de UVF ciblé sont présentées dans la figure 2.
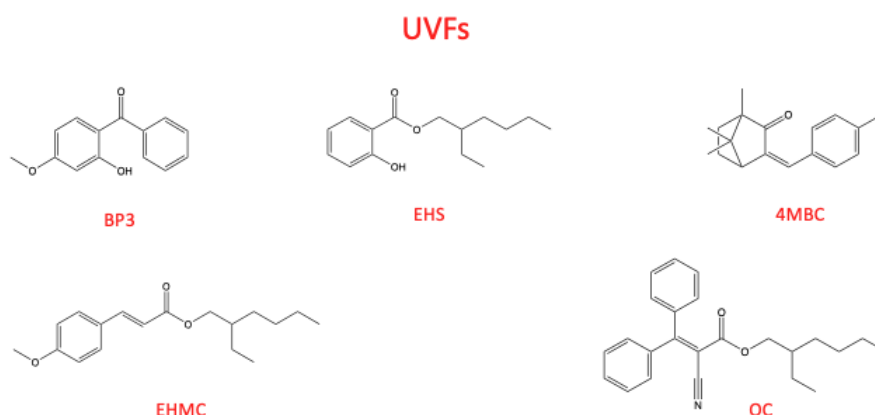
Figure 1: Structures des UVF ciblés.

1.4.1.2 Devenir et bioaccumulation chez les poissons et l'humain

Les UVF peuvent pénétrer dans l'environnement aquatique de plusieurs manières, notamment par l'application de produits personnels lors d'activités de loisirs (Tsui et al., 2014) et les rejets des eaux usées traitées par les stations d'épuration, où les UVF ne sont pas complètement éliminés pendant le traitement (Kameda et al., 2011). Les UVF peuvent être transportés partout dans l'environnement. Ils ont été détectés dans divers composants environnementaux tels que l'eau de mer (Chen et al., 2019), l'eau douce (Liu et al., 2014), les sédiments (Wick et al., 2016) et le biote (Nakata et al., 2009a ; Lu et al., 2016a ; Lu et al., 2017 b ; Lu et al., 2018 ;; Lu et al., 2019 ; Castilloux, A.D et al., 2022). Cette distribution est contrôlée par les conditions environnementales ainsi que les caractéristiques physicochimiques du composé (telle que la solubilité, la répartition entre les phases aqueuses et organiques, ainsi que le potentiel d'adsorption sur les surfaces solides) (Tableau1).

Les UVF sont des composés hydrophobes, ils ont tendance à se concentrer dans les tissus des organismes vivants [Binelli and Provini, 2004]. Les poissons peuvent les accumuler dans

leurs tissus adipeux à la suite d'une exposition à des sources d'eau et de nourriture contaminées (Gago-Ferrero et al., 2015). En effet, la bioamplification peut jouer un rôle dans l'accumulation de ces composés chez les poissons (Gago-Ferrero et al., 2015). Une fois dans l'organisme, les UVF sont transportés vers les différents organes via la circulation sanguine. Le principal organe de stockage des UVF chez le poisson est le foie (Peng et al., 2020). Les différentes propriétés des UVF déterminent leur capacité à persister et à se bioaccumuler dans la chaîne alimentaire marine, ce qui peut avoir un impact sur la santé humaine suite à la consommation de produits issus des pêches (Kameda et al., 2011; Nakata et al., 2009a).

Tableau 1: Noms chimiques, numéros de registre CAS, acronymes et propriétés physicochimiques de UVFs ciblé par le présent projet.

Nom chimique	CAS No.	Acronyme	Poids moléculaire (g/mol)	Solubilité dans l'eau (mg/L)	Log K_{ow}[a]
2-Hydroxy-4-methoxybenzophenone	131-57-7	BP-3	228.3	68.6	3.52
Ethylhexyl methoxycinnamate	5466-77-3	EHMC	290.4	0.15	5.80
4-Methylbenzylidene camphor	36861-47-9	4-MBC	254.4	0.2	5.92
2-Ethylhexyl salicylate	118-60-5	EHS	250.3	0.72	5.97
2-Ethylhexyl-2-cyano-3,3-diphenylacrylate	6197-30-4	OC	361.5	3.8×10^{-3}	6.88

[a] Prédit par la modélisation EPI [Estimation Program Interface] Suite [V4.11].

L'humain peut aussi être exposé aux UVF par l'intermédiaire de produits cosmétiques et écrans solaires (Binelli and Provini, 2004). Des études ont suggéré que les UVF peuvent atteindre la circulation sanguine et s'accumuler à travers le temps dans le corps humain (Giokas et al., 2007 ; Ballestín and Bartolomé, 2023). Les UVF ont été détectés dans l'urine et le lait maternel, ce qui représente un risque d'exposition du nouveau-né à ces contaminants (Molins-Delgado et al., 2018 ; Stoeckelhuber et al., 2020).

1.4.1.3 Toxicité des UVF chez les poissons et l'homme

Des études ont démontré la toxicité de nombreux UVF utilisés dans les produits solaires. Les benzophénones et le camphre ont été associés à une possible perturbation endocrinienne à l'égard de différents organismes tels que les poissons (Wang et al., 2016). Certaines recherches *in vitro* et *in vivo* ont rapporté que ces filtres peuvent se lier à des récepteurs chimiques, tels que le récepteur Ah (Kameda et al., 2011). Certains dérivés de benzophénone telle que l'homosalate (HMS) de 2-hydroxy-4-méthoxybenzophénone (BP-3 ; 131-57-7) et le camphre de 4-méthylbenzylidène (4-MBC ; 36861-47-9) ont été identifiés comme des antagonistes du récepteur des androgènes (Schreurs et al., 2004). Le BP-3 peut avoir un effet négatif sur les poissons en diminuant la production d'œufs, l'éclosion et les niveaux de testostérone (Ghazipura et al., 2017).

Chez l'humain, le BP-3 a aussi été associé au cancer de la glande mammaire (Kariagina et al., 2020). Le BP-3 est également reconnu comme un perturbateur endocrinien, qui peut provoquer divers effets indésirables sur la reproduction (Wang et al., 2016). Comme l'ont démontré des tests in vivo et in vitro, l'exposition à ces composés chimiques a provoqué une variété d'effets perturbateurs hormonaux, y compris des effets perturbateurs sur les œstrogènes, les androgènes ainsi que et des effets perturbateurs sur l'hormone thyroïdienne et le récepteur progestérone (Wang et al., 2016). Il a également été démontré que le transfert maternel peut se faire par le placenta et probablement aussi par le lait maternel (Stoeckelhuber et al., 2020), ce quiceci représente un risque d'exposition du fœtus à ces contaminants. Des modèles in vivo ont révélé d'autres effets nocifs des UVF comme la cytotoxicité, les anomalies comportementales et la neurotoxicité sure (Kockler et al., 2012 ; Ballestín and Bartolomé, 2023).

1.4.2 BZT-UV

1.4.2.1 Propriétés

Les BZT-UV sont utilisés dans de nombreux produits en plastique, notamment les matériaux de construction, les pièces automobiles, la cire, la peinture, les adhésifs, les films, les chaussures, les lunettes et certains équipements sportifs. Ils sont utilisés pour empêcher le jaunissement et la détérioration des produits (Nakata et al., 2009b). Les BZT-UV ont généralement une structure 2-hydroxyphényl benzotriazole avec des substitutions alkyles sur le cycle phénol (Figure 3).
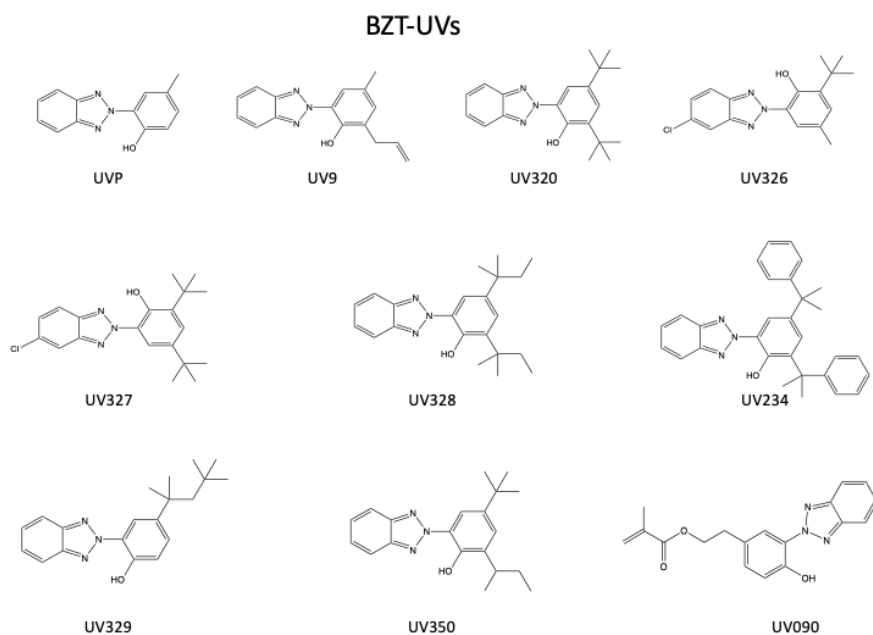
Figure 2: Structures des BZT-UVs cibles.

Ces composés ont la capacité d'absorber le rayonnement ultraviolet à spectre complet (Kim et al., 2011b ; Nakata et al., 2009 b). Ils sont utilisés comme photostabilisateurs en absorbant et rapportant les UV et ainsi assurer une protection contre les UVA et les UVB (290-350 nm) (Egambaram et al., 2020). Les BZT-UV se trouvent principalement sous leurs formes neutres dans l'environnement. Ce sont des acides faibles avec un pKa d'environ 7-10, ce qui augmente leur caractère hydrophobe (Kim et al., 2015 ; Liu et al., 2014). Les demi-

vies estimées des BZT-UV dans les sédiments vont de 340 à 540 jours, de 38 à 60 jours dans l'eau et de 0,5 à 1,2 jour dans l'air (Kim et al., 2019). Leurs faibles solubilités dans l'eau et leurs coefficients Log K_{ow} élevés (exemple UV328 : 0,015 mg/L ; Log K_{ow}>5) suggèrent qu'ils peuvent s'accumuler dans les sédiments et dans les organismes (Cantwell et al., 2015).

Tableau 2: Noms chimiques, numéros de registre CAS, acronymes et propriétés physicochimiques des BZT-UV cibles.

Nom chimique	CAS No.	Acronymes	Poids moléculaire (g/mol)	Solubilité dans l'eau (mg/L)	Log K_{ow}[a]
2-(2H-benzotriazol-2-yl)-p-cresol	2440-22-4	UVP	225,3	25,6	3,00
2-[3-(2H-benzotriazol-2-yl)-4-hydroxyphenyl]ethyl methacrylate	96478-09-0	UV090	323.4	14.9	3.93
2-(2H-benzotriazol-2-yl)-4-methyl-6-(2-propenyl)phenol	2170-39-0	UV9	265.3	13.1	4.39
2-(2H-benzotriazol-2-yl)-4,6-bis(1-methyl-1-phenylethyl)phenol	70321-86-7	UV234	447.6	1.6×10^{-3}	7.67
2-Benzotriazole-2-yl-4,6-di-*tert*-butylphenol	3846-71-7	UV320	323.4	0.15	6.27
2-*tert*-Butyl-6-(5-chloro-2H-benzotriazol-2-yl)-4-methylphenol	3896-11-05	UV326	315.8	0.68	5.55
2.4-Di-*tert*-butyl-6-(5-chloro-2H-benzotriazol-2-yl) phenol	3864-99-1	UV327	357.9	0.026	6.91
2-(2H-benzotriazol-2-yl)-4,6-di-*tert*-pentylphenol	25973-55-1	UV328	351.5	0.015	7.25
2-(2H-benzotriazol-2-yl)-4-(1,1,3,3-tetramethyl butyl)phenol	3147-75-9	UV329	323.4	0.17	6.21
2-(2H-benzotriazol-2-yl)-4-(*tert*-butyl)-6-(*sec*-butyl)phenol	36437-37-3	UV350	323,4	0,14	6,31

[a]Prédit par la modélisation de l'interface du programme d'estimation (EPI) Suite (V4.11).

1.4.2.2 Devenir et Bioaccumulation chez les poissons et l'homme

Les stations d'épuration (STEP) ont été reconnues comme la principale source des BZT-UV qui se retrouvent dans les écosystèmes aquatiques (Ramos et al., 2016). Ces composés ont été détectés dans diverses matrices environnementales, plus particulièrementen particulier dans les eaux usées et les boues des stations d'épuration (Montesdeoca-Esponda et al., 2015), dans les sédiments marins et d'eau douce (Nakata et al., 2009b), les organismes aquatiques (Nakata et al., 2009b) et dans la poussière domestique (Kim et al., 2012). Ces résultats indiquent que les BZT-UV sont largement répandus dans l'environnement.

Comme les UVF, la bioaccumulation des BZT-UV se produit chez les poissons par absorption de ces composés par les branchies, qui atteignent ainsi la circulation sanguine (Peng et al., 2017). Cette bioaccumulation paraît spécifique au composé et à l'espèce (Kim et al., 2011a ; Kim et al., 2011b). Cependant, les BZT-UV, ayant une forte affinité pour les tissus adipeux, (Log K_{ow} élevé) se concentrent dans les graisses et les huiles présentes dans les tissus des poissons (Giraudo et al., 2020). Ils s'accumulent notamment dans le plasma sanguin, le foie et la bile des poissons (Kim et al., 2011b ; Lu et al., 2017a ; Lu et al., 2016 b). Les BZT-UV peuvent également être accumulées par les poissons qui consomment d'autres organismes contenant ces composés, tels que des algues ou les minuscules crustacés du zooplancton (Peng et al., 2020). Les BZT-UV peuvent alors se bioamplifier dans la chaîne alimentaire, présentent ainsi un risque pour l'environnement (Giraudo et al., 2020).

Chez l'Homme, l'accumulation des BZT-UV peut se produire de plusieurs façons. Ils peuvent être ingérés par l'alimentation, notamment par la consommation de poisson et d'autres organismes aquatiques contaminés (Kim et al., 2011b). Ces composés peuvent pénétrer dans la circulation sanguine et se bioaccumuler dans les tissus adipeux de l'organisme. Les BZT-UV ont été détectées dans les tissus adipeux du corps humain, (Wang et al., 2015), le lait maternel (Kameda et al., 2011) et l'urine (Asimakopoulos et al., 2013).

1.4.2.3 Toxicité des BZT-UV chez les poissons et l'Homme

Les BZT-UV peuvent causer une toxicité hépatique. Par exemple, l'exposition au 2-(3.5-di-tert-butyl-2-hydroxyphényl) benzo-triazole (UV320) et au 2-(3.5-di-*tert*-amyl-2-hydroxyphényl) benzotriazole (UV328) chez les rats a entraîné des toxicités chroniques spécifiques au sexe dans le foie, les reins, la rate et la thyroïde (Hirata-Koizumi et al., 2007). Des toxicités hépatiques telles que l'augmentation du poids du foie et l'hypertrophie des hépatocytes ont également été observées chez les sujets ayant reçu des doses répétées de 2-(2H-benzotriazol-2-yl)-4,6-bis(1-methyl-1-phenylethyl) phenol (UV234) (Ruan et al., 2012).

D'autre part, bien que les embryons d'éleuthérocoque de poisson-zèbre exposés aux stabilisants BZT-UV n'aient pas présenté d'activité œstrogénique ou androgénique (Fent et al., 2014), l'exposition aux 2-(2H-benzotriazol-2-yl)-p-cresol (UVP) et aux 2-*tert*-butyl -6-(5-chloro-2H-benzotriazol-2-yl)-4-methylphenol (UV326) peut entraîner un déséquilibre métabolique et des dommages au niveau du développement (Fent et al., 2014). Cependant, les stabilisateurs BZT-UV n'ont pas été toxiques pour la daphnie aux concentrations environnementales (Kim et al., 2011a).

Chez l'Homme, l'exposition directe à certains BZT-UV comme l'UVP peut avoir des effets secondaires immédiats tels que la dermatite et l'irritation de la peau (Yamano et al., 2001). En plus d'interagir avec l'albumine sérique humaine (protéine de transport la plus abondante dans le plasma humain) (Zhang et al., 2016), les stabilisateurs BZT-UV comme UVP et UV326 peuvent également agir sur le récepteur humain des hydrocarbures aryliques (AhR), ce qui peut avoir un impact négatif sur la réponse immunologique (Nagayoshi et al., 2015).

1.5 APPROCHE GÉNÉTIQUE QPCR

La méthode employée pour distinguer les espèces de poissons *S. fasciatus et S. mentella* repose sur la PCR en temps réel (qPCR) utilisant le SYBR Green. Les amorces spécifiques, conçues pour cibler des régions distinctes d'ADN, présentent des températures de fusion (Tm) propres à chaque espèce. L'échantillon d'ADN extrait des poissons est soumis à une

réaction de qPCR dans un thermocycleur en temps réel, où la fluorescence est mesurée à chaque cycle. L'analyse de la courbe de fusion permet de déterminer la température à laquelle l'ADN propre à chaque espèce fond. La présence de *S. fasciatus* est confirmée à 74 °C, et celle de *S. mentella* à 76 °C. Ainsi, cette méthode offre une approche ciblée et sensible pour l'identification des espèces, sous réserve de conditions expérimentales optimales (Senay et al., 2023).

1.6 APPROCHE DES RATIOS ISOTOPIQUES

Dans l'objectif de déterminer le niveau trophique des espèces, l'analyse des isotopes stables et de la composition de l'azote peut être effectuée au moyen d'un spectromètre de masse à rapport isotopique en continu (CF-IRMS). Ce dispositif, composé d'un Deltaplus XP MS de ThermoScientific Inc. couplé à un analyseur élémentaire COSTECH 4010 de Costech Analytical Technologies, Inc équipé d'un passeur automatique de blanc zéro, suit la méthode décrite par Glaz et al. (2014).

1.7 PROBLÉMATIQUE DE LA RECHERCHE

L'étude de la présence de THg, de MeHg et d'UVA dans le sébaste revêt une importance cruciale en raison de leur impact potentiel sur la santé humaine environnementale. Le sébaste connaît un retour spectaculaire dans l'estuaire et le golfe du Saint-Laurent, ce qui soulève des préoccupations quant à sa future consommation potentielle et aux contaminants qu'il pourrait contenir, transférant ainsi ces substances à l'Homme. Le THg et le MeHg, en tant que substances toxiques, peuvent s'accumuler dans les tissus des poissons qui, s'ils sont consommés en grandes quantités, peuvent entraîner de graves problèmes de santé, en particulier chez les femmes enceintes, les mères allaitantes et les jeunes enfants. Les UVA, également préoccupants, peuvent influer la qualité et la sécurité des produits de la mer, notamment les poissons. À notre connaissance, il n'existe pas de données sur la présence et la distribution du THg, MeHg et les UVA dans le sébaste du SLEG. En comblant cette lacune, cette étude offre une perspective inédite sur les niveaux et la distribution de ces contaminants dans le sébaste du SLEG. Ce manque de données quant aux connaissances actuelles, surtout compte tenu du retour spectaculaire du sébaste dans le SLEG et de son potentiel accroissement de la consommation humaine, souligne l'urgence de cette

étude pour évaluer les risques potentiels pour la santé des consommateurs et de l'environnement.

1.8 OBJECTIF DE LA RECHERCHE ET PLAN DU MÉMOIRE

L'objectif principal de la présente étude est de fournir de l'information sur le statut et les tendances spatiales des concentrations du mercure et methylmercure ainsi que les absorbants ultraviolets organiques présents dans le sébaste atlantique de fond, au niveau de l'estuaire et le golfe du Saint-Laurent (EGSL).

Les objectifs spécifiques sont les suivants :

Analyser les concentrations de mercure, de méthylemercure et des absorbants UV dans les échantillons de muscles du sébaste atlantique.

Déterminer la distribution spatiale des contaminants visés dans le sébaste de l'estuaire et le golfe du Saint-Laurent.

Déterminer le lien entre les concentrations des contaminants visés et les caractéristiques du sébaste atlantique, tel que les isotopes stables, le poids, la taille, le sexe et l'âge (répartis en deux catégories d'âge).

Évaluer le risque de l'exposition potentielle à ces contaminants sur la santé humaine.

Il s'agit de mieux comprendre la répartition et le degré d'exposition de ces contaminants et ainsi répondre aux objectifs de la recherche. La prochaine partie, qui est la deuxième section, comporte un premier article qui présente un aperçu général de la problématique dans l'estuaire et le golfe du Saint-Laurent au Québec, Canada, et met l'accent sur les concentrations et la répartition spatiale du THg et MeHg dans le sébaste et évalue les risques liés au mercure pour la santé humaine. Enfin, dans la troisième partie, le deuxième article s'attarde aux concentrations en absorbants UV dans le sébaste et évaluation du risque d'exposition humaine aux stabilisateurs benzotriazole ultraviolets (BZT-UV) et aux filtres ultraviolets (UVF).

CHAPITRE 1 SPATIAL DISTRIBUTION AND SPECIATION OF MERCURY IN A RECOVERING DEEPWATER REDFISH (SEBASTES MENTELLA) POPULATION FROM ST. LAWRENCE ESTUARY AND GULF, CANADA

1.1 CONTRIBUTION À LA RECHERCHE ET PRÉSENTATION

Cet article publié dans le journal 'Environmental Pollution' est le fruit d'un travail d'équipe. En tant qu'auteure principal j'ai effectué le prétraitement des échantillons pour mesurer le mercure et le méthylmercure dans le muscle du sébaste. Les résultats ont permis d'établir les niveaux de chaque polluant et de confirmer leur présence dans le sébaste du Saint-Laurent. J'ai également traité les échantillons, analysé les données, interprété les résultats et rédigé la première version de l'article ainsi que le traitement des commentaires reçus des co-auteurs. La direction assurée par **Zhe Lu** a contribué de manière significative à son succès. Il a participé activement à l'interprétation des résultats et à l'évaluation des résultats du projet. **Dominic E. Ponton** et **Marc Amyot** de l'Université de Montréal (UdeM) ont participé à la conceptualisation du projet de recherche, à l'analyse du mercure et méthylemercure ainsi que la révision et l'édition de l'article. **Geneviève Parent** du Ministère des Pêches et Océans Canada (MPO) a réalisé l'analyse génétique pour l'identification de l'espèce cible (*Sebastes mentella*). La méthodologie, qui comprenait l'analyse des isotopes stables, était sous la direction de **Mathieu Babin**. Les informations biologiques des spécimens utilisés dans l'étude ont été fournies par **Caroline Senay** de MPO, qui a également participé à la révision et à l'édition de l'article. Les nombreuses présentations produites dans le cadre de ce projet, y compris celles données à Ecotoq 2022, SETAC North America 2022, Québec Océan 2023 et Chapitre Saint-Laurent 2023, ont été révisées par tous les coauteurs. Les échantillons de sébastes ont été fournis par le codirecteur **Dominique Robert**, qui a également révisé dans leur intégralité tous les documents et présentations créés pour ce programme de master.

Auteurs : Moualek, Fella ; Bélanger, Dominic ; Babin, Mathieu ; Parent, Geneviève J. ; Ponton, Dominic .E., Amyot, Marc ; Senay, Caroline ; Robert, Dominique & Lu, Zhe.

1.2 RÉSUMÉ

La pollution par le mercure (Hg) constitue une menace importante pour l'environnement, en particulier sous la forme de méthylmercure (MeHg). Cependant, on sait peu de choses sur la distribution et les facteurs d'influence du Hg dans les poissons de fond d'eau profonde (>200m), ce qui est crucial pour évaluer les risques pour la santé des poissons et des humains. Au Canada, le sébaste (*Sebastes mentella*) a été désigné comme une espèce menacée depuis 2010. Après un moratoire de 25 ans sur la pêche, la population de sébastes de l'estuaire et du golfe du Saint-Laurent se rétablit, et la reprise de la pêche commerciale et de la consommation humaine est attendue. Cette étude visait à étudier la distribution du MeHg et du Hg total (THg) dans le muscle du sébaste, ainsi que les facteurs influençant cette distribution, et à évaluer les risques pour la santé humaine associés à la consommation de sébaste. Les échantillons de sébaste (*n*=123) ont été prélevés par Pêches et Océans Canada en 2019. Les concentrations de THg et de MeHg dans le muscle de sébaste ont été déterminées à 93±183 ng/g (moyenne±SD, poids humide) et 78,2±149 ng/g, respectivement. Le MeHg représentait 93±8% du THg dans le muscle du sébaste. Les grands sébastes (>30 cm) ont accumulé 20 à 30 fois plus de Hg que les petits sébastes (17 à 30 cm). Les petits sébastes de l'estuaire et du golfe occidental avaient des niveaux plus élevés de MeHg et de THg que ceux du chenal laurentien et du nord-est du golfe. Les prédicteurs significatifs des concentrations de MeHg dans le muscle du sébaste ont été déterminés comme étant la longueur du poisson, l'humidité du muscle, $\delta\,^{15}$N, et N%. La consommation de MeHg par la population générale avec un taux moyen de consommation de poisson ne devrait pas avoir d'effets néfastes. Cette étude établit une base de référence pour la surveillance future du Hg dans les eaux profondes de cette région. D'autres recherches sont nécessaires pour élucider les relations de cause à effet entre les divers paramètres environnementaux et biologiques qui influencent l'accumulation de Hg dans le biote des eaux profondes.

Mots-clés : Grands fonds, espèces menacées, exposition humaine, évaluation des risques pour la santé, suivi de référence.
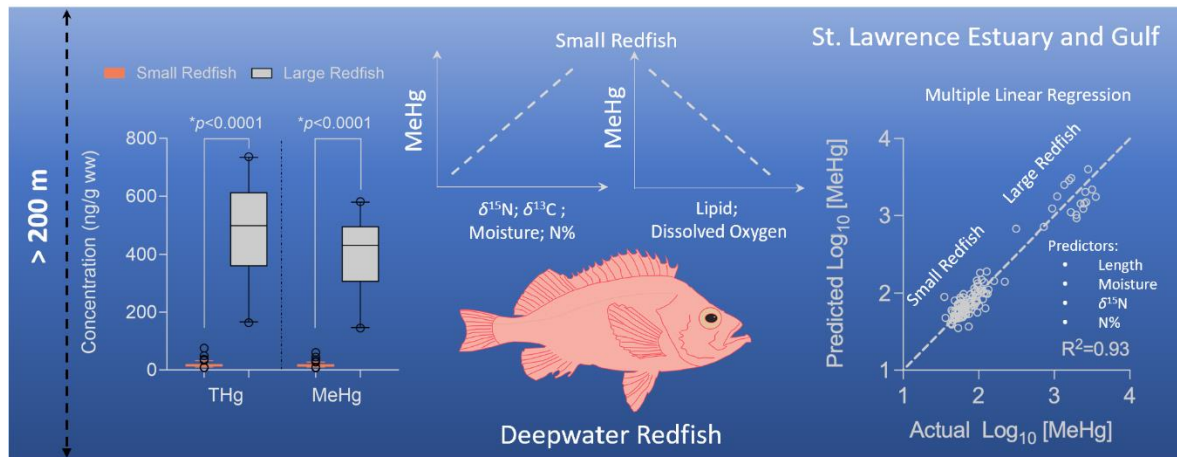
Figure 3: Résumé graphique.

1.3 INTRODUCTION

Mercury (Hg) is a global pollutant that can be emitted into the environment from both natural (e.g., volcanic eruptions and weathering of rocks) and anthropogenic (coal combustion and mining) origins (Ramirez-Llodra et al., 2011). Hg has the potential to be conveyed to the marine environment via atmospheric deposition, as well as through the discharge of rivers and wastewater (Blukacz-Richards et al., 2017). Once in the environment, Hg can be transformed into the highly toxic form of methylmercury (MeHg) by various microorganisms (Villar et al., 2020). It is well established that MeHg is highly bioaccumulative and can biomagnify in food webs. Exposure to MeHg, even at low levels, can result in severe impacts on the health of both human and wildlife. For example, due to its high lipophilicity and high affinity with the cysteine group in proteins, MeHg can quickly cross cell membranes and the blood-brain barrier (Al-Sulaiti et al., 2022). This can result in a range of adverse effects in humans, including central nervous system dysfunction, chromosomal abnormalities and disorders, and immune system disruption (Al-Sulaiti et al., 2022). In fish, chronic Hg exposure can result in neurotoxic effects and reproductive toxicity (Al-Sulaiti et al., 2022; Zheng et al., 2019). Because of these risks, Hg has been designated as one of the top ten major health concern chemicals by the World Health Organization (WHO) (WHO, 2020).

Factors influencing concentrations of total Hg (THg) and MeHg in marine fish have gained significant attention due to the ecological and commercial roles that these organisms play, as well as their contributions to human exposure to these pollutants (Sofoulaki et al., 2019). Contaminated fish consumption is one of the primary routes of Hg exposure to humans (Al-Sulaiti et al., 2022). Nevertheless, the knowledge of the distribution of THg and MeHg in the deep-sea (median depth of occurrence>200 m) fish, which are considered a sink of these pollutants in the ocean, remains limited. It has been reported that the THg and MeHg concentrations in the fish muscle increased with depth in both demersal and pelagic fish species occurring in the Cantabrian Sea (North-East Atlantic, 50-1868 m), indicating that deep-sea fish species may be more contaminated with these pollutants than those species living in surface waters (Romero-Romero et al., 2022). These findings raise concerns about THg and MeHg pollution in deep-sea fish and their environment. In addition, it is also not clear how environmental and biological factors can impact and predict the levels of these pollutants in deep-sea fish, and the potential health risks that deep-sea fish consumption may pose to humans.

Deepwater redfish (*Sebastes mentella*) (also known as beaked redfish; hereafter redfish) primarily distributes in the deep layer, from 100 to 1000 m, of North Atlantic Ocean ecosystems (Fisheries and Oceans Canada, 2021; Cadigan et al., 2022). Redfish are a slow-growing, long-lived species that can live up to 75 years and grow up to a length of 42 cm (Senay et al., 2021). In the St. Lawrence Estuary and Gulf (SLEG) (Canada), the redfish population collapsed in the early 1990s, which was attributed to overfishing that occurred in a period of low productivity and recruitment caused by abnormally cold temperatures (Fisheries and Oceans Canada, 2021; Gascon, 2003; Senay et al., 2019;2021). The decline of redfish prompted the implementation of a fishing moratorium as a management measure to allow for the recovery of the population (Savenkoff et al., 2006). After two decades of stability at low biomass level, massive redfish recruitment occurred in 2011-2013 during a period of warming conditions (Fisheries and Oceans Canada, 2021;2022; Senay et al., 2021). Without significant variations of the total trawlable biomass of other species in the past 20 years, the biomass of redfish increased rapidly to represent >80% of the total demersal

biomass caught in the bottom-trawl survey conducted by Fisheries and Oceans Canada in 2021, in comparison to 15% in the 1995-2012 period (Fisheries and Oceans Canada, 2022). Despite redfish exploitation still being under moratorium, it is anticipated that the rapid increase in spawning biomass will lead to the resumption of commercial fishing shortly (Senay et al., 2021). Consequently, the forthcoming consumption of redfish may serve as a potential pathway of exposure for humans to various contaminants, including THg and MeHg, and necessitates investigation beforehand.

To the best of our knowledge, there is no existing data on the presence and distribution of THg and MeHg in redfish from the SLEG. Therefore, the aims of this study are to (i) analyze the concentrations and spatial variations of THg and MeHg in the muscles of redfish from the SLEG, (ii) examine the associations of different biological and environmental factors with MeHg and THg concentrations in SLEG redfish muscles, and (iii) evaluate the potential health risks to humans from MeHg exposure associated with the consumption of redfish. This study's findings establish a baseline for future monitoring and modeling of THg and MeHg levels in deep-sea fish from the SLEG and provide critical information to consumers and decision-makers to determine the safety of consuming redfish from this region.

1.4 MATERIALS AND METHODS

1.4.1 Sampling and Fish species determination

Redfish samples were collected in 2019 by bottom trawling during the monitoring survey conducted annually by Fisheries and Oceans Canada in August-September, along the SLEG (Canada) (Figure 5). Fish weight and length were measured on the vessel upon capture, and sex was determined through dissection and visual inspection of the gonads. All fish manipulations were carried out based on the recommendation of the Canadian Council of Animal Protection (Batt et al., 2005). Environmental parameters including water depth (the water column depth and the depth the fish were caught were the same because the bottom trawling method was used), dissolved oxygen, salinity and temperature were measured during sampling and details are shown in Bourdages et al. (2022). Redfish samples were

wrapped in aluminum foil, sealed in Ziplock polyethylene bags, and transported on ice to the laboratory. Fish species determination was based on published method (Senay et al., 2023). To distinguish the target deepwater redfish from the morphologically similar Acadian redfish (*Sebastes fasciatus*), pectoral fin rays were sampled on *Sebastes* spp. and then conserved at -20 °C. Species determination was done at the laboratory of genomics of the Maurice Lamontagne Institute of Fisheries and Oceans Canada (Mont-Joli, Canada). Briefly, DNA was extracted using QuickExtract™ (Lucigen, Middleton, USA). A genus specific qPCR assay was used with SYBR™Green (Thermo Fisher Scientific™, Waltham, USA) to discriminate *S. fasciatus* (melting temperature: 74°C) from *S. mentella* (melting temperature: 76°C) (Senay et al., 2023). Note that this test cannot discriminate *S. fasciatus* from *S. norvegicus* but *S. norvegicus* is rarely captured in the Gulf of St. Lawrence. All 123 muscle samples identified as redfish *Sebastes mentella* were used for the analyses of THg and MeHg.
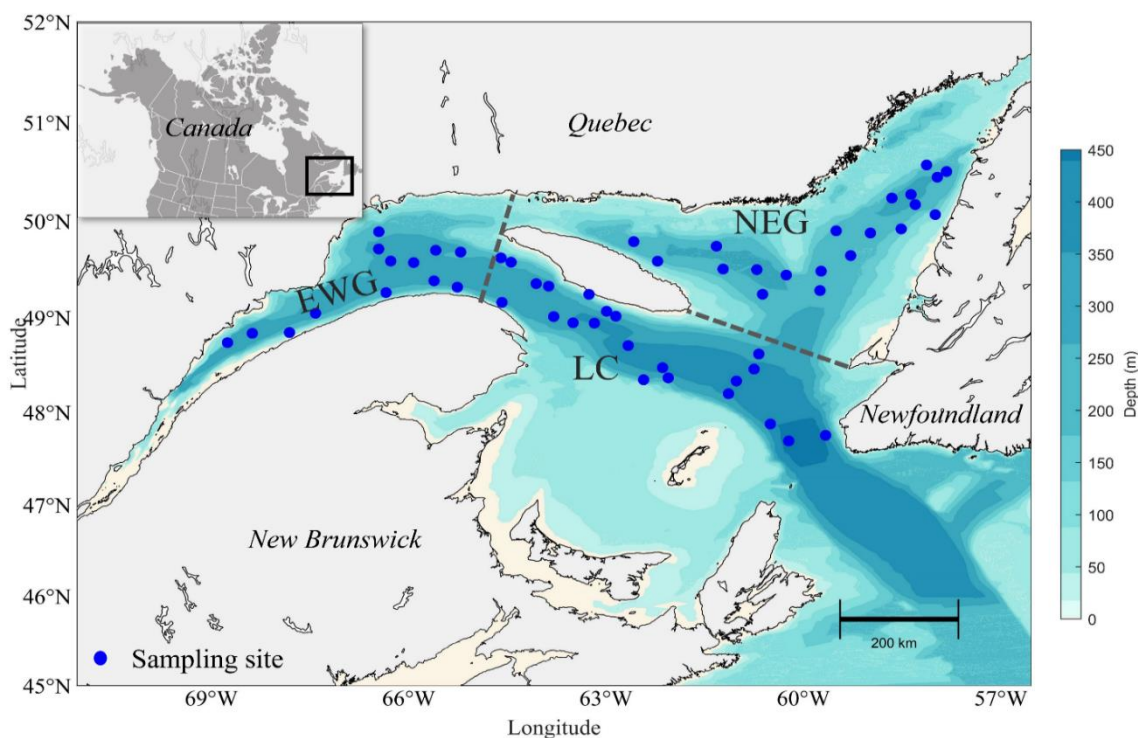
Figure 4: Redfish sampling locations in three areas of the St. Lawrence Estuary and Gulf: Estuary - Western Gulf (EWG), Laurentian Channel (LC) and Northeast Gulf (NEG).

Collected redfish were dominated by the 2011 cohorts with size ranging between 20 and 25 cm (65% of total fish collected) (Figure S1, annex I). In the present study, the redfish samples with size <30 cm are defined as the "small group" (n=103), while those >30 cm (individuals from cohorts prior to 2011) are defined as "large group" (n=20). This study focused on comparing three distinct subareas within the SLEG, which exhibit topographic heterogeneity (Brown-Vuillemin et al., 2022). These subareas (Figure 5) include: (1) the Estuary-Western Gulf (n=32 total; small group: n=28; large group: n=4), encompassing the estuary and the western portion of the St. Lawrence Gulf characterized by relatively shallow water depths (maximum depth approximately 300 m); (2) the Northeast Gulf (n=39 total; small group: n=34; large group: n=5), which includes Esquiman and Anticosti Channels with a maximum depth of about 335 m; and (3) the Laurentian Channel (n=39 total; small group: n=31; large group: n=8), which can reach a maximum water depth of approximately 550 m. In addition, the sampling locations of 13 samples (small group: n=10; large group: n=3) were not recorded. The fish were carefully skinned using ceramic scalpel and only the muscles of the fish were collected and weighted, as it is known to be the major tissue to accumulate of MeHg (Teunen et al., 2022) and consumed by humans. The fish muscle samples were freeze-dried, ground using glass mortar and pestle, and stored at - 20 °C until further analysis.

1.4.2 Sample preparation analysis and quality control

1.4.2.1 Total mercury (THg) and methylmercury (MeHg) analyses

The analyses of THg and MeHg were carried out at the Université de Montréal (Montréal, Québec, Canada) following the published method (Charette et al., 2021). THg was analyzed using Direct Mercury Analyzer (DMA 80; Milestone Inc). First, the samples were weighed (0.01-0.04 g) into a nickel combustion vessel and then introduced on the DMA 80, where they were thermally decomposed at 660 °C and Hg vapors were selectively trapped on gold amalgamator for analysis by atomic absorption spectrophotometry. The DMA threshold analysis ranged from 0.05 to 600 ng.

MeHg concentrations were determined by Tekran 2700 Mercury Vapor Analyzer (Tekran 2700; Tekran Instruments Corporation). Before analysis, 0.01–0.04 g of dry sample was digested in 5mL of 4M nitric acid solution (HNO_3) at 65°C over night. Digested materials were ethylated in sodium acetate buffer at pH=4.9, followed by gas chromatography separation with Cold Vapor Atomic Fluorescence Spectroscopy detection (CVAFS) (Tekran 2700). Water content was determined in all samples (average: 84.1 ± 3.0 %), and dry weight concentrations were converted to a wet weight basis based on water content of each sample.

1.4.2.2 Stable isotope analysis

Stable isotopes and nitrogen compositions were analyzed using a Continuous-Flow Isotope Ratio Mass Spectrometer (CF-IRMS). The CF-IRMS consisted of a Deltaplus XP MS (ThermoScientific Inc.) coupled with a COSTECH 4010 elemental analyzer (Costech Analytical Technologies, Inc) equipped with a zero blank autosampler. Caffeine, Nannochloropsis and Mueller Hinton Broth calibrated from National Institute of Standards and Technology (NIST) primary standard, were used repeatedly throughout every 36 samples sequence, as the standard for in-lab normalization regressions to determine sample delta values. Analytical errors (standard deviation (SD)) for replicate standard analyzes were $\pm$ 0.13 ‰ for $\delta^{15}N$ and $\pm$ 0.17 ‰ for $\delta^{13}C$. Quantification of nitrogen was based on external secondary standard (Caffeine and Nannochloropsis) with an approximate calibration range of 0.025 to 0.250 mg and the relative SD of calibration slopes was 2%. Certified reference material from Elemental Mirco Analysis (B2151 and B2159) were used for quality control. To test the method's repeatability, a redfish sample was analyzed six times and the SD was 0.07‰ for $\delta^{15}N$, 0.06 ‰ for $\delta^{13}C$, and 0.4% for N%.

1.4.2.3 Lipid content determination

A mixture of 5mL hexane/dichloromethane (*1/1, v/v*) was added to the redfish muscle (0.5g, dw) sample, followed by 30 seconds vortex, 5 minutes sonication, and 5 minutes centrifugation (1,167*g*). The supernatant was transferred to a new pre-weighted glass tube. This extraction procedure was repeated three times and the supernatants were combined. The

combined extract was concentrated to dryness using a gentle stream of N_2 and lipid content (dry weight based) was measured gravimetrically.

1.4.2.4 Age of Redfish

Given the difficulties of using otoliths to determine the age of redfish (Saborido-Rey et al., 2004; Stransky et al., 2005), the Von Bertalanffy growth curve, which models size as a function of age for the 1980 cohort of redfish (Fisheries and Oceans Canada, 2022), was used to determine the age of collected redfish. This approach still has a certain level of uncertainty between cohorts and particularly for old individuals who are no longer growing and for whom the sizes-at-age are overlapping. Therefore, relationship between fish age and MeHg or THg concentrations was not evaluated at individual level. Consequently, the analysis solely focused on examining the overall pattern between younger and older redfish. The results revealed that the age of small redfish was between 5 and 13 years, and that of large redfish was between 13 and 50 years. As expected, the group of large redfish (age: 13 - >50 years) had higher levels of MeHg and THg. This could be due to the redfish's longevity (40-70 years) (Senay et al., 2021), which increases their exposure and accumulation period to Hg. Given that the growth rate may vary for different cohorts, combining fish size and age could better estimate Hg levels in redfish.

1.4.2.5 Quality control

Laboratory glassware was cleaned with diluted hydrochloric acid (10%) and ultra-pure water before being dried (Kim et al., 2016). The precision of the chemical analysis was verified using standard reference materials including Tort-3, Dorm-4 and Dolt-5 for THg and Dorm-4 and Dolt-5 for MeHg (National Research Council of Canada). The recoveries were in the range of 97%-109% for THg and 87%-110% for MeHg (Table S1, annex II). A reagent blank sample was extracted and evaluated together with the other samples for each batch, without adding the fish sample. The reagent blank samples were free of Hg contamination.

1.4.3 Human health risk assessment

The detailed risk assessment method is described in Kortei et al (2020). Briefly, it is based on: (a) the determination of estimated weekly intakes (EWI) of MeHg, and (b) the comparison of the EWI with the "reference dose"(RfD).

The adult EWI (µg/kg/week) for MeHg was estimated, following this formula:

$$EWI = (C_{fish} \times Consumption_{fish}) / body\ weight \qquad (Eq.1)$$

where C_{fish} is the 50th or 95th percentile of observed MeHg concentrations in all redfish muscle (µg/kg wet weight (ww)); Consumption $_{fish}$ is the weekly consumption of fish in Canada, which is estimated as 0.05 kg/week/person (annual fresh and frozen sea fish, edible weight in 2022 in Canada: 2.64 kg/person) (Statistic Canada, 2023) for average fish consumers group and 0.28 kg/week (40 g/day) for the high consumers group (Health Canada, 2007); and body weight is Canadian average human body weight (women: 66.8 kg, men: 81.6 kg; average: 74.2 kg) (Statistic Canada, 2015). HQ was calculated as follows:

$$HQ = EWI / RfD \qquad (Eq.\ 2)$$

where HQ (unitless) is the ratio between EWI (Eq.1) and the RfD which is 3.2 µg/kg/week for general adults and 1.6 µg/kg/week for childbearing women (United Nations Environment Programme (UNEP)/WHO, 2008). HQ values of <1 indicate that the population will unlikely be subjected to adverse health impacts, however HQ values > 1 indicate that the population may be exposed to health concerns. Generally, HQ of 0.1 to 1, 1 to 10, and HQ > 10 correspond to low, moderate, and high health risks from MeHg, respectively (Rantetampang & Mallongi, 2014).

The study focused on two demographic groups: adults of the general population and women of childbearing age. Women of childbearing age were selected as a target group for the risk assessment because they are deemed to be the group most susceptible to the impacts of MeHg (Bello et al., 2023). The exposure scenarios are as follows: In Scenario A, we assumed that the individuals being evaluated consume an average amount of fish per week

in Canada (0.05 kg/week). We then computed the EWI for two different percentiles of observed MeHg concentrations in all small and large redfish muscle: the 50th percentile (16.4 ng/g ww; Scenario A1) and the 95th percentile (473 ng/g ww; Scenario A2). In Scenario B, we assumed that the individuals are high fish consumers per week (0.28 kg/week) and calculated the EWI for the 50th percentile (16.4 ng/g ww; Scenario B1) and 95th percentile (473 ng/g ww; Scenario B2) of observed MeHg concentrations in redfish muscle, with B2 representing the worst-case exposure.

The maximum allowable daily consumption rate (CRlim; kg/day) is a measure of the highest level of a substance that can be consumed daily over a lifetime without posing a significant risk to health. The CRlim of MeHg due to redfish consumption was calculated following this formula (Raissy et al., 2013):

$$CRlim = [(RfD/7) \times body\ weight]/\ C_{fish} \qquad (Eq.\ 3)$$

1.4.4 Data analysis

Data were analyzed using GraphPad Prism 9.5 (La Jolla, CA, USA), Excel 16.43 (Redmond, WA, USA) and R4.3.1 (with RStudio 2023.06.0) (Boston, MA, USA). The normality and homoscedasticity of data were tested with Shapiro-Wilk and Squared Ranks test, respectively. Non-parametric tests (e.g., Mann-Whitney test, Kruskal-Wallis test, and Spearman correlation) were used to analyze data that deviated from the normal distribution even after log transformation. Both wet weight (ww) and dry weight (dw) based concentrations are reported for the comparison with existing literature. Mean (with standard deviation (SD) and sometimes in standard error (SE)) and median concentrations are provided to facilitate comparisons to published results.

The first tier of analysis was descriptive to illustrate the variation and distribution of MeHg and THg concentrations in small and large redfish and the spatial variations based on the raw data. Because redfish length was not correlated with MeHg or THg concentrations in either the small or large groups, the concentration data used for such comparisons in the first tier analysis were not corrected for fish size. The significance of differences of

concentrations (raw data) between small and large groups was analyzed by Mann-Whitney test. The concentration differences (raw data) among three sampling areas were tested using Kruskal-Wallis test followed by a post-hoc Dunn test.

The second tier analysis estimate the least squares mean of $\log_{10}$ transformed MeHg and THg concentrations (dw) in small or large redfish for comparison among three sampling areas (package 'lsmeans' version 2.30-0 in R) (Lenth 2016). All measured environmental (depth, temperature, dissolved oxygen, and salinity), biological (fish length, sex, weight, lipid content, moisture in muscle, $\delta^{15}N$, $\delta^{13}C$, and N%) parameters and sampling areas were initially added to a linear model and those environmental and biological variables that showed significant effects (small redfish: sex, lipid content, moisture in muscle, dissolved oxygen, $\delta^{15}N$; large redfish: moisture in muscle) were used for the final least squares mean estimation. This relativized estimate statistically accounts for the effects of these variables, which allows for spatial comparisons of MeHg and THg relative availability to redfish among three sampling areas. Welch's ANOVA test was used for the comparisons of least squares mean among three sampling areas.

Spearman correlation and simple linear regression were employed to examine the relationships between the $\log_{10}$ transformed concentrations of MeHg or THg (dw) and each biological or environmental variable. These correlation and regression analyses were conducted for small and large redfish separately because the two size groups of redfish are separate clusters, and analyzing two groups of fish together can violate the basic assumptions (i.e., continuous data and normality of residuals) for these analyses. Then, multiple linear regression was used to build a predictive model of MeHg or THg concentration (dw) in the muscle of all redfish (small and large group together) and small redfish based on multiple explanatory biological/environmental variables, following this initial equation: $\log_{10}$ [MeHg] or [THg] (dw) = $\beta0 + \beta1\times$length $+ \beta2\times$sex $+ \beta3\times$weight $+ \beta4\times$lipid content in muscle $+ \beta5\times$ moisture in muscle $+ \beta6\times$depth $+ \beta7\times$temperature $+ \beta8\times$dissolved oxygen $+ \beta9\times$salinity $+ \beta10\times\delta^{15}N + \beta11\times\delta^{13}C + \beta12\times$N% $+ \varepsilon$. In the given equation, $\beta0$ to $\beta12$ are considered as constants and ε represents the error term. These variables were selected because they may affect the distribution, speciation and fate of Hg in the aquatic environment,

including the accumulation of Hg in fish. Age was not included in this equation because it was solely estimated with some uncertainties and details are presented in title 1.4.2.4. To improve the stability and reliability of the model's estimates and predictions, certain independent variables such as weight (with length) and salinity (with temperature) were excluded from the model due to multicollinearity (variance inflation factor (VIF) > 4). The significant variables were finally selected for the multiple linear regression model. We considered test results as statistically significant where $p \leq 0.05$.

1.5 RESULTS AND DISCUSSION

1.5.1 Concentrations and spatial variations of THg and MeHg in redfish muscle

For all redfish muscle samples, the concentrations of THg and MeHg were 93.3 ± 183 ng/g ww (mean ± SD) (median: 16.9 ng/g, range: 7.40-737 ng/g, ww) and 78.2 ± 149 ng/g ww (median: 16.4 ng/g, range: 7.14-581 ng/g, ww), respectively (Table 4). MeHg accounted for 93 ± 8 % (mean ± SD) of THg in the redfish muscle. Except for 3% of samples (all of them were large redfish), the concentrations of MeHg in most redfish muscle samples were below the international limit allowed for commercialization set by the Food and Agriculture Organization (FAO)/WHO, which is 500 ng/g ww (FAO/WHO, 2003). Significantly higher (about 20-30 times) concentrations of THg and MeHg were found in large redfish (>30 cm) compared to small redfish (<30 cm) (Figure S2, annex I) ($p < 0.0001$). The small individuals had an average concentration of 17.6 ± 8.9 ng/g ww (mean ± SD) (median 15.7 ng/g, range: 7.40-75.8 ng/g, ww) for THg and 16.6 ± 7.4 ng/g ww (median 14.9 ng/g, range: 7.14-60.5 ng/g, ww) for MeHg, while the large individuals had an average concentration of 483 ± 154 ng/g ww (median 497 ng/g, range: 164-737 ng/g, ww) for THg and 395 ± 123 ng/g ww (median 431 ng/g, range: 145-581 ng/g, ww) for MeHg.

Spatial variations in MeHg and THg levels (raw concentration) were observed for small redfish but not for large redfish (Figure 6 & S3, annex I). Small redfish from the Estuary-Western Gulf had higher levels of MeHg and THg compared to samples from the Laurentian Channel and the Northeast Gulf (Figure 6 & S3 annex I). The different spatial variation pattern of Hg in small and large redfish could be linked to the difference in sample size,

which is much smaller for large redfish and thus, it is more difficult to detect spatial variations in Hg levels. In addition, larger fish at higher trophic levels exhibit a longer integration time for environmental signals and a slower response to the changes in Hg levels in the environment (Blanchfield et al., 2022).

The least squares mean of MeHg and THg, which reflects the relative availability of Hg to the redfish in the sampling areas, were not statistically different for both small and large redfish (Figure 6 & S3 annex I). These results suggest that the Hg availability to redfish among the three sampling areas was similar, and the spatial variation of the actual concentration of Hg in redfish was affected by the differences in biological and environmental variables of the sampling areas. In the St. Lawrence Gulf, small and large redfish commonly overwinter in the Cabot Strait (Campana et al., 2007). This migration behavior of redfish suggests possible habitat overlap around the Cabot Strait in winter, which could lead to a reduced disparity in Hg availability to the redfish collected from different areas of the SLEG in the summer.

In comparison to other species examined in this area (Lavoie et al., 2010) (Table S2, annex I), redfish in the present study tended to exhibit higher concentrations of MeHg. For example, the mean MeHg concentration in small redfish from the present study was 77.7 ± 4.04 ng/g dw (mean ± SE), which was higher than capelin (*Mallotus villosus*) (17.5 ± 1.3 ng/g dw), Atlantic herring (*Clupea harengus*) (69.2 ± 6.1 ng/g dw), American sandlance (*Ammodytes americanus*) (54.7 ± 20.1 ng/g dw), comparable with American plaice (*Hippoglossoides platessoides*) (77.4 ± 18.8 ng/g dw), but lower than witch flounder (*Glyptocephalus cynoglossus*) (100 ± 27 ng/g dw) that also live in deep environments from the SLEG (Lavoie et al., 2010). In addition, the concentration of MeHg in the muscle of large redfish (2050 ± 191 ng/g dw) was approximately 20 to 100 times higher than that found in the previously mentioned species from SLEG (Lavoie et al., 2010). These results are generally consistent with the previous research conducted in the Cantabrian Sea (North-East Atlantic) by Romero-Romero et al. (2022). These previous findings suggest that deep-sea fish species tend to accumulate higher levels of MeHg in their tissues compared to surface-dwelling species (Romero-Romero et al., 2022). This pattern can be attributed to the deep-

sea species occupying higher trophic positions and being long-lived (Romero-Romero et al., 2022).
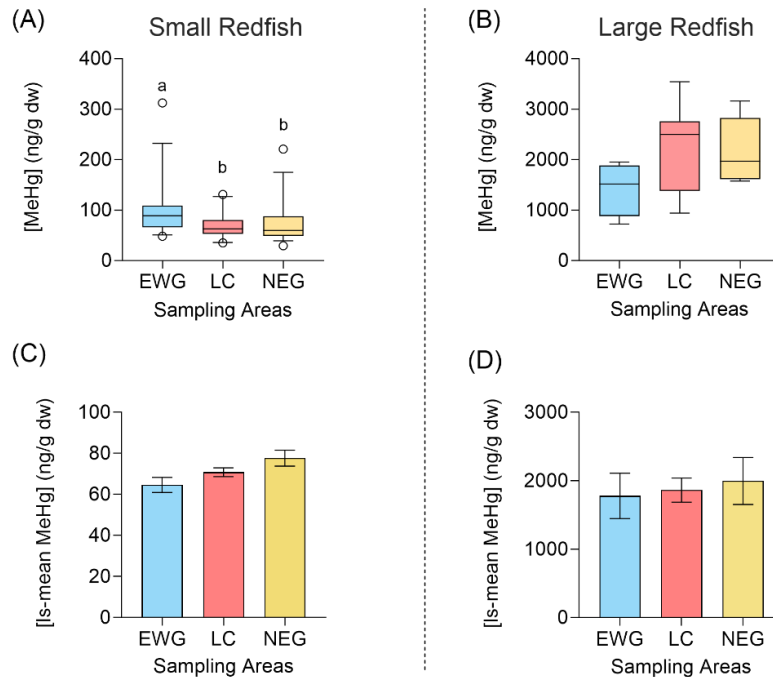
Figure 5: Spatial distribution of MeHg concentrations (dw) in (A) small and (B) large redfish, as well as least squares mean (ls-mean) MeHg concentrations ± standard error (dw) in (C) small and (D) large redfish from the three sampling areas.
EWG: Estuary-Western Gulf; LC: Laurentian Channel; NEG: Northeast Gulf. Boxplots are defined as follows: center line, median; boxplot edges, 25th and 75th percentiles of distribution; whiskers, 5th and 95th percentiles of the distribution. Black circles are outliers. Different letters in (A) indicate significant differences.

When comparing redfish from different sampling areas, the mean concentration of THg in large redfish from SLEG (480 ±30 ng/g ww; 38.4±1.1 cm; mean± SE) was higher than in similar size redfish from the Barents Sea (60±10 ng/g ww; 41.2±0.5 cm) and the Norwegian Sea (130 ± 10 ng/g ww; 34.4±0.2cm), but lower than in redfish from Skagerrak (670±12 ng/g ww; 29.2 ± 0.1cm) (Azad et al., 2019). Overall, the results suggest that the concentration of THg in redfish varies among different areas, with SLEG having an intermediate concentration for the large individuals compared to redfish from other global areas. Factors influencing THg accumulation patterns in redfish from different areas, such as proximity to pollution sources, atmospheric deposition, trophic transfer, water chemistry, and environmental variables, may warrant further research.

Table 3: Environmental and biological parameters (mean ± SD and (median) or range) of redfish, and the concentrations of THg (ng/g) and MeHg (ng/g) (mean ± SD). [1]Sample ratios of male (M) and female (F).

Group		Depth (m)	Oxygen (mM)	δ^{15}N (‰)	δ^{13}C (‰)	N (%)	Weight (g)	Length (cm)	Sex[1]	THg (ng/g)	MeHg (ng/g)
Small 17 – 30 cm	EWG	279±66 -293	87±38 -73	12.4±0.7 (12.5)	-20.2±0.6 (-20.2)	13.3±0.8 (13.4)	136 ±62 -121	21.9±2.9 (21.4)	M:46% F:54%	21.2±12.1 (ww) 102±63.5 (dw)	19.8±9.2 (ww) 95.2±48.9 (dw)
	LC	335±100 -343	133±47 -124	11.3±0.3 (11.4)	-20.7±0.3 (-20.7)	12.8±0.6 (12.9)	187 ±52 -186	24.3±2.0 (24.5)	M:29% F:71%	15.6±5.4 (ww) 72.7±26.1 (dw)	14.7±5.3 (ww) 68.8±25.3 (dw)
	NEG	242±52 -256	112±56 -90	11.4±0.5 (11.4)	-20.9±0.4 (-20.8)	12.8±0.8 (12.7)	174 ±33 -171	23.5±1.2 (23.6)	M:35% F:65%	16.6±8.3 (ww) 74.3±40.2 (dw)	16.0±7.6 (ww) 71.4±36.2 (dw)
Large ≥ 30 cm	EWG	310±40 -302	82±14 -81	14.9±0.4 (14.9)	-19.4±0.3 (-19.5)	13.6±0.7 (13.6)	950±631 -797	39.1±8.6 (37.6)	M:25% F:75%	366±151(ww) 1710±636(dw)	306±127 (ww) 1430±528 (dw)
	LC	421±37 -413	137±12 -139	14.9±0.4 (15.1)	-19.4±0.3 (-19.4)	13.9±0.8 (14.2)	786±265 -648	37.9±3.4 (36.3)	M:75% F:25%	526±170(ww) 2870±1080(dw)	417±135 (ww) 2280±871 (dw)
	NEG	269±56 -302	94±23 -88	14.4±0.7 (14.4)	-19.6±0.1 (-19.6)	14.2±0.4 (14.3)	809±191 -873	38.7±2.9 (39.5)	M:20% F:80%	451±94 (ww) 2560±694 (dw)	380±80 (ww) 2170±661 (dw)

1.5.2. Relationships between biological or environmental variables and Hg levels in redfish

1.5.2.1 Biological variables

$\delta^{15}N$ and $\delta^{13}C$. Positive correlations were found between $\delta^{15}N$ and $\delta^{13}C$ (all redfish: Spearman correlation coefficient r_s=0.64, p<0.0001; small redfish: r_s=0.40, p<0.0001; large redfish: r_s=0.66, p=0.0015) and large redfish showed greater $\delta^{15}N$ and $\delta^{13}C$ than small redfish (Figure S4 & S5, annex I). These results suggest that the larger redfish were at higher trophic levels and consuming more benthic prey, which is consistent with previously documented variations in the dietary content of redfish over their lifetimes (Brown-Vuillamin et al. 2022, 2023; Senay et al., 2021). Brown-Vuillemin et al. (2022, 2023) showed that the diet of redfish <30 cm (redfish samples collected between 2015 and 2019) was strongly dominated by zooplankton, while that of fish >30 cm was driven by shrimp and fish. Notably, the small redfish sampled from the Estuary-Western Gulf exhibited higher $\delta^{15}N$ and $\delta^{13}C$ signatures than those from the Laurentian Channel and Northeast Gulf (Figure S5, annex I), possibly attributable to elevated terrestrial input (e.g., wastewater effluent) from the coastal region of the estuary (Lavoie et al, 2010). In addition, the $\delta^{13}C$ signatures of small redfish (Figure S6, annex I) suggest that the individuals from Estuary-Western Gulf had a combination of pelagic and benthic diets, while Laurentian Channel and Northeast Gulf mainly had pelagic diet, which could reflect the reported differences in diet composition among these areas (Brown-Vuillemin et al., 2022).

Positive correlations were found between MeHg levels and $\delta^{15}N$ or $\delta^{13}C$ signatures in small redfish ($\delta^{15}N$: $r_s = 0.70$; $p < 0.0001$; $\delta^{13}C$: $r_s = 0.34$; $p = 0.0004$) (Figure S7, annex I). Conversely, no such correlation was observed for the large redfish (Figure S7, annex I). Similar results were found for THg, as illustrated in Figures S8, annex I. These results should be interpreted with caution because this study did not collect baseline species to standardize redfish $\delta^{15}N$ and $\delta^{13}C$ data. Future research can address this issue to better elucidate redfish trophic levels and the links between $\delta^{15}N$ or $\delta^{13}C$ and contaminants levels. Nonetheless, by dividing the small redfish into three sampling areas, we still observed positive correlations between $\delta^{15}N$ and MeHg or THg in each area (Figure S6, annex I), indicating the

accumulation of MeHg or THg in redfish varied with prey composition. In contrast, δ^{13}C was only positively correlated with MeHg or THg in the Estuary-Western Gulf (Figure S6, annex I), implying that feeding sources and habitat use may play more important roles in affecting the levels of Hg in redfish from Estuary-Western Gulf than the other two sampling areas.

These findings support previously reported positive relationships between MeHg and δ^{15}N or δ^{13}C in the SLEG food web, which includes a variety of invertebrates, fish, and seabirds (Lavoie et al., 2010). The data on small redfish closely follow the relationship with other species, including its potential preys (Figure S9, annex I) (Lavoie et al., 2010). However, the large redfish accumulated much more MeHg than those species (from SLEG food web) with similar δ^{15}N or δ^{13}C signatures (Figure S9, annex I) (Lavoie et al., 2010), indicating that factors other than δ^{15}N or δ^{13}C may be responsible for the large redfish high MeHg levels (e.g., age). One other important aspect for this species, is that the different redfish size groups reflect different cohorts. The food web may have changed a lot during the last 30 years (large *vs* small fish) and should be investigated further.

Size. When analyzing small and large redfish separately, no correlation was observed between MeHg or THg levels and fish weight or length (Figure S7 & S8, annex I). It is worth noting that there were weak negative relationships between size (length or weight) and δ^{15}N for small redfish from Laurentian Channel or δ^{13}C for small redfish from Estuary-Western Gulf (Figure S10, annex 1). This suggests that small redfish individuals, which consume prey from higher trophic levels (Laurentian Channel) and/or benthic species (Estuary-Western Gulf), tend to have smaller sizes. While these findings may appear contradictory to general expectations, it is important to consider that negative relationships between fish length and trophic level have been observed in many fish species from different regions (Burress et al., 2016; Keppeler et al., 2020). These relationships may be influenced by variations in diet composition and the sizes of digestive tracts of fish (Burress et al., 2016; Keppeler et al., 2020). However, limited information is available on the relationship between trophic level and size for deep-sea fish and further investigation is necessary.

Moisture, lipid, protein content and sex. Moisture and N%, an indicator of protein levels, exhibited a positive correlation (r_s=0.71, p<0.0001), whereas the lipid content present in the muscle of redfish demonstrated a negative association with these factors (moisture *vs.* lipid: r_s=-0.64, p<0.0001; N% *vs.* lipid: r_s=-0.58, p<0.0001). Given the negative relationship between protein and lipid in the muscle, the same quantity of dried muscle will exhibit a higher protein content if it has a lower lipid content, and vice versa.

The protein fraction of fish muscle is a well-known site for storing MeHg. This is attributed to the high affinity of MeHg for the thiol groups present in the amino acid cysteine, with which it forms stable complexes (Ajsuvakova et al., 2020; Nogara et al., 2019). Indeed, the present study found that MeHg concentrations were positively correlated with N% (small redfish: r_s=0.51, p<0.0001) and moisture (small redfish: r_s=0.47, p<0.0001; large redfish: r_s=0.53, p=0.015), (Figure S7, annex I). MeHg concentrations were negatively related to lipid content in small redfish (Figure S7, annex I). This is because a higher lipid content is associated with a lower protein fraction and, as a result, reduced MeHg bound to muscle. Similar results were found for THg, as presented in Figure S8, annex I. These results suggested that the presence of MeHg or THg in redfish muscle varies depending on the composition of the muscle.

The small redfish exhibited variations in muscle compositions across different sampling areas (Figure S11, annex I). Samples obtained from Estuary-Western Gulf display higher moisture and N% levels but lower lipid content (Figure S9, annex II). As a result, these differences in the muscle composition of redfish from distinct sampling area can influence the MeHg and THg levels. The present study's findings concerning the correlation between MeHg and protein in redfish align with prior observations for striped bass (*Morone saxatilis*) and northern pike (*Esox lucius*) (Charette et al., 2021). The toxicological implication is that the MeHg concentrations in redfish muscle may vary when the muscle composition changes with its physiological state (e.g., spawning) and/or environmental conditions (e.g., prey availability), which consequently affect its toxicity in fish. In addition, the present study found no discernible variations for the MeHg or THg levels between male (small: 18.2 ± 9.0 ng/g ww (mean ± SD) (median: 16.9 ng/g ww); large: 388 ± 133 ng/g ww

(median: 431 ng/g ww) and female redfish (small: 15.9 ± 6.7 ng/g ww (median: 13.5 ng/g ww); large: 372 ± 118 ng/g ww (median: 381 ng/g ww).

1.5.2.2 *Environmental variables*

Environmental variables differed among the three sampling areas (Figure S12, annex I) but had less impact on MeHg or THg levels in redfish than biological variables in the current study. Only water-dissolved oxygen and temperature had weak negative correlations with MeHg or THg concentrations (Figure S7&S8, annex I). The concentrations of MeHg and THg in redfish muscle samples did not correlate with water depth or salinity. Detailed discussions about environmental variables are presented in the following.

Oxygen. A weak negative correlation was observed between water dissolved oxygen levels and MeHg (r_s= -0.25; p = 0.01) or THg (r_s= -0.23; p = 0.02) concentrations for small redfish (Figure S7 & S8, annex I). The reason for this could be that MeHg production and solubility are typically negatively related to dissolved oxygen levels (Cuvin-Aralar, 1990; Regnell et al., 1996). Consequently, lower dissolved oxygen concentration results in higher aqueous concentrations of MeHg in the water, which can then be absorbed by surrounding aquatic organisms, including fish. Additionally, a reduction in dissolved oxygen levels could lead to a higher uptake of water by fish and consequently increase the accumulation of MeHg in fish (Wang et al., 2011). THg in small redfish also follow a weak inverse relationship with the dissolved oxygen in water (Figure S8, annex I). For different sampling areas, Estuary-Western Gulf showed lower dissolved oxygen levels compared to Laurentian Channel and Northeast Gulf (Figure S12, annex I). This lower oxygen environment could potentially contribute to the methylation of Hg (Cuvin-Aralar, 1990; Regnell et al., 1996) and higher MeHg levels (raw concentration) in small redfish from Estuary-Western Gulf, as discussed in 3.1 in the main text.

Temperature. Weak negative association was found between MeHg or THg levels in small redfish and water temperature (MeHg: r_s= -0.25; p =0.017; THg: r_s= -0.27; p =0.0008) (Figure S7&S8, annex I). Northeast Gulf showed higher water temperature compared to Estuary-Western Gulf and Laurentian Channel (Figure S12, annex I). Multiple factors could

contribute to the net impact of temperature on MeHg or THg levels in redfish. At warmer water temperatures, fish may experience higher metabolic rates, resulting in increased feeding and respiration (Dijkstra et al., 2013; Laske et al., 2023). This can lead to faster growth rates, which may dilute the concentration of Hg in the fish, resulting in a lower overall Hg concentration (Simoneau et al., 2005; Ward et al., 2010).

Depth and Salinity. The water column (same as the depth at which fish were caught) at sampling sites in the Laurentian Channel was deeper than the other two sampling areas (Figure S12, annex I). Despite the observation that SLEG fish species residing in deeper waters tend to display elevated levels of MeHg accumulation in their tissues (as elaborated in section 3.1 of the main text) (Lavoie et al., 2010), no correlation between MeHg (or THg) concentrations and the depth of redfish collection was established ($p>0.05$). Therefore, the influence of water depth on MeHg (or THg) accumulation in fish may be more prominent at the inter-species level, as opposed to within a single species. To elucidate the factors influencing the exposure and bioaccumulation of different forms of Hg in deep-sea species, it is necessary to conduct additional research on the speciation of Hg at water depths >200 m in the SLEG as well as conduct research on redfish diet. Moreover, Laurentian Channel showed higher water salinity than the other two sampling areas (Figure S12, annex I), and no correlation was found between MeHg or THg levels in the redfish muscle and water salinity of the sampling site. The hypothesis that salinity affects the moisture content in redfish muscle was tested by conducting a correlation analysis between these two variables for small redfish. However, the analysis results ($r_s=0.03$, $p=0.78$) failed to support this hypothesis.

1.5.2.2 Multiple linear regression

The result shows that fish length, moisture, $\delta^{15}N$ and N% are significant predictors of MeHg concentrations (dw) in the redfish (small and large together), while length, moisture, $\delta^{15}N$ are significant factors for predicting THg levels (dw) in redfish (small and large together). When considering only the small redfish group, length, moisture, $\delta^{15}N$ are significant predictors for both MeHg and THg. For large redfish, only muscle moisture was determined as the significant predictor, which is not different from the single linear regression results.

The multiple linear regression parameters are shown in the Table 5. Overall, the model fits the data very well (all redfish: R^2=0.93 for MeHg and THg; small redfish: R^2=0.59 for MeHg and R^2=0.60 for THg), indicating that the included independent variables explain a large portion of the variance in MeHg or THg concentrations (dw) in redfish. Figure S13, annex I shows the relationship between the actual measured concentrations of MeHg or THg and the predicted values using the model. It illustrates the good agreement between the observed Hg concentration and the values estimated by the model.

Table 4: Multiple linear regression analysis of the concentrations of log10 [MeHg] (dw) and log10 [THg] (dw) in redfish muscle from fish length, moisture, δ15N and N%.
NA: not applicable. Results for large fish are not shown because only moisture is a significant predictor, and the simple linear regression results are shown in Figure S7&S8, annex I.

			MeHg			
	Variable	Estimate β	Standard Error	t	p	VIF
	Intercept	-4.26	0.58	7.36	<0.0001	NA
	Length	0.004	0.0003	11.78	<0.0001	2.078
All Fish	Moisture	2.69	0.88	3.04	0.003	1.628
	$\delta^{15}N$	0.21	0.02	11.36	<0.0001	2.849
	N%	0.05	0.02	2.36	0.02	1.709
	Intercept	-1.84	0.57	3.24	0.002	NA
Small	Length	0.002	0.0005	3.70	0.0004	1.089
Redfish	Moisture	1.57	0.72	2.19	0.03	1.133
	$\delta^{15}N$	0.17	0.02	9.99	<0.0001	1.193
			THg			
	Variable	Estimate β	Standard Error	t	p	VIF
	Intercept	-4.53	0.59	7.63	<0.0001	NA
All Fish	Length	0.004	0.0003	12.1	<0.0001	2.002
	Moisture	3.61	0.84	4.29	<0.0001	1.371
	$\delta^{15}N$	0.23	0.02	12.9	<0.0001	2.411
	Intercept	-2.16	0.59	3.69	0.0004	NA
Small	Length	0.002	0.0005	4.42	<0.0001	1.089
Redfish	Moisture	1.78	0.74	2.42	0.02	1.133
	$\delta^{15}N$	0.18	0.02	9.98	<0.0001	1.193

1.5.3 Human health risk assessment

1.5.3.1 HQs of different scenarios

To assess the potential health risks associated with consuming redfish following the reopening of the fishery, this study estimated the EWI and HQ of different scenarios of human exposure to MeHg via redfish consumption, as it represents the common form of Hg exposure (Hellberg et al., 2012). The EWI and HQ for each scenario is presented in Table 6. The EWI for MeHg in scenario B2 (adults of the general population: 1.78; women of childbearing age: 1.98 µg/kg bw/week) for both groups exceeds the reference dose of United States Environmental Protection Agency (US EPA) (2001) (0.1 µg/kg bw/day or 0.7 µg/kg bw/week), the Minimum Risk Level recommended by the Agency for Toxic Substances and Disease Registry (2023) (0.1 µg/kg bw/day or 0.7 µg/kg bw/week), and Provisional Tolerable Weekly Intake (1.6 µg/kg bw/week) recommended by FAO/WHO (FAO/WHO, 2010). This indicates that in certain worst-case scenarios, the consumption of redfish muscle could result in exposure to MeHg that exceeds some of the recommended threshold dose for both the general population and women of childbearing age.

HQ for all scenarios ranges between 0.003 and 0.56, except for scenario B2 for women of childbearing age where it is 1.24 (extreme scenario) (Table 6). Overall, these findings suggest that adults from the general population who consume redfish will be exposed to MeHg at levels that are considered safe and will not experience known non-cancerogenic related adverse health risks (HQ between 0.003 and 0.56). However, women of childbearing age who consume the large redfish that contain the high concentrations (95 percentile) of MeHg may have moderate risks related to MeHg exposure (HQ=1.24).

1.5.3.2 The maximum allowable fish consumption

To better assess and define potential risks to human health, exposure assessment data must be combined with an understanding of the amount of fish that can be consumed safely over a given time period without adverse effects. Using the MeHg tolerable intake limit of 0.46 µg/kg bw/day (3.2 µg/kg bw/week) set by the FAO/WHO (FAO/WHO, 2010), and

assuming an individual weighing 74.2 kg, the maximum allowable consumption rates of SLEG small redfish range from 564 to 4,890 g/day (3,950-33,500 g/week) (ww), while for large redfish, the rates are between 59 and 235 g/day (412-1,650 g/week) (ww) depending on the MeHg levels (minimum to maximum concentrations) present in the muscle tissue. For women of childbearing age (assuming the weight is 66.8kg) with lower tolerable intake limit of 0.23 µg/kg bw/day (1.6 µg/kg/week), the maximum allowable consumption rates of SLEG small and large redfish are 254 to 2,160 g/day (1,780-15,100 g/week) and 26 to 106 g/day (185-741 g/week), respectively.

Table 5: Estimated weekly intake (EWI) based on fish consumption and the estimated hazard quotient (HQ) in 4 different scenarios.
Scenario A1: fish consumption is 0.05 kg/week; 50th percentile of observed MeHg concentrations in all redfish muscle (16.4 ng/g ww). Scenario B2: fish consumption is 0.28 kg/week; 95th percentile of observed MeHg concentrations in all redfish muscle (473 ng/g ww). Average weight used for calculation is 74.2 kg for general population (AGP) and 66.8 kg for childbearing women (WCA). HQ calculation is based on RfD of 3.2 µg/kg/week for AGP and 1.6 µg/kg/week for WCA. * Worst case scenario.

	Scenario A1		Scenario A2		Scenario B1		Scenario B2*	
	Average Consumers				High Consumers			
	50th of MeHg level		95th of MeHg level		50th of MeHg level		95th of MeHg level	
Group	AGP	WCA	AGP	WCA	AGP	WCA	AGP	WCA
EWI (µg/kg/week)	0.01	0.01	0.32	0.35	0.06	0.07	1.78	1.98
HQ	0.003	0.006	0.10	0.22	0.02	0.04	0.56	1.24

1.6 CONCLUSION

In the SLEG, redfish is an endangered deep-sea species under a fishing moratorium. But the rapid biomass increase of redfish in recent years may result in the resumption of commercial fishing shortly, which raises the concern of human exposure to Hg via redfish consumption. The results of this study reveal that MeHg and THg levels are approximately 20-30 times higher in large redfish (>30 cm and >13 years old) than in small redfish. Large

redfish from SLEG had an intermediate level of Hg compared with similar-sized redfish from Europe. Small redfish located in the Estuary-Western Gulf showed higher accumulation of MeHg and THg compared to individuals of the same size distributed in the Laurentian Channel and Northeast Gulf. In large redfish, no significant spatial variations in MeHg and THg were found. The least squares mean of MeHg and THg suggest the relative availability of Hg to the redfish from three sampling areas were not statistically different. According to the modelling results, fish length, muscle moisture, δ15N, and N% were significant predictors of MeHg concentrations (dw) in redfish muscle. The results of the human health risk assessment indicate that MeHg in redfish muscle is unlikely to have a negative impact on the general population of average fish consumers. However, women of childbearing age who are high consumers of fish may experience moderate risk if they consume highly contaminated large redfish, although this is an extreme scenario that is unlikely to occur. This study establishes a baseline for monitoring MeHg and THg in deep-sea fish for the SLEG. However, the limited sample size of large redfish caught in this study and lack of stable isotope data from baseline species may limit the spatial comparison and interpretation of how biological and environmental variables may affect Hg accumulation in redfish. Further investigation is needed to elucidate better the cause-effect relationships between biological/environmental parameters and the concentrations of MeHg or THg in deep-sea species to improve the understanding of their fate and impacts in these less studied environments.

CHAPITRE 2 ORGANIC UV ABSORBENTS IN THE DEEPWATER REDFISH (*SEBASTES MENTELLA*) FROM THE ST. LAWRENCE ESTUARY AND GULF: DISTRIBUTION AND HUMAN HEALTH RISK ASSESSMENT

CONTRIBUTION À LA RECHERCHE ET PRÉSENTATION

Plusieurs personnes ont collaboré dans la publication de cet article dans le journal 'Science of The Total Environment'. En tant que première auteure, j'ai appliqué les techniques pour mesurer les absorbeurs d'UV dans le muscle de sébaste. Ces techniques ont permis de déterminer les concentrations de chaque contaminant et de vérifier leur présence dans le sébaste du Saint-Laurent. Afin d'offrir les résultats et leur interprétation, qui seront fournis dans les sections suivantes, j'ai également procédé au traitement et à l'analyse des échantillons. J'ai également rédigé la première version de l'article et traiter les commentaires des co-auteurs. **Mathieu Babin** s'est occupé de la méthodologie, notamment les analyses des isotopes stables et le soutien technique pour les analyses des absorbants UV. **Geneviève Parent** du Ministère des Pêches et Océans Canada (MPO) a effectué les analyses génomiques pour l'identification de l'espèce de cible (*Sebastes mentella*) ; **Dominic E. Ponton** et **Marc Amyot** de l'Université de Montréal (UdeM) ont contribué à l'investigation, la révision et l'édition de l'article. **Caroline Senay** du MPO a fourni les données biologiques pour les spécimens étudiés et a contribué à la révision et l'édition de l'article. Tous les co-auteurs ont participé à la révision des différentes présentations qui ont été effectuées pour ce projet, notamment aux colloques Ecotoq 2022, SETAC 2022, Québec Océan 2023 et Chapitre Saint-Laurent 2023. **Dominique Robert,** en tant que codirecteur, a permis de fournir les échantillons de sébaste, il a effectué aussi la révision complète de tous les documents et présentations produits tout au long de ce programme de maîtrise. La réussite de ce projet a été grandement facilitée par la direction de **Zhe Lu**. Il a activement contribué à la mise en place des techniques analytiques, à l'interprétation des résultats et à l'examen des résultats du projet.

Auteurs : Fella Moualek, Mathieu Babin, Geneviève J. Parent, Dominic E. Ponton [c], Caroline Senay [b], Marc Amyot [c], Dominique Robert, Zhe Lu

2.1 RÉSUMÉ

Les absorbants UV (UVA), tels que les filtres UV organiques (UVF) et les stabilisateurs UV à base de benzotriazole (BZT-UV), sont utilisés dans une large gamme de produits de consommation et industriels et sont des contaminants dont la présence dans l'environnement est de plus en plus préoccupante. Toutefois, leur présence et leur devenir dans les environnements d'eaux profondes sont mal compris. Cette étude a examiné l'occurrence et la distribution de cinq UVF et de dix BZT-UV dans le muscle (n=127) de sébastes (*Sebastes mentella*) prélevés en 2019 dans l'estuaire et le golfe du Saint-Laurent (Canada) afin de mieux comprendre la bioaccumulation de ces contaminants chez les poissons d'eau profonde. Les petits sébastes (<30 cm) avaient tendance à accumuler plus d'UVA par rapport à leur poids que les spécimens plus grands (>30 cm). L'UVF 2-hydroxy-4-méthoxybenzophénone (BP-3) a été l'UVA le plus fréquemment détecté (présente dans 34% des échantillons), avec des concentrations atteignant 413 ng/g (poids sec). Bien que les effets physiologiques du BP-3 sur le sébaste soient inconnus, environ 6 % des muscles de sébaste contenaient des concentrations de BP-3 supérieures à 25 ng/g (poids humide), un niveau connu pour être associé à des effets néfastes sur le métabolisme du poisson zèbre (*Danio rerio*). D'après les données isotopiques δ ^{15}N et δ ^{13}C, les sébastes consomment plus de proies pélagiques, et les individus de niveau trophique inférieur ont un contenu lipidique plus élevé et accumulent plus de BP-3 dans leurs muscles. Cette constatation pourrait aider à expliquer pourquoi les petits sébastes du Nord-Est du Golfe avaient des niveaux de BP-3 plus élevés que les petits sébastes de l'estuaire, du golfe occidental et du chenal laurentien du SLEG. Quatre BZT-UV ont été détectés dans le muscle du sébaste, mais la fréquence de détection était inférieure à 30 %. Le quotient de danger estimé pour ces contaminants était inférieur à $2,3\times10^{-2}$ pour les populations canadiennes en général, ce qui indique qu'il est peu probable qu'ils posent des risques pour la santé humaine suite à la consommation de sébaste. Les facteurs influençant la bioaccumulation des UVA chez le sébaste, ainsi que les effets que les UVA peuvent avoir sur les espèces d'eau profonde, devraient faire l'objet de recherches plus approfondies.

Mots-clés :

Benzophénone-3, filtres UV, stabilisateurs UV à base de benzotriazole, eaux profondes, bioaccumulation, évaluation des risques pour la santé humaine.
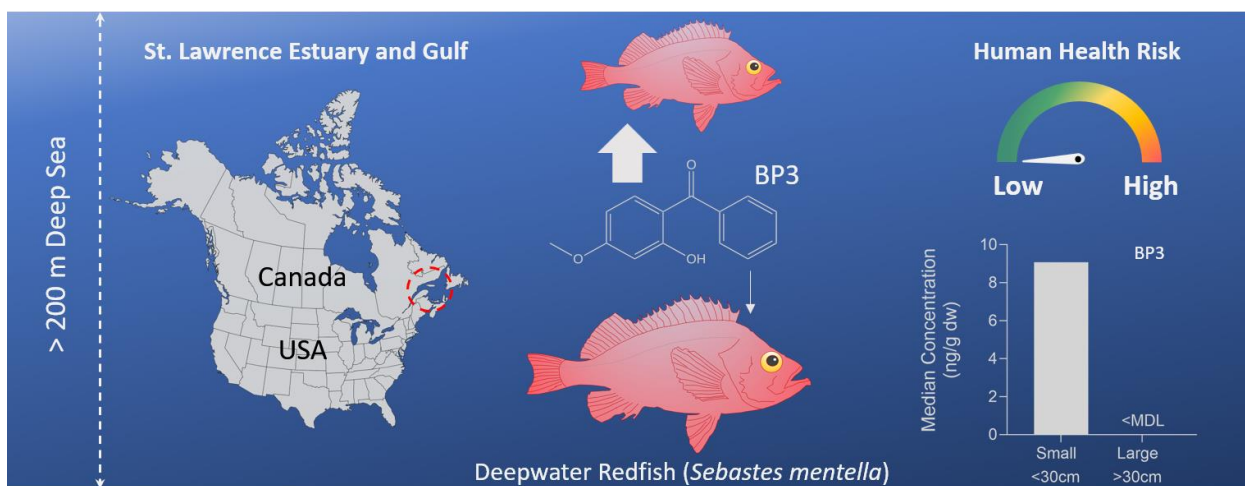
Figure 6: Résumé graphique.

2.3 INTRODUCTION

Organic UV absorbents (UVAs), including UV filters (UVFs) and benzotriazole UV stabilizers (BZT-UVs), are contaminants of emerging concern. They are widely used in personal care products (e.g., sunscreens), cosmetics, plastics, paints, automobile polymeric components, varnishes, and many others to protect human skin from sunburn or prevent industrial and commercial products from sunlight induced degradation and color change of materials (Mao et al., 2019; Nakata et al., 2009).

These compounds may enter the environment during the production (Cantwell et al., 2015), usage (e.g., sunscreen may be directly released to the water during watersports and recreation activities) (Giokas et al., 2007), and waste disposal (e.g., wastewater) (Ruan et al., 2012; Lu et al., 2017b). Some of them are known to have natural sources (e.g., benzophenones in mango and muscat grape) (Suzuki et al., 2005). UVAs have been widely detected in environmental matrices such as water (Castilloux et al., 2022), sediment (Peng et al., 2017b), biota (Peng et al., 2017a), and human tissues including milk (Kim et al., 2019) and placenta (Valle-Sistac et al., 2016). Exposure to UVAs may lead to various adverse effects, such as the disruption of reproductive behavior (Ghazipura et al., 2017; Zhuang et al., 2017), the activation of aryl hydrocarbon receptor-mediated toxicities (Nagayoshi et al., 2015), the perturbation of the thyroid system (Fent et al., 2014; Liang et al., 2017), in fish and mammals. Therefore, UVAs have sparked increasing environmental concern. Recently, 2-(2H-benzotriazol-2-yl)-4,6-di-*tert*-pentylphenol (UV328), one of the BZT-UVs, was recommended to be phased out by 2026 and globally banned by 2044

by the Stockholm Convention on Persistent Organic Pollutants (POPs) (United Nations Environment Programme, 2023).

However, the occurrence and fate of UVAs in the deep-sea (>200m) environment are largely unknown, which impedes the risk assessments of these contaminants. Deep-sea environment is considered as the final reservoir of POPs and many other contaminants in the ocean because numerous contaminants tend to bind with particles and transport to the deep-sea via marine snow effects (Froescheis et al., 2000). Deep-sea fish species are known to accumulate more POPs than the species living in the upper water layer (Froescheis et al., 2000). But this pattern is based on the very slow degradation/biotransformation of POPs, low water solubility and high sorption of POPs with particles, which may not be the case for many UVAs or other emerging contaminants.

In the St. Lawrence Estuary and Gulf (SLEG) (Canada), deepwater redfish (*Sebastes mentella*) stock, which has been considered as endangered by the Committee on the Status of Endangered Wildlife in Canada (COSEWIC) in 2010 (COSEWIC, 2010), is rapidly recovering after a fishing moratorium of more than 25 years, following a series of strong year classes in 2011, 2012 and 2013. Redfish primarily feed on copepods, shrimp, and fish (e.g., capelin (*Mallotus villosus*)) (Brown-Vuillemin et al., 2023; Senay et al., 2021;2023). They are bentho-pelagic fish and older fish tend to live in deeper waters than younger fish (Planque et al., 2013; Senay et al., 2021). The larvae stay in the surface water, the juveniles gradually migrate to deeper areas as they grow, and the adults can be found in the seabed as deep as 500 m in the SLEG (Senay et al., 2021; 2023). Even though redfish exploitation is still prohibited, it is anticipated that the rapid increase in reproductive biomass will soon lead to the reinstatement of commercial fishing (Senay et al., 2021). Thus, it is essential to monitor the levels of different types of contaminants in the redfish to support the next large-scale fishery in the region and protect human health. In addition, redfish have previously been identified as one of the main potential vectors of contaminants to top predators (e.g., marine mammals) in the Arctic (Tomy et al., 2004), so the current dramatic population increase may have a significant impact on contaminant dynamics in the SLEG food web. To this end, this study aims to (1) investigate the occurrence and distribution of UVAs in the deepwater redfish from the SLEG to establish a baseline for future monitoring and (2) estimate human daily intake and conduct a preliminary human health risk assessment whenever possible.

2.4 MATERIALS AND METHODS

2.4.1 Sampling

Genetically identified deepwater redfish samples (*n*=127 total; small redfish (<30cm): *n*=106; large redfish (>30cm): *n*=21) were collected by bottom trawling along the SLEG (Figure 7) between August and September 2019, during the annual research survey of the Fisheries and Oceans Canada. For each sampling station, small and large redfish were caught during the same bottom trawling, and the depth of the net varied within about 20 m. Information on species identification can be found in the Supplementary Data and details are available in Senay et al. (2023). In addition, 13 samples (small *n*=10; large *n*=3) were analyzed but their locations were not recorded. The whole fish samples were wrapped in aluminum foil and sealed in Ziplock plastic bags before being transferred to the laboratory on ice. The biological and environmental variables of redfish samples are summarized in Table S1, annex II (Moualek et al., 2023). The dorsal muscles of redfish were carefully isolated using a pre-cleaned (with acetone) metallic scalpel. The weights of the samples were measured before and after freeze-drying to calculate the moisture content. The freeze-dried fish muscle samples were ground to powder with a glass mortar and pestle and stored at - 20 °C in amber glass jars until further analysis.
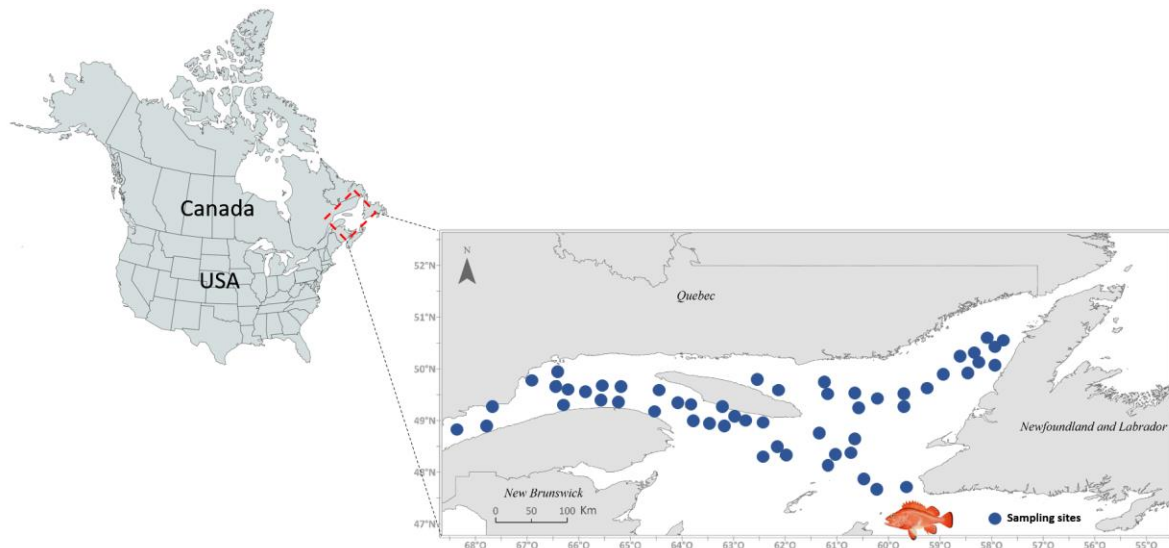

Figure 7: Redfish sampling locations in the St. Lawrence Estuary and Gulf.

Table 6: Biological (mean ± standard deviation) of small and large deepwater redfish samples and environmental variables from the Estuary- Western Gulf (EWG), Laurentian Channel (LC) and Northeast Gulf (NEG) of the St. Lawrence Estuary and Gulf.
(Moualek et al., 2023). NA: data not available. The methods of the measurement of environmental variables can be found in Bourdages et al (2022).

Group Region		Length (mm)	Weight (g)	Lipid content (%)	Moisture (%)	Depth (m)	Temperature (°C)	Oxygen (Micromoles)	Salinity (psu)	$\delta^{15}N$ (‰)	$\delta^{13}C$ (‰)
Small	EWG	219±28	136±61	11.0±5.1	79±1	279±65	5.6±1.2	87±38	34.5±0.5	12.4±0.7	-20.2±0.6
	LC	242±19	186±51	13.4±5.9	79±1	332±113	5.7±1.5	140±57	34.6±0.8	11.3±0.3	-20.7±0.3
	NEG	235±12	174±33	17.5±7.8	77±2	242±51	6.3±0.6	111±55	34.4±0.6	11.5±0.7	-20.9±0.4
Large	EWG	391±86	950±631	5.7±4.0	79±2	310±40	6.3±0.1	82±14	34.7±0.1	14.9±0.4	-19.4±0.3
	LC	379±35	786±265	6.7±10.2	81±2	421±37	6.1±0.1	137±12	35.0±0.02	14.9±0.4	-19.4±0.3
	NEG	387±29	809±191	1.7±1.4	82±2	269±56	6.4±0.2	94±23	34.5±0.1	14.4±0.7	-19.6±0.1
Samples from unknown locations		NA	NA	12.2±7.0	79±2	NA	NA	NA	NA	12.9±1.6	-20.2±0.8

2.4.2 Chemicals and regents

The name and chemical-physical properties of the target UVAs are shown in Table S2, annex II and the structures are presented in Figure S1, annex II. Analytical standards of 2-hydroxy-4-methoxybenzophenone (BP3), 4-methylbenzylidene camphor (4MBC), 2-(2H-benzotriazol-2-yl)-4,6-bis(1-methyl-1-phenylethyl)phenol (UV234), 2-benzotriazole-2-yl-4,6-di-*tert*-butylphenol (UV320), 2,4-di-*tert*-butyl-6-(5-chloro-2H-benzotriazol-2-yl) phenol (UV327), UV328, 2-(2H-benzotriazol-2-yl)-4-(1,1,3,3-tetramethyl butyl)phenol (UV329), 2-(2H-benzotriazol-2-yl)-4-(*tert*-butyl)-6-(*sec*-butyl)phenol (UV350), diphenylamine-d_{10}, and benzophenone (BP)-d_{10} were purchased from Toronto Research Chemicals (Toronto, ON, Canada). The standards of ethylhexyl methoxycinnamate (EHMC), 2-ethylhexyl salicylate (EHS), 2-ethylhexyl-2-cyano-3,3-diphenylacrylate (OC), 2-(2H-benzotriazol-2-yl)-p-cresol (UVP), 2-[3-(2H-benzotriazol-2-yl)-4-hydroxyphenyl]ethyl methacrylate (UV090), 2-(2H-benzotriazol-2-yl)-4-methyl-6-(2-propenyl)phenol (UV9), and 2-*tert*-butyl-6-(5-chloro-2H-benzotriazol-2-yl)-4-methylphenol (UV326) were purchased from Sigma-Aldrich (Oakville, ON, Canada). UV328-d_4 was obtained from ASCA GmbH (Berlin, Germany). HPLC grade acetonitrile, *n*-hexane, dichloromethane, and

acetone were purchased from Sigma Aldrich (Oakville, ON, Canada). The Quick, Easy, Cheap, Effective, Rugged, and Safe (QuEChERS) dispersive solid phase extraction (SPE) kits "QuEChERS Enhanced Matrix Removal – Lipid" (EMR) and the polish tubes of NaCl/MgSO$_4$ were purchased from Agilent Technologies Canada (Mississauga, ON, Canada).

2.4.3 Sample preparation

A stringent glassware cleaning method was followed, including rinsing with distilled water, cleaning with laboratory detergent, deionized water rinsing, oven drying, and a final rinse with acetone right before use. Redfish muscle sample (0.5g dry weight (dw)) was transferred to a solvent cleaned glass test tube. Isotope labeled surrogate standards (20 ng of BP-d$_{10}$ and UV328-d$_4$) were spiked into each sample before extraction. Sample preparation method was adapted from Fujita et al. (2022) with some modifications. Briefly, the sample was vortexed with 4 mL of acetonitrile for 1 minute, followed by 5 minutes of sonication and 5 minutes of centrifugation (1,167 ´g). The extraction was repeated 3 times, and the extracts were combined. The solvent extract was concentrated to 5 mL under a gentle stream of N$_2$. This extract was cleaned by EMR kit (Agilent, Mississauga, Canada) and dried with salts. The EMR sorbents and salts (NaCl and MgSO$_4$) were transferred to separate glass tubes respectively before use. First, the concentrated extract was added to the EMR tube, followed by 1 minute of vortexing, 1 minute of up and down shaking, and 5 minutes of centrifugation (1,167 ´g). Then the supernatant was transferred to the salts tube and treated by 30 seconds of vortexing, 1 minute of up and down shaking, and 5 minutes of centrifugation (1,167 ´g). The supernatant was finally transferred to a glass centrifuge tube and concentrated to dryness using a gentle stream of N$_2$. The sample was reconstituted in 0.5 mL of hexane for instrument analysis. Diphenylamine-d$_{10}$ (20 ng) was added to the sample as internal standard before instrumental analysis. A gas chromatography mass spectrometer (GC-MS) (Trace ultra GC coupled with an PolarisQ MS) (Thermo Fisher Scientific Inc., Waltham, USA) was used for sample analysis based on published method (Castilloux et al., 2022). The GC-MS methods and experimental parameters are shown in Table S3, annex II.

2.4.3.1 Lipid weight and stable isotope analyses

Redfish muscle sample (0.5 g, dw) was mixed with 5 mL of hexane/dichloromethane (1/1, v/v) and subjected to a 30 seconds vortex to determine extractable lipid content. This was followed

by 5 minutes of sonication and 5 minutes of centrifugation at 1,167 ´g. The resulting supernatant was transferred to a pre-weighted glass tube and this extraction process was repeated three times. The combined extract was then dried using a gentle stream of N2 to obtain the extractable lipid weight gravimetrically.

Using lyophilized muscle, samples from individual redfish were analyzed for stable isotopes of nitrogen and carbon in accordance with the procedure published by Glaz et al. (2014), using a DeltaPlus XP mass spectrometer (Thermo Fisher Scientific Inc., Waltham, USA) in Countinuous-flow Isotope Ratio Mass Spectrometry mode (CF-IRMS) with a Costech Analytical model 4010 Elemental Analyzer (Costech Analytical, Valencia, USA). Repeatability was tested for three standards (Caffeine (16 measurements), Nannochloropsis (12 measurements) and Mueller Hinton Broth (12 measurements) and the standard deviation (SD) was 0.17‰ and 0.13‰ for δ13C and δ15N, respectively. For redfish, one sample was measured six times and the SD was 0.06‰ for δ13C and 0.07‰ for δ15N.

3.4.4 Quality control

Glass materials were used in the experiment to prevent the samples contact with plastics. The tubes, syringes, and vessels used during the experiment were all pre-cleaned using solvents. Personnel refrained from using personal care products during the experiments to avoid contamination. The method detection limit (MDL) was determined following the United States Environmental Protection Agency (US EPA)'s guidelines (US EPA, 2016) based on seven samples (target contaminants were not detected in these samples) spiked with 5 ng of each compound in 0.5 g sample. The MDL was calculated using the SD of the final detected concentration (3.14 × SD) (US EPA, 2016). For the compound (BP3) detected in some blanks, MDL was determined using the highest level in the procedure blanks for analytes (US EPA, 2016) and subtracted from the samples. For every 9-11 samples, three procedural blanks and two spike-recovery samples (spike levels: 20 ng and 50 ng) were analyzed. For every five samples, one standard (20 ng/mL) and two *n*-hexane blanks were analyzed by the GC-MS as controls. Repeatability for real samples was determined by analyzing 10% of samples twice and the deviation from the mean value of two analytical results was within 11%. Calibration curves included standards with eight different concentrations (1, 2, 5, 10, 20, 50, 100, and 150 ng/mL). Target contaminants having concentrations beyond the calibration curve's concentration range were diluted and reanalyzed.

The parameters for method performance (MDLs and recoveries) are presented in Table S4, annex II.

2.4.4 Data analysis

Data were analyzed using GraphPad Prism 9.5 (La Jolla, CA, USA) and R (v2022.07.2). The robust regression on order (ROS) method in the NDexpo (https://expostats.ca) was used to estimate descriptive statistics (data <MDL were estimated and used for descriptive statistics) for target contaminants with censored values <80 % (Helsel, 2012). The maximum likelihood method in R (v2022.07.2; clikcorr package, v1.0) (Li et al., 2018), a method for testing correlations including censored data, was used to analyze the associations between log_{10}-transformed BP3 concentrations and each biological/environmental variable for redfish. The 13 samples without sampling site information were used for the correlation analysis between BP3 and δ^{13}C, δ^{15}N, lipid content in muscle, and moisture content in fish muscle. The correlation analysis was not conducted for other UVAs due to the low detection frequency (<30%). The cencorreg function in the Data Analysis for Censored Environmental Data (NADA2) package (v1.1.3) in R was used to compute regression models between log_{10}-transformed BP3 and various explanatory variables (δ^{13}C, δ^{15}N, water salinity, dissolved oxygen, water temperature, water depth, lipid content in muscle, moisture content in fish muscle, fish weight, and fish length) (Helsel, 2012). The 13 samples without sampling site information were not used for the regression analysis. Age was not included in the modeling since there is presently no good method for measuring redfish age and age modeling based on size data has huge uncertainty once the fish cease growing. Concentrations are reported on dw basis and not lipid corrected because no correlation was found in this study between target contaminant concentrations (dw) and the extractable lipid content of redfish (e.g., BP3: likelihood r = 0.18, *p* = 0.15) (Hebert and Keenleyside, 1995). Wet weight (ww) based concentrations are reported in some cases to facilitate comparisons with literature and used for human health risk assessment. The significance level was set as p≤0.05.

2.5 RESULTS AND DISCUSSION

2.5.1 Concentrations of UVAs in redfish muscle

The recovery for target UVAs ranged from 70±15% to 94±34% (mean±SD) and 61±16% to 95±20% for the spike levels at 20 ng and 50 ng, respectively. The concentrations of detectable

target UVAs in redfish samples are summarized in Table 8 and the spatial distribution is illustrated in Figure 9. One UVF (BP3) and four BZT-UVs (UV350, UV234, UV328, and UV090) were detected in the muscle of redfish. Target UVAs were much more frequently detected in small redfish compared to large redfish (Table 9). In small redfish, BP3 and UV350 were the predominant target UVAs, with an average contribution of 53% and 33% respectively to the total detected UVAs. Overall, the detection frequency was low (<50% for each compound) for target UVAs in the SLEG redfish. However, the occurrence of UVAs in redfish muscle indicated that deep-sea biota could accumulate these contaminants.

Table 8: Concentration (median and range, ng/g, dw) of UVFs and BZT-UVs in the muscle of deepwater redfish from SLEG. DF: detection frequency; NA: median concentration was not estimated due to the detection frequency <20%.

UVAs		Small Redfish (*n*=106)			Large Redfish (*n*=21)		
		DF %	Median	Range	DF %	Median	Range
UVFs	BP-3	41	9.07	<MDL -413	0	NA	<MDL
BZT-UVs	UV350	30	7.24	<MDL-148	5	NA	<MDL -26.1
	UV090	10	NA	<MDL-35.7	0	NA	<MDL
	UV328	5	NA	<MDL-12.8	0	NA	<MDL
	UV234	13	NA	<MDL-244	0	NA	<MDL

The estimated log K_{ow} for the target UVAs ranges from 3 to 8 (Castilloux et al., 2022), implying potential bioaccumulation of these contaminants. However, their field-based bioaccumulation factors in the fish from the St. Lawrence River in Canada (upstream of SLEG) were lower than previously modeled results (Castilloux et al., 2022), possibly due to faster biotransformation in fish than expected (Zhang et al., 2021). In addition, the primary tissues that accumulate UVAs differ between species. Most investigated fish species, except lake sturgeon (*Acipenser fulvescens*) (higher levels in muscle), accumulate more UVAs in the liver (Lu et al., 2017a; Tang et al., 2019; Castilloux et al., 2022), whereas beluga whales (*Delphinapterus leucas*) accumulate UVAs in the blubber (Blouin et al., 2022). These factors may be related to the low detection of UVAs in the redfish muscle. Moreover, to elucidate the factors influencing the bioaccumulation of UVAs in deep-sea species, it is necessary to conduct additional research on

the distribution of UVAs in the water and sediment at water depths >200 m in the SLEG as well as conduct research on redfish diet.
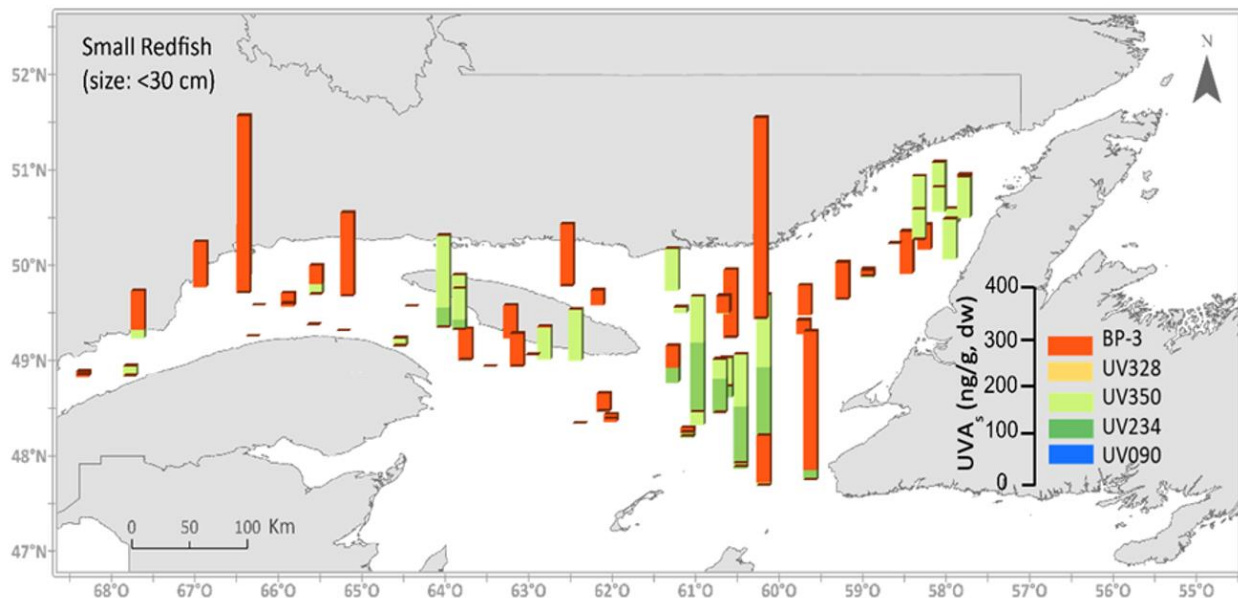
Figure 8: Average spatial distribution of UV absorbents in the muscle of small redfish from the St. Lawrence Estuary and Gulf.

2.5.1.1 BP-3 concentrations and its relationships with environmental/biological variables

BP3 was the most frequently (41%) detected UVA in the small redfish and the concentration ranged between <MDL and 413 ng/g (dw), with an estimated median and mean (data <MDL were counted in the estimation, details are described in section 2.6) of 9.07 ng/g dw (2.00 ng/g wet weight (ww)) and 37.0 ng/g dw (8.15 ng/g, ww), respectively. In contrast, BP3 was not detected in any large redfish. Large variations in BP-3 levels between sites within each sampling site were found for small redfish (Figure 8). Determining whether the samples from these sites share any distinguishing characteristics that could explain the elevated BP-3 levels is crucial. For example, fish from sites close to local contamination sources (e.g., wastewater treatment plants) may have higher exposure to BP3 (Mao et al., 2019; Castilloux et al., 2022). These factors require additional analysis and consideration to completely elucidate the spatial patterns of BP3 and their environmental implications.

Table 9: Occurrence of BP-3 (ng/g, dw) in marine fish tissues from different locations. ND: not detected. NA: not available. 1Scientific name was not provided in the literature.

Fish Species	Location	Tissue	Year	DF (%)	Mean	Range	References
Cod (*Gadus morhua*)				0	NA	ND	
Mackerel (*Scomber scombrus*)	Mediterranean Sea; North Sea; Atlantic Ocean	Muscle	2014-2015	78	15.7	ND-82.2	Cunha et al., 2018
Monkfish (*Lophius piscatorius)*				100	40.6	5-98.7	
Plaice/Sole[1]				0	NA	ND	
Tuna[1]				50	1.3	ND-2.5	
Atlantic cod (*Gadus morhua*)	North Sea; Inner Oslofjord (Norway)	Liver	2013	47	NA	ND-1037	Langford et al., 2015
Emerald rockcod (*Trematomus bernacchii*)	Ross Island (Antarctic)	Whole body homogenates	2009-2010	57	NA	ND-14.1	Emnet et al., 2015
lebranche mullet (*Mugil liza*)	Guanabara Bay (Brazil)	Muscle	2009-2010	100	7.4	3.5-15.4	Molins-Delgado et al., 2018
Wild fish (9 species)	Pearl River Estuary (China)	Whole body homogenates	2013	NA	NA	ND-1.1	Peng et al., 2015
Small Redfish (*Sebastes mentella*) (<30 cm)	St. Lawrence Estuary and Gulf (Canada)	Muscle	2019	41	37	ND-413	Present study

BP3 has been detected in wild marine fish samples worldwide, and its endocrine-disrupting properties in organisms are of environmental concern (Cuccaro et al., 2022). The distribution and level of BP3 vary greatly depending on different factors such as geographic area, fish species and tissue analyzed (Mao et al., 2019). When compared to previously reported findings in marine fish from various places, the BP3 levels detected in the muscle of small redfish in the present study tend to be greater (Table 09). The estimated mean BP3 level in the muscle of small redfish (37

ng/g, dw), for example, was comparable to Monkfish (*Lophius Americanus*) (41 ng/g, dw) from the Atlantic Ocean but higher than other fish species from the Atlantic Ocean, Antarctic, and the Pearl River Estuary in China (Table 09) (Cunha et al., 2018; Emnet et al., 2015; Molins-Delgado et al., 2018; Peng et al., 2015).

The distribution pattern of BP3 may be related to the carbon sources, diet compositions and trophic levels of redfish. The higher levels of BP3 detected in small redfish (Table 11), together with their significantly lower $\delta^{13}C$ and $\delta^{15}N$ relative to large redfish (Table S1, annex II), indicating that pelagic-eating redfish and those inhabiting lower trophic levels accumulate more BP3. When only considering small redfish, they also follow this pattern ($\delta^{13}C$ *vs.* BP3: likelihood r = -0.24, *p* = 0.03 for all redfish or small redfish, same results). These results implied that redfish foraging in the pelagic zone tend to accumulate more BP3. This BP3 distribution pattern suggests also that the accumulation of BP3 in redfish from the water column is more essential than from the benthic flux. Large redfish from SLEG consumed primarily shrimp and fish, whereas zooplankton was the dominant prey for small redfish (Brown-Vuillemin et al., 2023; Senay et al., 2023). Due to these dietary differences, the small redfish occupy a lower trophic level than the large specimen, as indicated by the $\delta^{15}N$ signatures (Table S1, annex II). Previous studies demonstrated that biomagnification behavior (trophic magnification or dilution) of BP3 in aquatic food webs was inconsistent (Peng et al., 2017a; Wang et al., 2022; Yang et al., 2020). In the present study, negative correlation was found between BP3 concentrations and $\delta^{15}N$ signatures when considering all redfish together (likelihood r = -0.50, *p* = 0.00002), probably derived by the noncontinuous distribution of $\delta^{15}N$ between small and large redfish. Such correlation was not found for small redfish (likelihood r = -0.21, *p* = 0.08). Thus, trophic dilution of BP3 cannot be fully concluded for the SLEG redfish. The trophodynamics of UVAs in the SLEG food web should be further investigated based on baseline corrected trophic levels and include more species.

The higher detection frequency and levels of BP3 in small redfish than the large group may be also related to the growth dilution effects. Growth dilution effects of BP3 was previously found in freshwater wild fish collected in Pearl River catchment, South China (Peng et al., 2020). Indeed, negative correlations were found between the BP3 concentrations and the redfish length (likelihood r = -0.46, p = 0.0008 for all redfish) and weight (likelihood r = -0.38, p = 0.003 for all redfish). But such correlations do not exist when analyzing only small redfish, implying that the

noncontinuous data distribution (Table S1, annex II) of length or weight derives the correlation found for all redfish.

Lipid content in redfish muscle is another possible reason affecting the distribution of BP3 (log Kow=3.52) (Tang et al., 2019). Although no correlation (likelihood r = 0.18, p = 0.15) was found between BP3 concentrations and the lipid content at individual level, small redfish (mean±SD 14.3±6.8%) had more (t test with Welch's correction, p<0.0001) lipid content than the large redfish (mean 5.0±6.9%) (Table S1, annex II), which is consistent with more BP3 found in small redfish group. No correlation was found between BP3 and other environmental/biological variables.

Salinity and fish weight were removed from the regression model due to variance inflation factors above 10. Non-significant variables were removed from the model using a stepwise approach and the final selected explanatory variables are $\delta^{15}N$ (p=0.02 based on Wald's test) and fish length (p=0.09). Because the p-value for fish length from the Wald's test is close to 0.05, a likelihood-ratio test was conducted based on the method described by Helsel et al (2012) to determine whether includes this variable and the p-value was calculated as 0.04. Therefore, the final estimated model is ln[BP3]=18.7-1.05´$\delta^{15}N$-0.022´length (likelihood R^2=0.17) when considering all redfish together. This model shows lower Akaike's Information Criterion (AIC) compared to the model only include $\delta^{15}N$ (AIC 248 vs 250) (ln[BP3]=15.1-1.19´$\delta^{15}N$) (likelihood R^2=0.14). Although these models are better to explain the variation of BP3 than the null model, they can only explain a very low portion of the variation of BP3 concentrations in redfish. For small redfish, using these environmental and biological variables cannot establish a regression model that is better than the null model. More research is necessary to better understand what factors (e.g., sources and biotransformation) driving the accumulation of BP3 in redfish and other deep-sea biota.

2.5.2 BZT-UV concentrations

UV350 was detected in 30% of small redfish samples with an estimated median concentration of 7.24 ng/g (mean 21.4 ng/g; <MQL-148 ng/g) (dw), which was higher than the large redfish (5%, <MQL-26.1 ng/g). The environmental occurrence data for UV350 is very

limited. In the St. Lawrence Estuary beluga, UV350 was found in only 4.5% of the blubber tissue, with concentrations below 2.5 ng/g (ww) (Blouin et al., 2022). In addition, this contaminant was previously detected in one (about 5 ng/g (dw)) liver sample of bream (Abramis brama) collected from a river of Germany, but not detectable in the fish from other three rivers in Germany (Wick et al., 2016). These findings indicate that UV350 accumulates in aquatic organisms, including deep-sea species, but at a generally low level.

UV234, UV328, and UV090 were also found in the redfish muscle, but the detection frequency was below 15% (Table 10). Akin to BP3 and UV350, these contaminants showed higher detection frequency and concentrations in small redfish compared to the large conspecifics (Table 11). UV328 and UV234 were detected less frequently or at lower concentrations in redfish than in wild fish reported before from other locations. For example, UV328 was detected in 73% of the muscle at a median concentration of 19 ng/g (ww) in lake sturgeon (Acipenser fulvescens) which is a long-lived species from the St. Lawrence River, which is upstream of the SLEG and more contaminated by surrounding large cities (Castilloux et al., 2022). In addition, as compared to the SLEG redfish, marine species from Manila Bay in the Philippines were more contaminated by UV328 (88% detection frequency, mean ND-207 ng/g, lipid weight (lw)), UV234 (55%, mean ND-63 ng/g, lw), and UV329 (41%, mean ND-33 ng/g, lw) than the SLEG redfish (Kim et al., 2011). The occurrence data for UV090 in organisms is very limited. For fish muscle, it was only sporadically detected in the lake sturgeon from the St. Lawrence River (6%, ND-111 ng/g, ww) (Castilloux et al., 2022). More data should be obtained from various matrices, species, and places to evaluate these substances' sources, environmental distribution, and exposure risks.

2.5.3 Estimated daily intake and hazard quotient

Humans can be exposed to UVAs through dermal contact (cosmetics), inhalation, or ingestion of food. In this study, exposure to the detected UVAs through redfish ingestion was assessed to understand the potential risk to human health. Due to the limited data, a deterministic risk model was used to evaluate the exposure. The estimated daily intake (EDI; ng/kg body weight (BW)/day) for UVAs in redfish for Canadian people was calculated based on the median and/or the maximum measured concentration of UVAs in redfish (CUVA, ng/g, ww), the daily ingestion rate (IR fish; g/day; assuming all consumed fish is redfish), and the BW (kg) of Canadian women and men as follows:

$$EDI = (CUVA \times IR\ fish)/\ BW \qquad\qquad (Eq.1)$$

According to Statistics Canada, the average daily fish consumption is 0.05 kg/week/person (7 g/day) (Annual fresh and frozen sea fish, edible weight in 2022 in Canada: 2.64 kg/person/year) for general population (Statistic Canada, 2023). The mean BW of Canadian adults is estimated as 66.8 kg for women and 81.6 kg for men (Statistic Canada, 2015). The median concentration-based EDI for BP3 and UV350 via redfish consumption were about 0.1 ng/kg/day (Table 10). The EDI based on the maximum measured concentrations of UVAs were in the range of 0.3 ng/kg/day (UV328 for men) to 10.6 ng/kg/day (BP3 for women) (Table 10).

Table 7: Estimated daily intake (EDI), no-observed adverse effect level (NOAEL), estimated reference dose (RfD) and hazard quotient (HQ) of detected UVAs through redfish consumption by Canadian population.
"Median" and "maximum" represent the scenarios of calculating EDI and HQ using median and maximum contaminant concentrations in redfish muscle, respectively. NA: not available.

Compounds	EDI (ng/kg/day)				NOAEL for rats (mg/kg/day)	Estimated Rfd (ng/kg/day for humans)	HQ			
	Median		Maximum				Median		Maximum	
	Women	Men	Women	Men			Women	Men	Women	Men
BP-3	0.1	0.1	10.6	8.7	200 (Mikkelsen et al., 2015)	20000	6.5×10^{-6}	5.5×10^{-5}	5.3×10^{-4}	4.3×10^{-4}
UV350	0.1	0.1	3.7	3.1	NA	NA	NA	NA	NA	NA
UV090	NA	NA	0.9	0.7	NA	NA	NA	NA	NA	NA
UV328	NA	NA	0.3	0.3	20 (US EPA, 2009)	2000	NA	NA	1.6×10^{-4}	1.4×10^{-4}
UV234	NA	NA	5.5	4.5	2.5 (US EPA, 2009)	250	NA	NA	2.3×10^{-2}	1.9×10^{-2}

Hazard quotient (HQ) which assesses the potential for non-cancer health risks from exposure to a contaminant, was calculated by the equation: HQ= EDI/RfD, where RfD is the reference dose (ng/kg/day), above which the health risks may occur. HQ <1 indicates that the human population is unlikely to experience adverse health effects. Because there is no widely accepted RfD available for these emerging contaminants, the RfD used in this study was derived from no-observed adverse effect level (NOAEL) for rats, divided by a safety factor of 10,000 as described by Kim et al (2012). The calculated HQ for the detectable UVAs in the redfish was below 2.3×10^{-2} (maximum level of

UV234 for women; worst scenario) (Table 10), which is much lower than 1, indicating that these contaminants are unlikely pose health risks to humans via redfish consumption. Even in other areas that consume far more marine fish than Canadians (e.g., roughly 10 times more in Japan, about 26 kg/year/person in 2020) (Food and Agriculture Organization of the United Nations), the highest HQ for target UVAs in the current study (maximum level of UV234 for women; worst scenario) were about five times lower than 1, which is still deemed safe.

2.6 CONCLUSION

The occurrence, fate, and impacts of contaminants of emerging concern, including UVAs, in the deep-sea are environmental concerns that have received less study. In the present study, BP3, UV350, UV234, UV328, and UV090 were detected in the muscle of deepwater redfish from the SLEG. Small redfish muscles showed higher concentrations of UVAs than large individuals, indicating different accumulation processes and potential risks of these contaminants between the two groups of redfish. Among all target UVAs, BP3 had the highest detection frequency and concentrations. The general pattern showed that redfish ingest more pelagic prey and at lower trophic levels tend to have more lipids and accumulate more BP3 in their muscle. Compared to other wild fish species in various locations reported previously, BP3 levels in the muscle of SLEG small redfish were generally among the high concentrations. In contrast, the detection rate of BZT-UVs in the SLEG redfish was lower than in other wild fish species reported before in other regions. Although some UVAs were detected in the SLEG redfish, the very low HQ values indicate they are unlikely to pose any health concerns to humans through redfish consumption. However, the toxicity of these contaminants in redfish is unknown, and the threats these contaminants may bring to the health of redfish or other deep-sea species should be researched further. Furthermore, it is crucial to investigate other factors affecting the bioaccumulation of these contaminants, such as their sources, partitioning and toxicokinetics in deep-sea fish, to elucidate their fate and risks better.

CONCLUSION GÉNÉRALE

Ce mémoire a permis d'approfondir nos connaissances sur la pollution au mercure total (THg) et méthylmercure (MeHg) ainsi que leurs implications environnementales. Il a également favorisé notre compréhension de l'occurrence et de la distribution des absorbants UV (UVAs), tels que les filtres UV organiques (UVFs) et les stabilisateurs UV à base de benzotriazole (BZT-UVs), dans les environnements des eaux profondes.

L'étude s'est particulièrement concentrée sur la distribution de ces contaminants dans un poisson des eaux profondes (> 200 m), le sébaste (*Sebastes mentella*) de l'estuaire et le golfe du Saint-Laurent, Canada, qui effectue un retour en force dans l'écosystème après avoir été designé comme espèce en voie de disparition par le Comité sur la situation des espèces en péril au Canada (COSEPAC) en 2010. Les échantillons de sébastes ont été collectés, après un moratoire de pêche de 25 ans, dans l'estuaire et le golfe du Saint-Laurent, où leur population se rétablit progressivement, ce qui permettra la reprise de la pêche commerciale et de la consommation humaine. Cependant, on ne connaît pas les niveaux de contaminants dans ces sébastes et les risques d'exposition humaine qui y sont liés, ce qui est important pour la protection de la santé humaine et de l'environnement marin.

Les résultats de l'étude du mercure ont révélé que les concentrations du THg et MeHg étaient inférieurs à la limite internationale autorisée pour la commercialisation fixée par FAO-OMS (500 ng/g p.h). Les sébastes provenant de l'estuaire et du golfe occidental présentaient des niveaux plus élevés de MeHg et de THg que ceux provenant du chenal laurentien et du nord-est du golfe. La taille du poisson, l'humidité du muscle, le rapport isotopique $\delta 15N$ et le pourcentage de l'azote (N%) ont été identifiés comme des prédicteurs significatifs des concentrations de MeHg dans le muscle du sébaste. Les résultats du mercure ont révélé que les individus de grande taille accumulaient significativement plus de mercure (20 à 30 fois plus) que ceux de petite taille.

De plus, cinq types d'UVAs, dont le 2-hydroxy-4-méthoxybenzophénone (BP-3) et quatre BZT-UVs (fréquence de détection < à 30 %) ont été détectés dans les muscles des sébastes. Les

individus de petite taille (<30 cm) avaient tendance à accumuler davantage d'UVA en proportion de leur poids par rapport aux spécimens plus grands (>30 cm).

La présence de BP-3 à des concentrations supérieures à 25 ng/g (poids humide) chez 6 % des sébastes pourrait être associée à des effets néfastes sur le métabolisme des poissons tel qu'observé dans d'autres études. Les données isotopiques $\delta^{15}N$ et $\delta^{13}C$ ont révélé que le régime alimentaire des sébastes était principalement composé de proies pélagiques et que les individus de niveaux trophiques inférieurs avaient une teneur plus élevée en lipides et accumulaient plus de BP-3 dans leurs muscles. Ce résultat pourrait expliquer pourquoi les petits sébastes du golfe du nord-est présentaient des niveaux de BP-3 plus élevés que ceux de l'estuaire et du golfe de l'ouest ainsi que du chenal laurentien.

Ces résultats ont démontré que le MeHg et le THg présentaient des niveaux plus élevés que les UVA dans le sébaste, et que les profils de distribution différaient entre le Hg et les UVA. Les niveaux de protéines ont affecté de manière significative l'accumulation de Hg dans le muscle du sébaste, tandis que la teneur en lipides a plus probablement influencé l'accumulation d'UVA dans le sébaste. Toutefois, la taille limitée de l'échantillon de grands sébastes capturés dans cette étude peut limiter la comparaison spatiale et l'interprétation de la manière dont les variables biologiques et environnementales peuvent affecter l'accumulation des contaminants dans ce groupe. En outre, la distribution des contaminants ciblés dans d'autres tissus du sébaste est inconnue, ce qui peut limiter notre compréhension des risques potentiels de ces contaminants sur la santé du sébaste, même si les humains ne consomment que le muscle du sébaste.

Malgré ces concentrations de THg et MeHg, il a été conclu que la consommation de sébaste par la population générale, à un taux de consommation moyen, ne devrait pas avoir d'effets néfastes sur la santé humaine. De même, l'évaluation du quotient de danger pour les UVAs a révélé des valeurs faibles pour la population générale canadienne, ce qui indique qu'ils ne posent probablement pas de risques pour la santé humaine lors de la consommation de sébaste.

Ce mémoire a mis en relief l'occurrence du THg, MeHg et des UVAs dans les muscles des sébastes des eaux profondes du Canada. Ces résultats fournissent une base de référence pour les

futurs suivis et soulignent l'importance de la surveillance continue de ces contaminants dans les environnements marins. En combinant les résultats sur l'accumulation de ces contaminants, il devient évident que des recherches supplémentaires sont nécessaires et pourraient se concentrer sur plusieurs aspects.

Tout d'abord, il serait essentiel d'approfondir la compréhension des facteurs qui influent sur la bioaccumulation du THg, du MeHg et des UVAs dans les espèces des eaux profondes. Cela pourrait inclure des investigations approfondies sur les caractéristiques environnementales spécifiques, les cycles biogéochimiques et les voies de contamination qui contribuent à l'accumulation de ces contaminants dans les muscles des sébastes. En outre, des études approfondies sur la source de ces contaminants pour les poissons des eaux profondes seraient cruciales. Identifier les points d'origine spécifiques du mercure et des UVA dans l'écosystème marin permettrait de mettre en place des mesures préventives plus ciblées et efficaces. En ce qui concerne les relations de cause à effet, des recherches approfondies pour comprendre comment les différents paramètres environnementaux (tels que la température, la salinité, etc.) et biologiques (comme le régime alimentaire, la biologie des espèces, etc.) influent sur l'accumulation de Hg et d'UVA dans les organismes des eaux profondes sont nécessaires. Cette compréhension plus approfondie permettrait de mieux prédire les tendances d'accumulation. Enfin, des études toxicologiques pour évaluer les risques sanitaires associés à la consommation de poissons des eaux profondes devraient être entreprises. Ces recherches pourraient aider à établir des limites de consommation sûres et à informer les politiques de gestion des ressources marines.

Dans l'ensemble, ces recherches supplémentaires contribueraient à renforcer la base scientifique nécessaire à la gestion durable des ressources marines, à la préservation de la santé humaine et à la protection de la biodiversité marine.

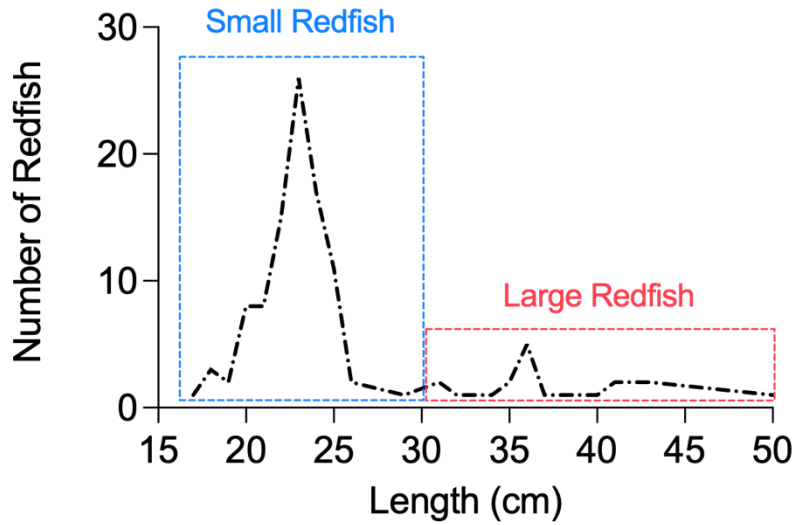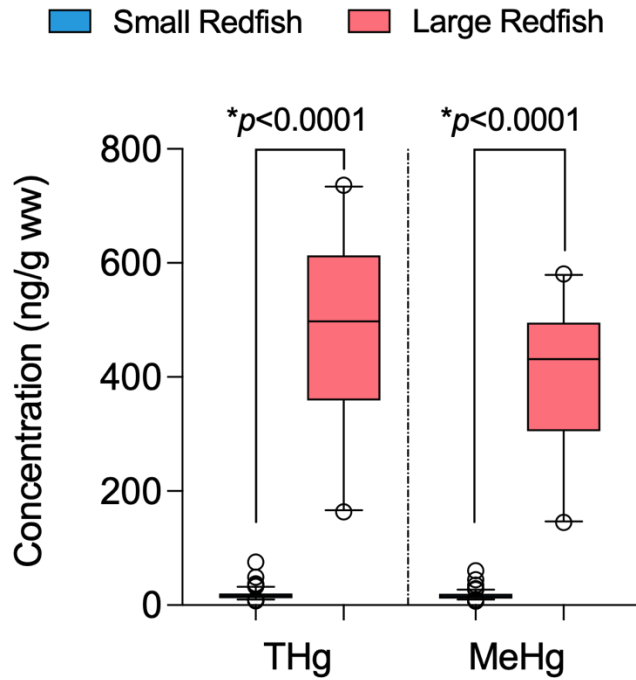Figure S1. Fish length distribution of collected redfish from St. Lawrence Estuary and Gulf.

Figure S2. Concentrations (ng/g ww) of THg and MeHg in the muscle of small (blue) and large (red) redfish. Boxplots are defined as follows: center line, median; boxplot edges, 25th and 75th percentiles of distribution; whiskers, 5th and 95th percentiles of the distribution. Black circles are outliers.

Figure S3. Spatial distribution of THg concentrations (dw) in (A) small and (B) large redfish, as well as least squares mean (ls-mean) THg concentrations ± standard error (dw) in (C) small and (D) large redfish from the three sampling areas. EWG: Estuary-Western Gulf; LC: Laurentian Channel; NEG: Northeast Gulf. Boxplots are defined as follows: center line, median; boxplot edges, 25th and 75th percentiles of distribution; whiskers, 5th and 95th percentiles of the distribution. Black circles are outliers. Different letters in (A) indicate significant differences.
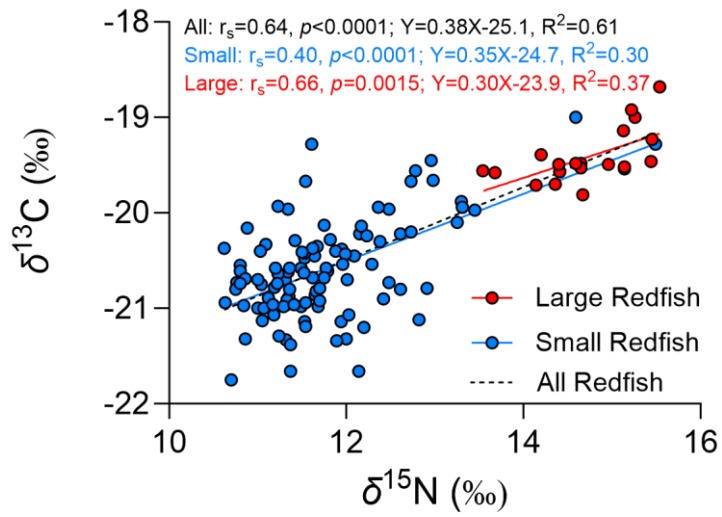
Figure S4. Relationship between $\delta^{15}N$ and $\delta^{13}C$ of all small (blue) and large (red) redfish from St. Lawrence Estuary and Gulf. Spearman correlation coefficient is shown as r_s; p represents the probability for the correlation to be caused by random variation; R^2 represents the coefficient of determination in simple linear regression.
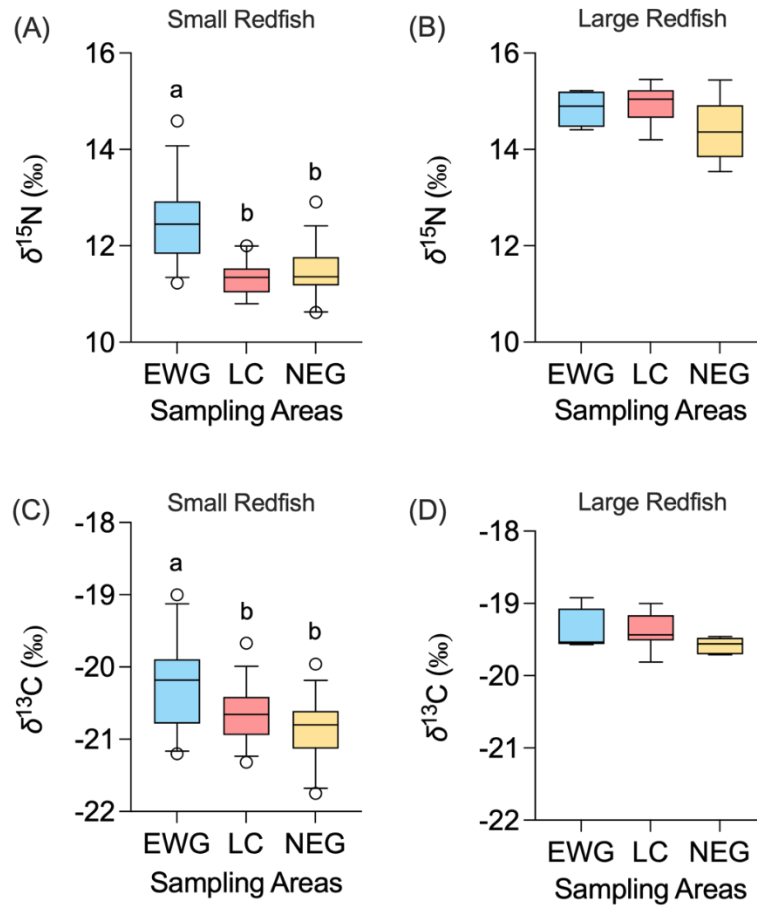
Figure S5. Spatial distribution of $\delta^{15}N$ in (A) small and (B) large redfish and $\delta^{13}C$ in (C) small and (D) large redfish from the three sampling areas. EWG: Estuary-Western Gulf; LC: Laurentian Channel; NEG: Northeast Gulf. Boxplots are defined as follows: center line, median; boxplot edges, 25th and 75th percentiles of distribution; whiskers, 5th and 95th 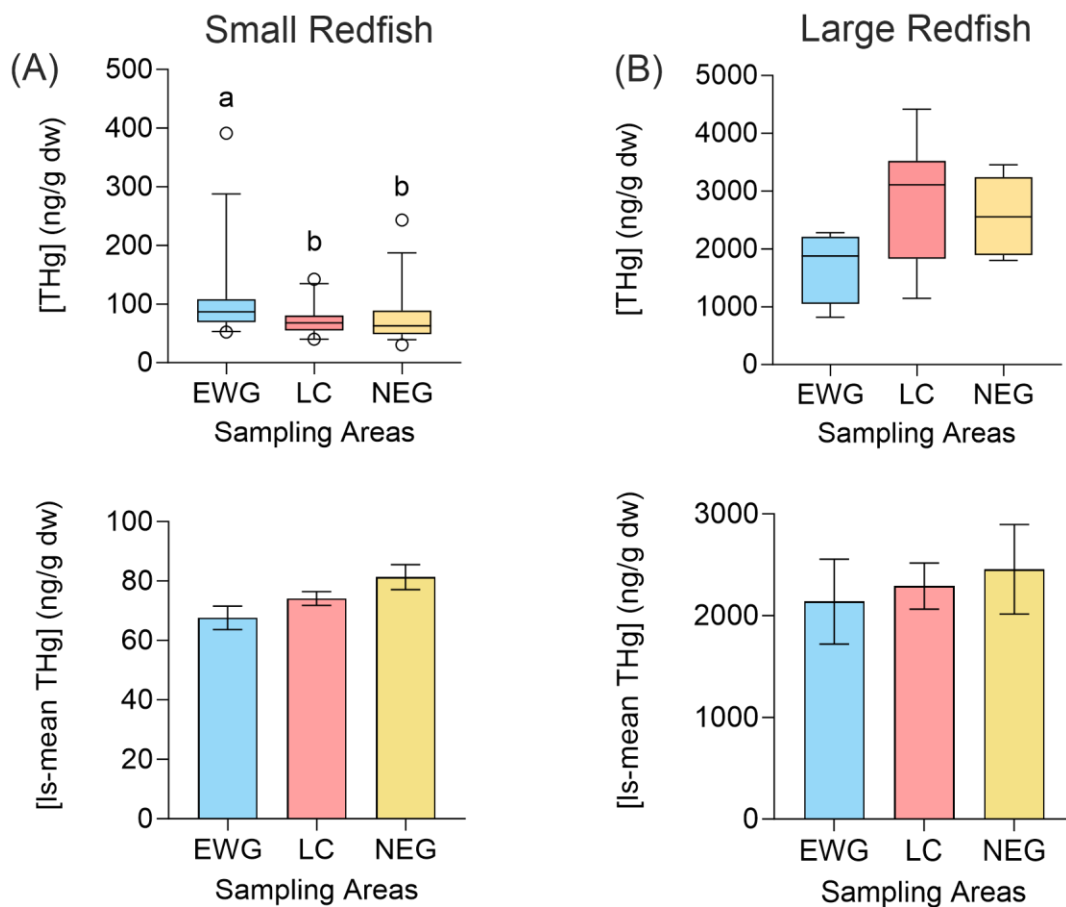percentiles of the distribution. Black circles are outliers. Different letters in (A) and (C) indicate significant differences.
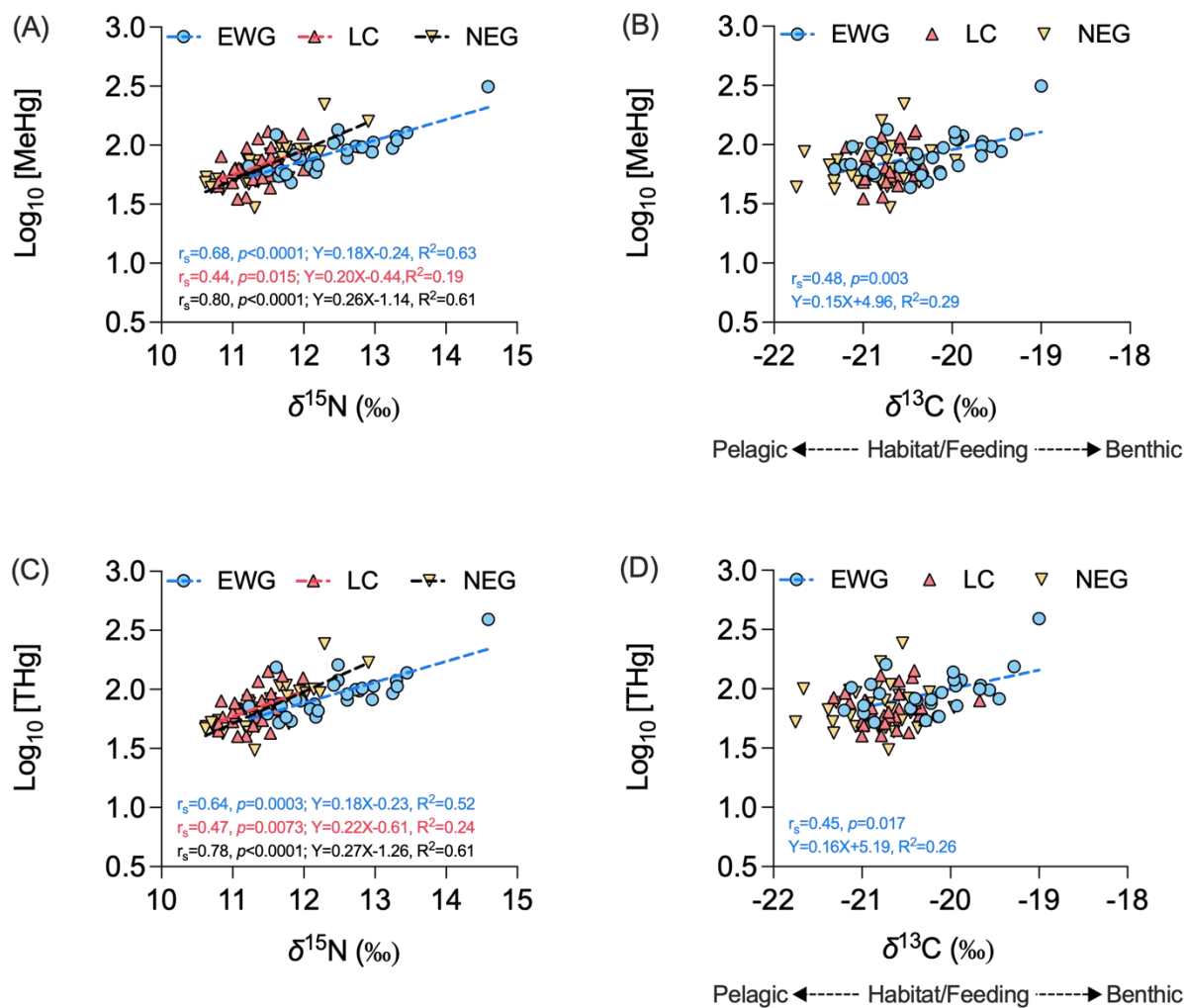
Figure S6. Relationships of $\log_{10}$[MeHg] (ng/g,dw) *vs.* (A) δ^{15}N or (B) δ^{13}C and $\log_{10}$[THg] (ng/g,dw) *vs.* (C) δ^{15}N or (D) δ^{13}C in small redfish from the three sampling zones. EWG: Estuary-Western Gulf ; LC: Laurentian Channel; NEG: Northeast Gulf. Spearman correlation coefficient is shown as r_s; *p* represents the probability for the correlation to be caused by random variation; R^2 represents the coefficient of determination in simple linear regression.

Figure S7. Relationships between $\log_{10}$[MeHg](dw) and (A) δ^{15}N, (B) δ^{13}C, (C) fish weight, (D) fish length, (E) moisture, (F) lipid, (G) N%, (H) $\log_{10}$ [dissolved oxygen], and (I) water temperature. Blue and red color represent small and large redfish, respectively. Spearman correlation coefficient is shown as r_s; p represents the probability for the correlation to be caused by random variation; R^2 represents the coefficient of determination in simple linear regression. In (H), log transformed data of dissolved oxygen are used because the linear regression slope of the original data is not significantly different from 0 for small redfish. Linear regression results are not shown for small redfish in (I) because the slope is not significantly different from 0 even after log transform of the temperature data.

Figure S8. Relationships between $\log_{10}$[THg](dw) and (A) δ^{13}C, (B) δ^{15}N, (C) fish weight, (D) fish length, (E) moisture, (F) lipid, (G) N%, (H) $\log_{10}$ [dissolved oxygen], and (I) water temperature. Blue and red color represent small and large redfish, respectively. Spearman correlation coefficient is shown as r_s; p represents the probability for the correlation to be caused by random variation; R^2 represents the coefficient of d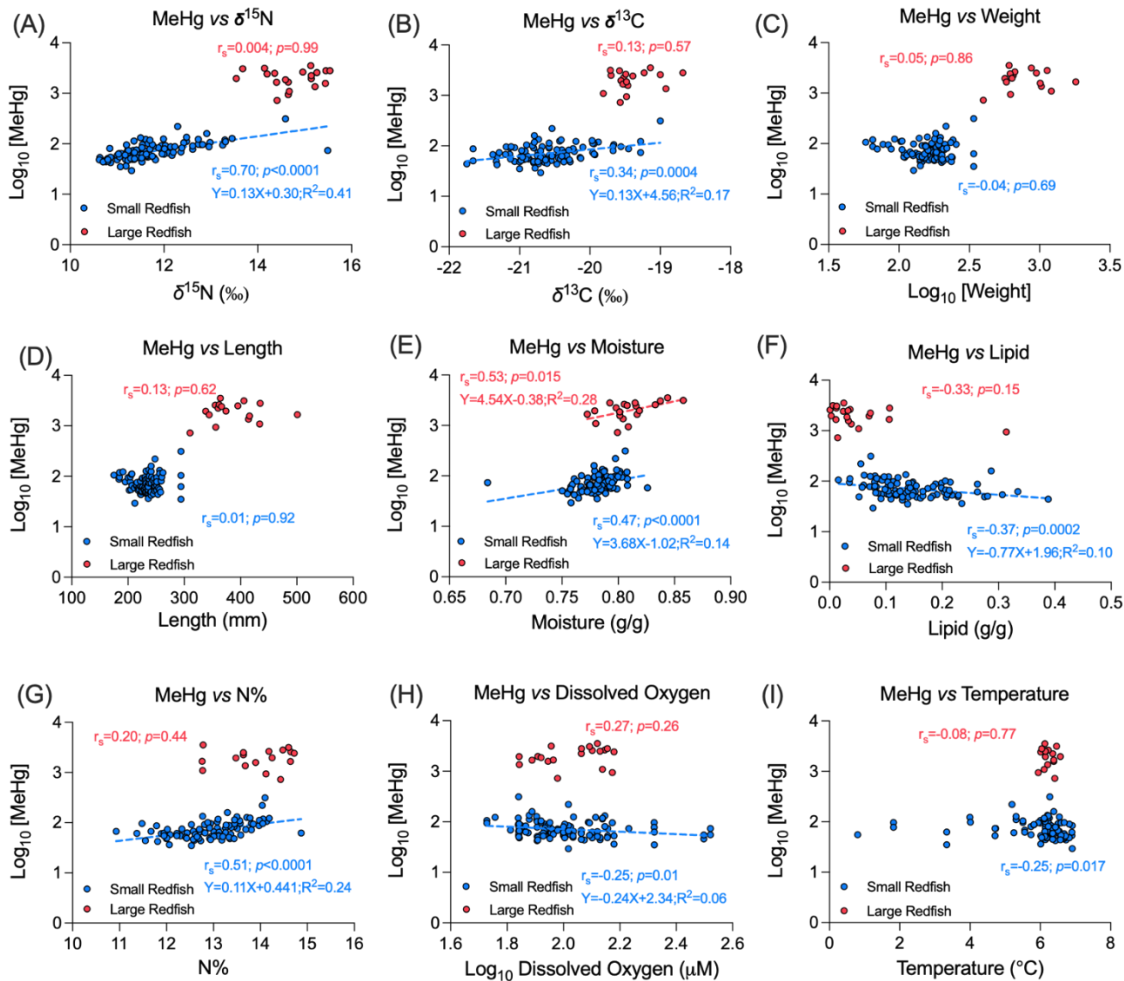etermination in simple linear regression. In (H), log transformed data of dissolved oxygen are used because the linear regression slope of the original data is not significantly different from 0 for small redfish. Linear regression results are not shown for small redfish in (I) because the slope is not significantly different from 0 even after log transform of the temperature data.
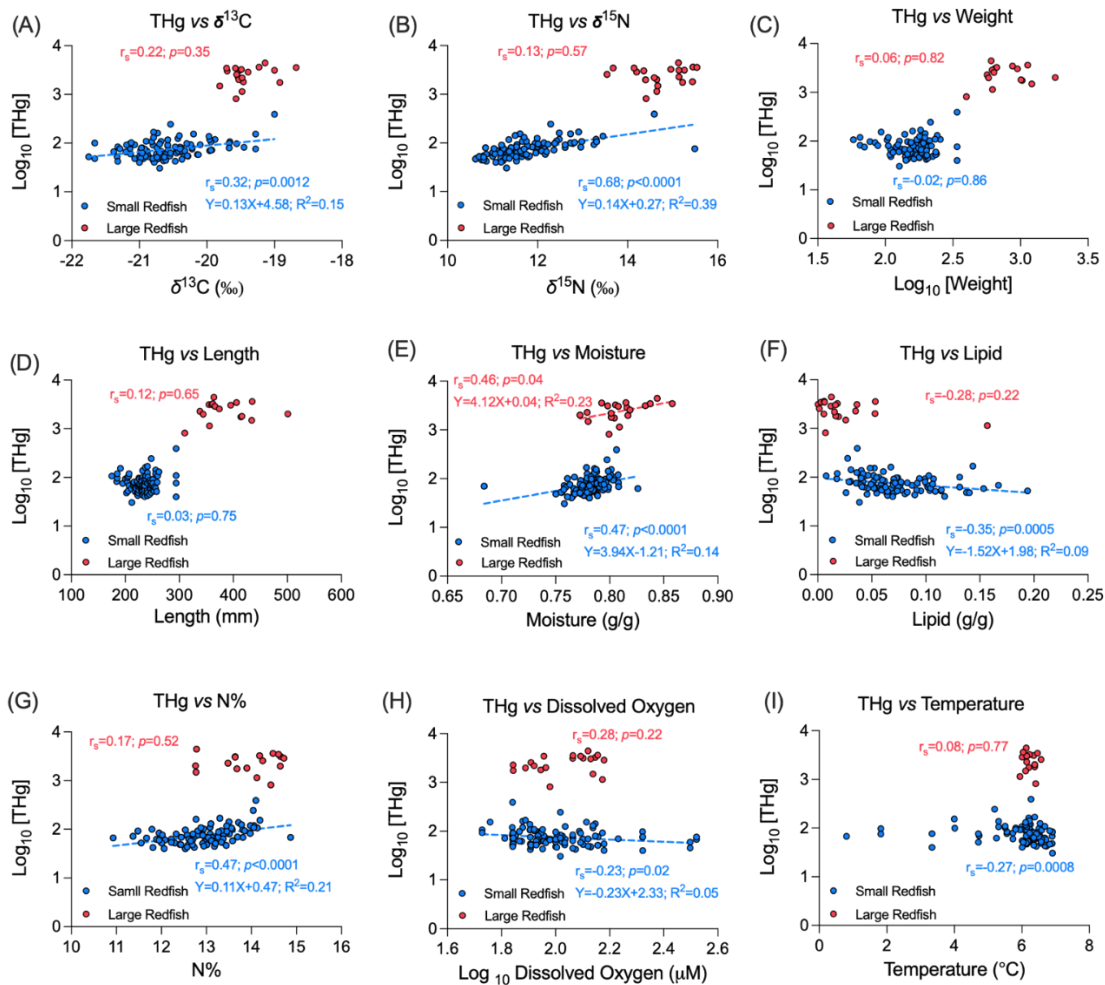
Figure S9. Log$_{10}$ [MeHg] (mean, calculated based on ng/g dw) in redfish and other species from the SLEG in relation to δ^{15}N (A) and δ^{13}C (B). The data for species other than redfish were gathered from Lavoie et al (2010) and samples were collected in 2006-2007. (Zooplankton: CFIN (*Calanus finmarchicus),* CHYP (*Calanus hyperboreus), MENO (Meganyctiphanes norvegica); Amphipoda: GAMA (Gammarellus sp.); Decapoda:* SHRI (Shrimps); *Fish: CAPE (Capelin (Mallotus villosus)), SAND (*American sandlance (*Ammodytes americanus*)), AMPL (American plaice (*Hippoglossoides platessoides*)), ATHE (Atlantic herring (*Clupea harengus*)), WIFL(Witch flounder (*Glyptocephalus cynoglossus*)). Spearman correlation coefficient is shown as r$_s$; *p* represents the probability for the correlation to be caused by random variation; R^2 represents the coefficient of determination in simple linear regression.

δ^{15}N vs Length

(A)   EWG   LC   NEG

Length (mm)

r_s=-0.48; p=0.006
Y=-28.0X+560;R^2=0.22

δ^{15}N

δ^{15}N vs Weight

(B)   EWG   LC   NEG

weight (g)

r_s=-0.48; p=0.005
Y=-63.0X+900;R^2=0.16

δ^{15}N

δ^{13}C vs Length

(C)   EWG   LC   NEG

Length (mm)

r_s=-0.51; p=0.005

δ^{13}C

δ^{13}C vs Weight

(D)   EWG   LC   NEG

Weight (g)

r_s=-0.52; p=0.005

δ^{13}C
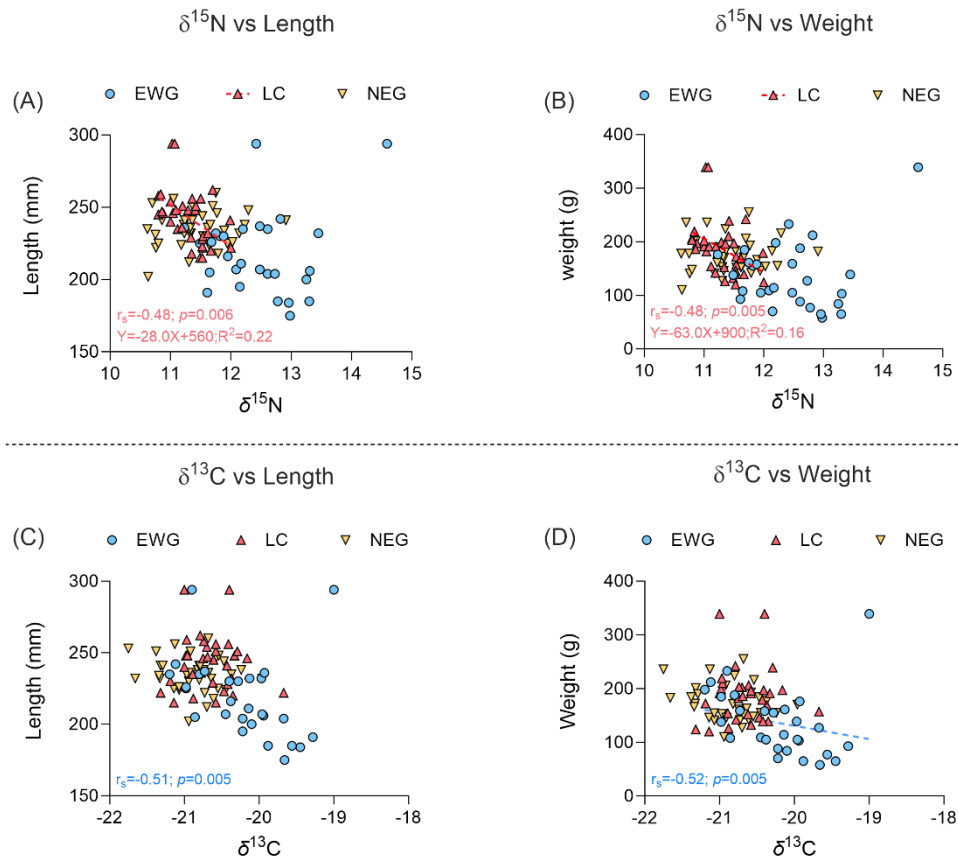
Figure S10. Relationships of fish size and δ^{15}N or δ^{13}C for small redfish ((A): length *vs.* δ^{15}N for small redfish from three sampling areas; (B) weight *vs.* δ^{15}N for small redfish from three sampling areas; (C) length *vs.* δ^{13}C for small redfish from three sampling areas; (D) weight *vs.* δ^{13}C for small redfish from three sampling areas). Spearman correlation coefficient is shown as r_s; *p* represents the probability for the correlation to be caused by random variation; R^2 represents the coefficient of determination in simple linear regression. Correlation results are not shown when it is not statistically significant. In (C) and (D), linear regression results are not shown for small redfish because the slope is not significantly different from 0. EWG: Estuary-Western Gulf; LC: Laurentian Channel; NEG: Northeast Gulf.
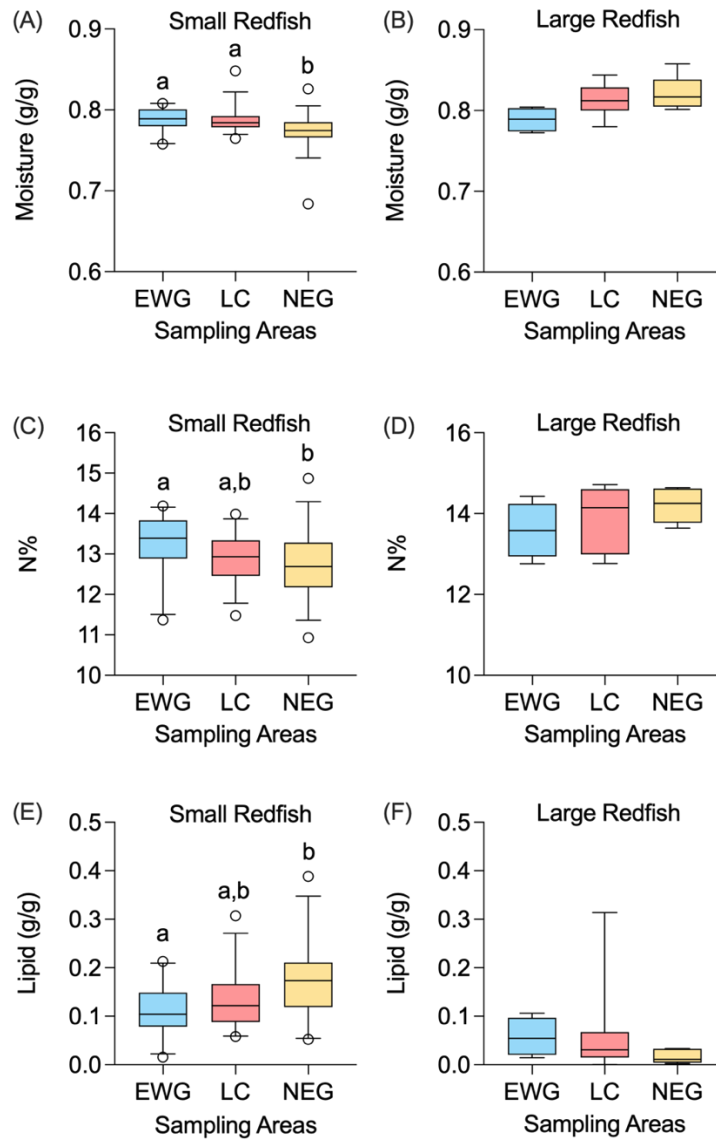
Figure S11. Spatial distribution of moisture (A and B), N% (C and D) and lipids (E and F) in small and large redfish from the three sampling areas. EWG: Estuary-Western Gulf; LC: Laurentian Channel; NEG: Northeast Gulf. Boxplots are defined as follows: center line, median; boxplot edges, 25th and 75th percentiles of distribution; whiskers, 5th and 95th percentiles of the distribution. Black circles are outliers. Different letters in (A), (C) and (D) indicate significant differences.
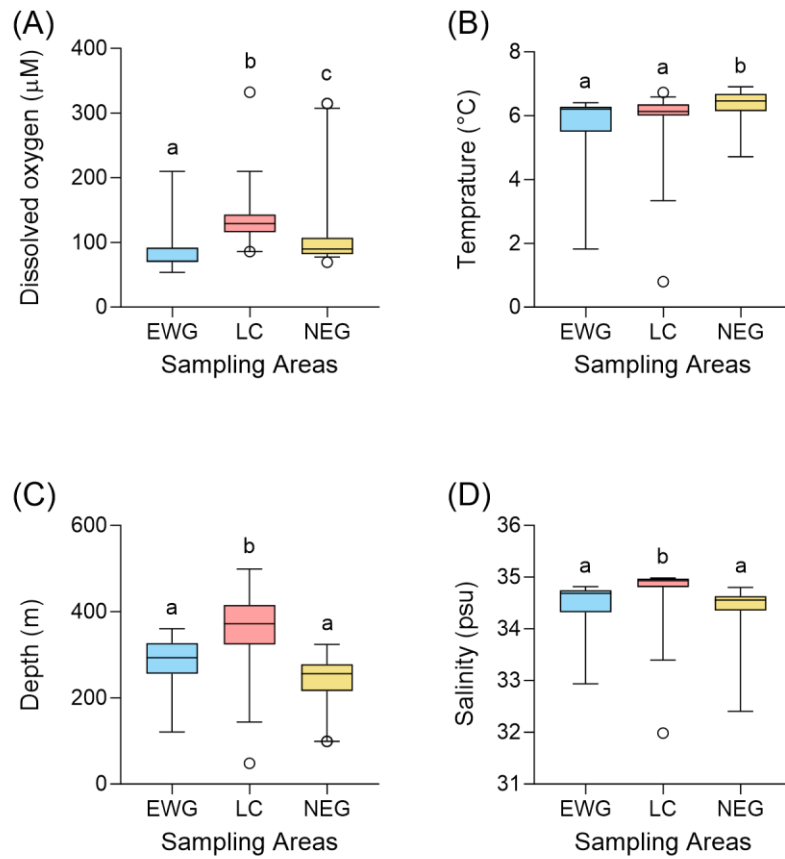
Figure S12. Spatial distribution of dissolved oxygen (A), temperature (B), depth (C) and salinity (D) from the three sampling areas. EWG: Estuary-Western Gulf; LC: Laurentian Channel; NEG: Northeast Gulf. Boxplots are defined as follows: center line, median; boxplot edges, 25th and 75th percentiles of distribution; whiskers, 5th and 95th percentiles of the distribution. Black circles are outliers. Different letters indicate significant differences.
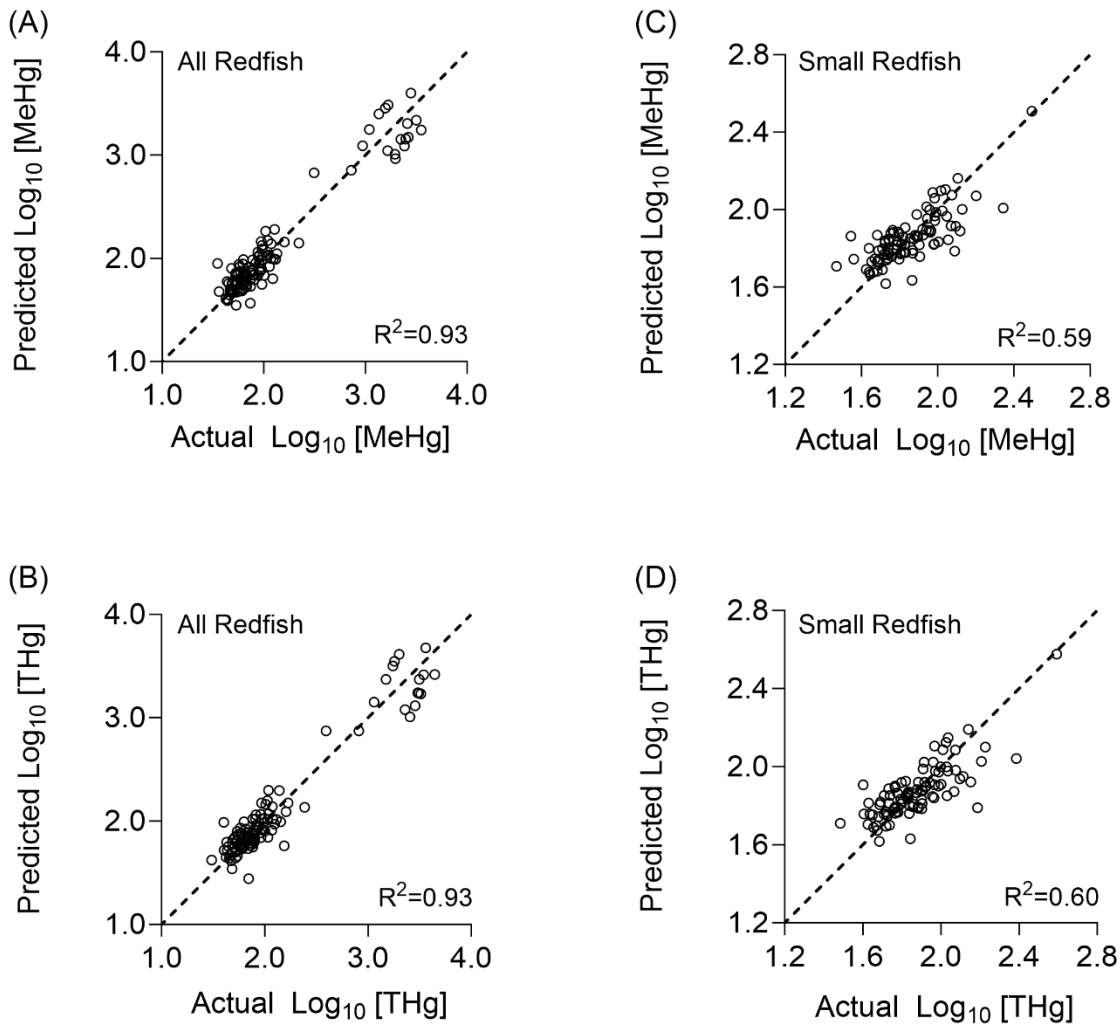
Figure S13. Linear regression of actual $\log_{10}$[MeHg] *vs*. predicted $\log_{10}$[MeHg] (dw) for all redfish (A) and small redfish (C), and actual $\log_{10}$[THg] *vs*. predicted $\log_{10}$[THg] (ng/g dw) for all redfish (B) and small redfish (D). Fish length, moisture, $\delta^{15}N$ and N% are used for the model of MeHg in all redfish (A), while fish length, moisture, and $\delta^{15}N$ are used for model of THg in all redfish (B), MeHg in all redfish (C) and MeHg in small redfish (D). R^2 is the coefficient of determination in multiple linear regression.

Table S1: Standard recoveries for THg and MeHg.

Reference Standard	Recovery	Relative Standard Deviation	*n*
THg			
Tort-3 (Lobster hepatopancreas)	97.0%	4.3%	4
Dorm-4 (Dogfish muscle)	109.1%	6.0%	16
Dolt-5 (Dogfish liver)	103.3%	4.7%	6
MeHg			
Dorm-4	86.6%	3.5%	13
Dolt-5	110.1%	2.7%	9

Table S2: Mean concentrations of MeHg in different fish species from St. Lawrence Estuary and Gulf.

Species	Location	Year of Sampling	Mean	SE	Unit	Reference
Fish						
Small redfish (*Sebastes mentella*)	SLEG	2019	77.7	4.04	(ng/g dw)	Present study
Large redfish (*Sebastes mentella*)			2050	191		
Small redfish (*Sebastes mentella*)			16.6	0.73	(ng/g ww)	
Large redfish (*Sebastes mentella*)			395	27.4		
Capelin (*Mallotus villosus*)	Estuary-Western Gulf	2006	17.5	1.3	(ng/g dw)	Lavoie et al., 2010
American sandlance (*Ammodytes americanus*)			54.7	20.1		
American plaice (*Hippoglossoides platessoides*)			77.4	18.8		
Witch flounder (Glyptocephalus cynoglossus)			100	27		
Atlantic herring (*Clupea harengus*)			69.2	6.1		
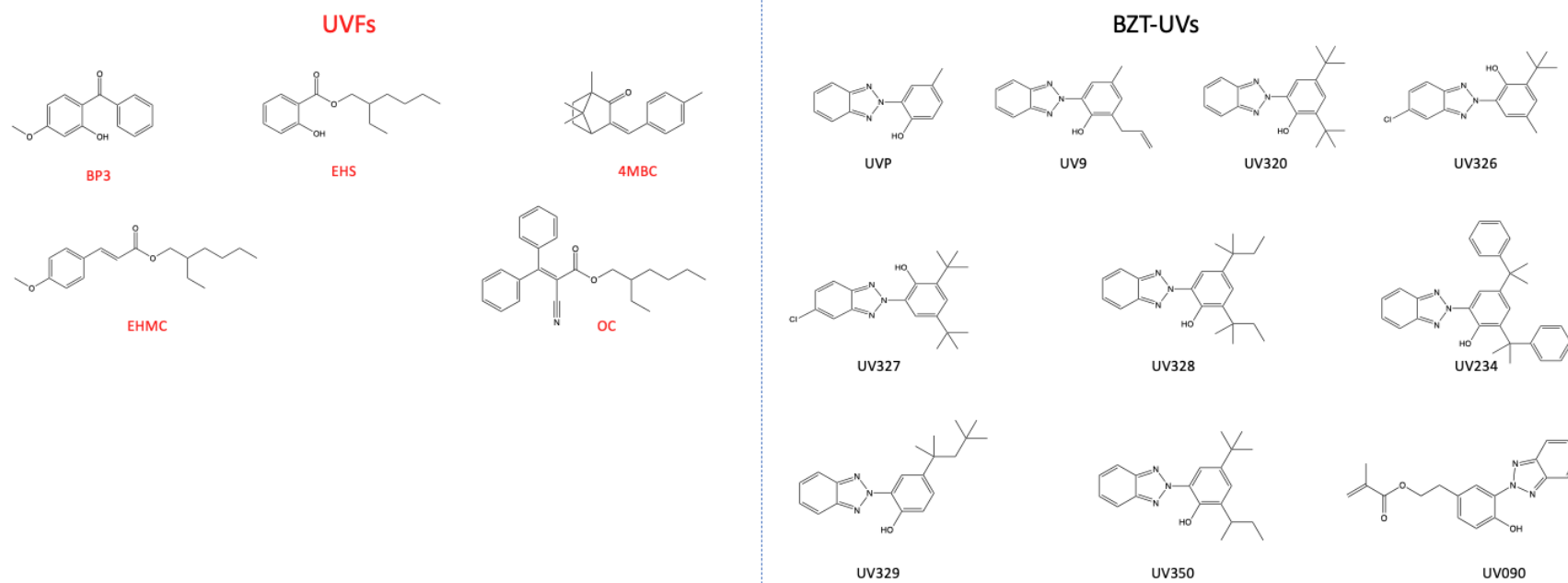
Figure S1. Structures of target UV absorbents.

Table S1: Biological and environmental variables (mean ± standard deviation) of small and large deepwater redfish samples from the Estuary- Western Gulf (EWG), Laurentian Channel (LC) and Northeast Gulf (NEG) of the St. Lawrence Estuary and Gulf (Moualek et al., 2023). NA: data not available. The methods of the measurement of environmental variables can be found in Bourdages et al (2022).

Group	Length (mm)	Weight (g)	Lipid content (%)	Moisture (%)	Depth (m)	Temperature (°C)	Oxygen (Micromoles)	Salinity (psu)	δ^{15}N (‰)	δ^{13}C (‰)
Small	233±22	166±53	14.3±6.8	78±2	284±89	5.9±1.2	114±55	34.5±0.6	11.8±0.7	-20.6±0.5
Large	384±46	834±350	5.0±6.9	81±2	350±82	6.2±0.2	111±29	34.8±0.2	14.7±0.6	-19.4±0.3

Table S2. Chemical names, CAS registry numbers, acronyms and physicochemical properties of target compounds.

No.	Chemical Name	CAS No.	Acronyms	Molecular weight (g.mol^{-1})	Water solubility[a] (mg. L^{-1})	Log K_{ow}[a]
1	2-Hydroxy-4-methoxybenzophenone	131-57-7	BP3	228.3	68.6	3.52
2	Ethylhexyl methoxycinnamate	5466-77-3	EHMC	290.4	0.15	5.80
3	4-Methylbenzylidene camphor	36861-47-9	4MBC	254.4	0.2	5.92
4	2-Ethylhexyl salicylate	118-60-5	EHS	250.3	0.72	5.97
5	2-Ethylhexyl-2-cyano-3,3-diphenylacrylate	6197-30-4	OC	361.5	3.8×10^{-3}	6.88
6	2-(2H-benzotriazol-2-yl)-p-cresol	2440-22-4	UVP	225.3	25.6	3.00
7	2-[3-(2H-benzotriazol-2-yl)-4-hydroxyphenyl]ethyl methacrylate	96478-09-0	UV090	323.4	14.9	3.93
8	2-(2H-benzotriazol-2-yl)-4-methyl-6-(2-propenyl)phenol	2170-39-0	UV9	265.3	13.1	4.39
9	2-(2H-benzotriazol-2-yl)-4,6-bis(1-methyl-1-phenylethyl)phenol	70321-86-7	UV234	447.6	1.6×10^{-3}	7.67
10	2-Benzotriazole-2-yl-4,6-di-*tert*-butylphenol	3846-71-7	UV320	323.4	0.15	6.27
11	2-*tert*-Butyl-6-(5-chloro-2H-benzotriazol-2-yl)-4-methylphenol	3896-11-05	UV326	315.8	0.68	5.55
12	2,4-Di-*tert*-butyl-6-(5-chloro-2H-benzotriazol-2-yl) phenol	3864-99-1	UV327	357.9	0.026	6.91
13	2-(2H-benzotriazol-2-yl)-4,6-di-*tert*-pentylphenol	25973-55-1	UV328	351.5	0.015	7.25
14	2-(2H-benzotriazol-2-yl)-4-(1,1,3,3-tetramethyl butyl)phenol	3147-75-9	UV329	323.4	0.17	6.21
15	2-(2H-benzotriazol-2-yl)-4-(*tert*-butyl)-6-(*sec*-butyl)phenol	36437-37-3	UV350	323.4	0.14	6.31

[a] Data are predicted by Estimation Program Interface (EPI) Suite (V4.11) modeling, K_{ow} represents n-octanol/water partition coefficient.

Table S3. GC-MS experimental parameters. NA: not applicable.

Compound	Quantification ion (*m/z*)	Confirmation ion (*m/z*)	Retention time (min)
Diphenylamine-d$_{10}$	179	NA	13.16
BP-d$_{10}$	192	NA	14.02
BP-3	227	151	21.13
4-MBC	155	254	21.62
UV-P	225	168	21.78
EHMC	178	161	26.34
UV-9	250	265	26.83
UV320	308	252	30.77
UV350	308	294	31.59
UV326	300	315	33.12
UV329	252	253	34.05
UV328-d$_4$	326	NA	36.40
UV328	322	252	36.43
UV327	342	344	36.65
OC	232	203	36.87
UV090	237	180	38.09
UV234	432	447	50.97

Method (Blouin et al., 2022, Castilloux et al., 2022): A Programmable Temperature Vaporization injector was used to inject three µL of sample. The initial injector temperature was set at 50 °C, held for 0.1 minute, and ramped to 120 °C at a rate of 14 °C/min, followed by a cleaning process at 300 °C at a rate of 2.5 °C/min (kept for 10 minutes), followed by a cleaning process at 330 °C and held for 5 minutes. The GC column was a 30 m RXI-5MS column from Chromatographic Specialties in Brockville, Ontario, Canada (0.25 mm diameter, 0.25 m film thickness). The oven temperature program began at 80 °C and was held for 2 minutes. The temperature was then gradually increased to 160 °C at a rate of 10 °C/min, then to 230 °C at a rate of 5 °C/min, and finally to 300 °C at a rate of 10 °C/min, followed by a 15-minute isothermal hold. The carrier gas was helium gas (1 mL/min). The temperature of the GC-MS transfer line was fixed to 300 °C. The MS was set to single ion monitoring (SIM) mode, with electron impact (EI) ionization at a 70 eV electron energy and a 200 °C ion source temperature.

Table S4. MDL and recovery (mean ± SD) for the target UV absorbents in muscle of redfish.

NA: not applicable

Analyte	MDL (ng/g, dw)	Recovery (%)					
		20ng			50 ng		
BP-d_{10}	NA	72%	±	27%	53%	±	18%
BP3	6.2	94%	±	34%	91%	±	28%
4-MBC	3.4	74%	±	21%	61%	±	16%
UVP	8.7	93%	±	20%	95%	±	20%
EHMC	5.9	77%	±	17%	70%	±	21%
UV-9	4.3	75%	±	20%	74%	±	21%
UV320	3.7	75%	±	16%	78%	±	22%
UV350	8.7	83%	±	17%	78%	±	22%
UV326	4.1	86%	±	18%	85%	±	17%
UV329	4.7	90%	±	19%	79%	±	16%
UV328-d_4	NA	74%	±	12%	73%	±	19%
UV328	5.1	71%	±	14%	67%	±	16%
UV327	5.7	74%	±	15%	74%	±	18%
OC	4.2	84%	±	14%	65%	±	16%
UV090	3.9	86%	±	15%	65%	±	14%
UV234	7.0	70%	±	15%	63%	±	12%

RÉFÉRENCES BIBLIOGRAPHIQUES

Adamou, T. Y., Riva, M., Muckle, G., Laouan-Sidi, E. A., & Ayotte, P. 2018. Socio-economic inequalities in blood mercury (Hg) and serum polychlorinated biphenyl (PCB) concentrations among pregnant Inuit women from Nunavik, Canada. Canadian Journal of Public Health. 109(5-6), 671-683. doi:10.17269/s41997-018-0077-y.

Agency of Toxic Substances and Disease Registry (MRLs), 2023. Minimal Risk Levels (MRLs) for hazardous substances | ATSDR. wwwn.cdc.gov. URL https://wwwn.cdc.gov/TSP/MRLS/mrlslisting.aspx (accessed 7.16.23).

Ajsuvakova, O.P., Tinkov, A.A., Aschner, M., Rocha, J.B.T., Michalke, B., Skalnaya, M.G., Skalny, A.V., Butnariu, M., Dadar, M., Sarac, I., Aaseth, J., Bjørklund, G., 2020. Sulfhydryl groups as targets of mercury toxicity. Coordination Chemistry Reviews 417, 213343. https://doi.org/10.1016/j.ccr.2020.213343

Al-Sulaiti, M.M., Soubra, L., Al-Ghouti, M.A., 2022. The causes and effects of mercury and methylmercury contamination in the marine environment: a review. Current Pollution Reports 8, 249-272. https://doi.org/10.1007/s40726-022-00226-7

Amyot, M., Lean, D.R., Poissant, L., Doyon, M.-R., 2000. Distribution and transformation of elemental mercury in the St. Lawrence River and Lake Ontario. Canadian Journal of Fisheries and Aquatic Sciences 57, 155–163. https://doi.org/10.1139/f99-248

Aschner, M., Aschner, J.L., 1990. Mercury neurotoxicity: Mechanisms of blood-brain barrier transport. Neuroscience & Biobehavioral Reviews 14, 169–176. https://doi.org/10.1016/s0149-7634(05)80217-9

Asimakopoulos, A.G., Wang, L., Thomaidis, N.S., Kannan, K., 2013. Benzotriazoles and benzothiazoles in human urine from several countries: A perspective on occurrence, biotransformation, and human exposure. Environment International 59, 274–281. https://doi.org/10.1016/j.envint.2013.06.007

Azad, A.M., Frantzen, S., Bank, M.S., Nilsen, B.M., Duinker, A., Madsen, L., Maage, A., 2019. Effects of geography and species variation on selenium and mercury molar ratios in Northeast Atlantic marine fish communities. Science of the Total Environment 652, 1482–1496. https://doi.org/10.1016/j.scitotenv.2018.10.405

Bakir, F., Damluji, S.F., Amin-Zaki, L., Murtadha, M., Khalidi, A., Al-Rawi, N.Y., Tikriti, S., Dhahir, H.I., Clarkson, T.W., Smith, J.C., Doherty, R.A., 1973. Methylmercury poisoning in Iraq. Science 181, 230–241. https://doi.org/10.1126/science.181.4096.230

Bello, T.C.S., Buralli, R., Cunha, M.P., Dórea, J., Diaz-Quijano, F., Guimarães, J., Marques, R.C., 2023. Mercury Exposure in Women of Reproductive Age in Rondônia State, Amazon Region, Brazil. International Journal of Environmental Research and Public Health. https://doi.org/10.3390/ijerph20065225

Benestan, L., Rougemont, Q., Senay, C., Normandeau, E., Parent, E., Rideout, R., Bernatchez, L., Lambert, Y., Audet, C., Parent, G.J., 2021. Population genomics and history of speciation reveal fishery management gaps in two related redfish species (*Sebastes mentella* and *Sebastes fasciatus*). Evolutionary Applications. 14, 588-606. https://doi.org/10.1111/eva.131438

Binelli, A., Provini, A., 2004. Risk for human health of some POPs due to fish from Lake Iseo. Ecotoxicology and Environmental Safety 58, 139–145. https://doi.org/10.1016/j.ecoenv.2003.09.014

Blanchfield, P.J., Rudd, J.W.M., Hrenchuk, L.E., Amyot, M., Babiarz, C.L., Beaty, K.G., Bodaly, R.A.D., Branfireun, B.A., Gilmour, C.C., Graydon, J.A., Hall, B.D., Harris, R.C., Heyes, A., Hintelmann, H., Hurley, J.P., Kelly, C.A., Krabbenhoft, D.P., Lindberg, S.E., Mason, R.P., Paterson, M.J., 2022. Experimental evidence for recovery of mercury-contaminated fish populations. Nature 601, 74–78. https://doi.org/10.1038/s41586-021-04222-7

Blouin, K., Malaisé, F., Verreault, J., Lair, S., Lu, Z., 2022. Occurrence and temporal trends of industrial antioxidants and UV absorbents in the endangered St. Lawrence Estuary beluga whale (*Delphinapterus leucas*). Science of The Total Environment 842, 156635. https://doi.org/10.1016/j.scitotenv.2022.156635

Blukacz-Richards, E.A., Visha, A., Graham, M.L., McGoldrick, D.L., de Solla, S.R., Moore, D.J., Arhonditsis, G.B., 2017. Mercury levels in herring gulls and fish: 42 years of spatio-temporal trends in the Great Lakes. Chemosphere 172, 476–487. https://doi.org/10.1016/j.chemosphere.2016.12.148

Bourdages, H., Brassard, C., Chamberland, J.M., Desgagnés, M., Galbraith, P., Isabel, L., Senay, C. 2022. Preliminary results from the ecosystemic survey in August 2021 in the Estuary and northern Gulf of St. Lawrence. Canadian Science Advisory Secretariat Science Advisory Report, 2022/011. URL https://publications.gc.ca/site/eng/9.908920/publication.html (accessed 7.14.23).

Bradley, M., Barst, B., Basu, N., 2017. A review of mercury bioavailability in humans and fish. International Journal of Environmental Research and Public Health 14, 169. https://doi.org/10.3390/ijerph14020169

Braune, B., Chételat, J., Amyot, M., Brown, T., Clayden, M., Evans, M., Fisk, A., Gaden, A., Girard, C., Hare, A., Kirk, J., Lehnherr, I., Letcher, R., Loseto, L., Macdonald, R., Mann, E.,

McMeans, B., Muir, D., O'Driscoll, N., Poulain, A., Reimer, K., Stern, G., 2015. Mercury in the marine environment of the Canadian Arctic: Review of recent findings. Science of The Total Environment 509-510, 67–90. https://doi.org/10.1016/j.scitotenv.2014.05.133

Breittmayer, J.P., Guido, R., Tuncer, S., 1980. Effet du cadmium sur la toxicité du mercure vis-a-vis de la moule *Mytilus edulis* (L.). Chemosphere 9, 725–728. https://doi.org/10.1016/0045-6535(80)90125-3

Brown-Vuillemin, S., Chabot, D., Nozères, C., Tremblay, R., Sirois, P., Robert, D., 2022. Diet composition of redfish (*Sebastes sp.*) during periods of population collapse and massive resurgence in the Gulf of St. Lawrence. Frontiers in Marine Science 9, 963039. https://doi.org/10.3389/fmars.2022.963039

Brown-Vuillemin, S., Tremblay, R., Chabot, D., Sirois, P., Robert, D., 2023. Feeding ecology of redfish (*Sebastes* sp.) inferred from the integrated use of fatty acid profiles as complementary dietary tracers to stomach content analysis. Journal of Fish Biology 102, 1049–1066. https://doi.org/10.1111/jfb.15348

Burress, E.D., Holcomb, J.M., Bonato, K.O., Armbruster, J.W., 2016. Body size is negatively correlated with trophic position among cyprinids. Royal Society Open Science 3, 150652. https://doi.org/10.1098/rsos.150652

Cadigan, N.G., Duplisea, D.E., Senay, C., Parent, G.J., Winger, P.D., Linton, B.R., Kristinsson, K., 2022. Northwest Atlantic redfish science priorities for managing an enigmatic species complex. Canadian Journal of Fisheries and Aquatic Sciences. 79, 1572–1589. https://doi.org/10.1139/cjfas-2021-0266

Campana, S.E., Valentin, A.E., MacLellan, S.E., Groot, J.B., 2016. Image-enhanced burnt otoliths, bomb radiocarbon and the growth dynamics of redfish (*Sebastes mentella* and *S. fasciatus*) off the eastern coast of Canada. Marine and Freshwater Research 67, 925. https://doi.org/10.1071/mf15002

Cantwell, M.G., Sullivan, J.C., Katz, D.R., Burgess, R.M., Bradford Hubeny, J., King, J., 2015. Source determination of benzotriazoles in sediment cores from two urban estuaries on the Atlantic Coast of the United States. Marine Pollution Bulletin 101, 208–218. https://doi.org/10.1016/j.marpolbul.2015.10.075

Castilloux, A.D., Houde, M., Gendron, A., De Silva, A., Soubaneh, Y.D., Lu, Z., 2022. Distribution and Fate of Ultraviolet Absorbents and Industrial Antioxidants in the St. Lawrence River, Quebec, Canada. Environmental Science & Technology 56. https://doi.org/10.1021/acs.est.1c07932

Charette, T., Rosabal, M., Amyot, M., 2020. Mapping metal (Hg, As, Se), lipid and protein levels within fish muscular system in two fish species (Striped Bass and Northern Pike). Chemosphere 265, 129036. https://doi.org/10.1016/j.chemosphere.2020.129036

Chen, X., Wang, J., Chen, J., Zhou, C., Cui, F., Sun, G., 2019. Photodegradation of 2-(2-hydroxy-5-methylphenyl)benzotriazole (UV-P) in coastal seawaters: Important role of DOM. Journal of Environmental Sciences 85, 129–137. https://doi.org/10.1016/j.jes.2019.05.017

Chiriac, F.L., Lucaciu, I.E., Paun, I., Pirvu, F., Gheorghe, S., 2022. *In vivo* bioconcentration, distribution and metabolization of Benzophenone-3 (BP-3) by *Cyprinus carpio* (European Carp). Foods (Basel, Switzerland) 11, 1627. https://doi.org/10.3390/foods11111627

Committee on the Status of Endangered Wildlife in Canada (COSEWIC), 2011. Assessment and Status Report on the Deepwater Redfish/Acadian Redfish complex *Sebastes mentella* and *Sebastes fasciatus* in Canada – 2010. www.canada.ca. URL https://www.canada.ca/en/environment-climate-change/services/species-risk-public-registry/cosewic-assessments-status-reports/deepwater-redfish-acadian-complex-2010.html#_Toc267065056 (accessed 6.25.23).

Cossa, D., Gobeil, C., 2000. Mercury speciation in the Lower St. Lawrence Estuary. Canadian Journal of Fisheries and Aquatic Sciences 57, 138–147. https://doi.org/10.1139/f99-237

Cuccaro, A., Freitas, R., De Marchi, L., Oliva, M., Pretti, C., 2022. UV-filters in marine environments: a review of research trends, meta-analysis, and ecotoxicological impacts of 4-methylbenzylidene-camphor and benzophenone-3 on marine invertebrate communities. Environmental Science and Pollution Research 29, 64370–64391. https://doi.org/10.1007/s11356-022-21913-4

Cunha, S.C., Trabalón, L., Jacobs, S., Castro, M., Fernandez-Tejedor, M., Granby, K., Verbeke, W., Kwadijk, C., Ferrari, F., Robbens, J., Sioen, I., Pocurull, E., Marques, A., Fernandes, J.O., Domingo, J.L., 2018. UV-filters and musk fragrances in seafood commercialized in Europe Union: Occurrence, risk and exposure assessment. Environmental Research 161, 399–408. https://doi.org/10.1016/j.envres.2017.11.015

Cuvin-Aralar, M.L.A., 1990. Mercury levels in the sediment, water, and selected finfishes of Laguna Lake, The Philippines. Aquaculture 84, 277–288. https://doi.org/10.1016/0044-8486(90)90093-3

Désy, J.-C., Archambault, J.-F., Bernadette, P.-A., Hubert, J., P.G.C., Campbell, 2000. Relationships between total mercury in sediments and methyl mercury in the freshwater gastropod prosobranch *Bithynia tentaculata* in the St. Lawrence River, Quebec. Canadian Journal of Fisheries and Aquatic Sciences 57, 164–173. https://doi.org/10.1139/f99-231

Dijkstra, J.A., Buckman, K.L., Ward, D., Evans, D.W., Dionne, M., Chen, C.Y., 2013. Experimental and natural warming elevates mercury concentrations in estuarine fish. PLoS ONE 8, e58401. https://doi.org/10.1371/journal.pone.0058401

Drevnick, P.E., Roberts, A.P., Otter, R.R., Hammerschmidt, C.R., Klaper, R., Oris, J.T., 2008. Mercury toxicity in livers of northern pike (*Esox lucius*) from Isle Royale, USA. Comparative Biochemistry and Physiology Part C: Toxicology & Pharmacology 147, 331–338. https://doi.org/10.1016/j.cbpc.2007.12.003

Egambaram, O.P., Kesavan Pillai, S., Ray, S.S., 2020. Materials Science Challenges in Skin UV Protection: A Review. Photochemistry and Photobiology 96, 779–797. https://doi.org/10.1111/php.13208

Emnet, P., Gaw, S., Northcott, G., Storey, B., Graham, L., 2015. Personal care products and steroid hormones in the Antarctic coastal environment associated with two Antarctic research stations, McMurdo Station and Scott Base. Environmental Research 136, 331–342. https://doi.org/10.1016/j.envres.2014.10.019

EPA, 2016. Definition and procedure for the determination of the method detection limit, revision 2. Environmental Protection Agency EPA.

FAO/WHO, 2003. Summary and conclusions of the sixty-first meeting of the Joint FAO/WHO Expert Committee on Food Additives.

FAO/WHO, 2010. Evaluation of certain food additives and contaminants: seventy-third report of the Joint FAO/WHO Expert Committee on Food Additives (https://www.who.int/publications/i/item/9789241209601; accessed April 13,2023).

Fent, K., Chew, G., Li, J., Gomez, E., 2014. Benzotriazole UV-stabilizers and benzotriazole: Antiandrogenic activity *in vitro* and activation of aryl hydrocarbon receptor pathway in zebrafish eleuthero-embryos. Science of the Total Environment 482-483, 125–136. https://doi.org/10.1016/j.scitotenv.2014.02.109

Fent, K., Chew, G., Li, J., Gomez, E., 2014. Benzotriazole UV-stabilizers and benzotriazole: Antiandrogenic activity in vitro and activation of aryl hydrocarbon receptor pathway in zebrafish eleuthero-embryos. Science of the Total Environment 482-483, 125–136. https://doi.org/10.1016/j.scitotenv.2014.02.109

Ferchiou, S., 2019. Mémoire de maîtrise Nouvelle approche chimique basée sur la bioaccumulation des retardateurs de flamme pour identifier et évaluer la diète récente du béluga du Saint-Laurent (*Delphinapterus leucas*). semaphore.uqar.ca. https://semaphore.uqar.ca/id/eprint/1645/ (accessed 7.15.23)

Fisheries and Oceans Canada (DFO), 2021. Impact of an expanding Redfish (*Sebastes* spp.) fishery on southern Gulf of St. Lawrence White Hake (*Urophycis tenuis*). Canadian Science Advisory Secretariat Science Advisory Report, 2021/033.

Fisheries and Oceans Canada (DFO), 2022. Redfish (*Sebastes mentella* and *Sebastes fasciatus*) stocks assessment in Units 1 and 2 in 2021. DFO Canadian Science Advisory Secretariat Science Advisory Report, 2022/039.

Fitzgerald, W.F., Engstrom, D.R., Mason, R.P., Nater, E.A., 1998. The Case for Atmospheric Mercury Contamination in Remote Areas. Environmental Science & Technology 32, 1–7. https://doi.org/10.1021/es970284w

Fjeld, E., Haugen, T.O., Vøllestad, L.A., 1998. Permanent impairment in the feeding behavior of grayling (*Thymallus thymallus*) exposed to methylmercury during embryogenesis. The Science of the Total Environment 213, 247–254. https://doi.org/10.1016/s0048-9697(98)00097-7

Food and Agriculture Organization of the United Nations, n.d. FAOSTAT. www.fao.org. URL https://www.fao.org/faostat/en/#data/FBS/report (accessed 6.25.23).

Froescheis, O., Looser, R., Cailliet, G.M., Jarman, W.M., Ballschmiter, K., 2000. The deep-sea as a final global sink of semivolatile persistent organic pollutants? Part I: PCBs in surface and deep-sea dwelling fish of the North and South Atlantic and the Monterey Bay Canyon (California). Chemosphere 40, 651–660. https://doi.org/10.1016/s0045-6535(99)00461-0

Fujita, K.K., Doering, J.A., Stock, E., Lu, Z., Montina, T., Wiseman, S., 2022. Effects of dietary 2-(2H-benzotriazol-2-yl)-4-methylphenol (UV-P) exposure on Japanese medaka (*Oryzias latipes*) in a short-term reproduction assay. Aquatic Toxicology 248, 106206. https://doi.org/10.1016/j.aquatox.2022.106206

Gago-Ferrero, P., Díaz-Cruz, M.S., Barceló, D., 2015. UV filters bioaccumulation in fish from Iberian river basins. Science of the Total Environment 518-519, 518–525. https://doi.org/10.1016/j.scitotenv.2015.03.026

Gascon, D., 2003a. Redfish multidisciplinary research zonal program (1995-1998): Final report. Canadian Technical Report of Fisheries and Aquatic Sciences 2462.

Gascon, D. (éd.)., 2003b. Programme de recherche multidisciplinaire sur le sébaste (1995-1998): Rapport final. Rapport technique canadien des sciences halieutiques et aquatiques. 2462 : xiv + 148 p.

Gaspar, L.R., Campos, P.M.., 2010. A HPLC method to evaluate the influence of photostabilizers on cosmetic formulations containing UV-filters and vitamins A and E. Talanta 82, 1490–1494. https://doi.org/10.1016/j.talanta.2010.07.025

Ghazipura, M., McGowan, R., Arslan, A., Hossain, T., 2017. Exposure to benzophenone-3 and reproductive toxicity: A systematic review of human and animal studies. Reproductive Toxicology 73, 175–183. https://doi.org/10.1016/j.reprotox.2017.08.015

Giokas, D.L., Salvador, A., Chisvert, A., 2007. UV filters: From sunscreens to human body and the environment. TrAC Trends in Analytical Chemistry 26, 360–374. https://doi.org/10.1016/j.trac.2007.02.012

Giraudo, M., Colson, T.-L.L., De Silva, A.O., Lu, Z., Gagnon, P., Brown, L., Houde, M., 2020. Food-Borne Exposure of Juvenile Rainbow Trout (*Oncorhynchus mykiss*) to Benzotriazole Ultraviolet Stabilizers Alone and in Mixture Induces Specific Transcriptional Changes. Environmental Toxicology and Chemistry 39, 852–862. https://doi.org/10.1002/etc.4676

Glaz, P., Sirois, P., Archambault, P., Nozais, C., 2014. Impact of Forest Harvesting on Trophic Structure of Eastern Canadian Boreal Shield Lakes: Insights from Stable Isotope Analyses. PLoS ONE 9, e96143. https://doi.org/10.1371/journal.pone.0096143

Gworek, B., Bemowska-Kałabun, O., Kijeńska, M., Wrzosek-Jakubowska, J., 2016. Mercury in Marine and Oceanic Waters—a Review. Water, Air, and Soil Pollution 227 (10): 371. https://doi.org/10.1007/s11270-016-3060-3

Ha, E., Basu, N., Bose-O'Reilly, S., Dórea, J.G., McSorley, E., Sakamoto, M., Chan, H.M., 2017. Current progress on understanding the impact of mercury on human health. Environmental Research 152, 419–433. https://doi.org/10.1016/j.envres.2016.06.042

Hammerschmidt, C.R., Sandheinrich, M.B., Wiener, J.G., Rada, R.G., 2002. Effects of Dietary Methylmercury on Reproduction of Fathead Minnows. Environmental Science & Technology 36, 877–883. https://doi.org/10.1021/es011120p

Health Canada. 2007. Human health risk assessment of mercury in fish and health benefits of fish consumption. Available on : http://hc-sc.gc.ca/fn-an/pubs/mercur/merc_fish_poisson_e.html

Hebert, Canada., 1995. To normalize or not to normalize? Fat is the question. scholar.google.com 14, 801–807.

Hellberg, R.S., DeWitt, C.A.M., Morrissey, M.T., 2012. Risk-benefit analysis of seafood consumption: A review. Comprehensive Reviews in Food Science and Food Safety 11, 490–517. https://doi.org/10.1111/j.1541-4337.2012.00200.x

Helsel, D.R., 2011. Statistics for Censored Environmental Data Using Minitab and R, 77th ed, Google Books. John Wiley & Sons.

Hirata-Koizumi, M., Watari, N., Mukai, D., Imai, T., Hirose, A., Kamata, E., Ema, M., 2007. A 28-Day Repeated Dose Toxicity Study of Ultraviolet Absorber 2-(2′-Hydroxy-3′,5′-di-tert-butylphenyl) benzotriazole in Rats. Drug and Chemical Toxicology 30, 327–341. https://doi.org/10.1080/01480540701522254

Jackson, A.C., 2018. Chronic neurological disease due to methylmercury poisoning. Canadian Journal of Neurological Sciences 45, 620–623. https://doi.org/10.1017/cjn.2018.323

Kameda, Y., Kimura, K., Miyazaki, M., 2011. Occurrence and profiles of organic sun-blocking agents in surface waters and sediments in Japanese rivers and lakes. Environmental Pollution 159, 1570–1576. https://doi.org/10.1016/j.envpol.2011.02.055

Kariagina, A., Morozova, E., Hoshyar, R., Aupperlee, M.D., Borin, M.A., Haslam, S.Z., Schwartz, R.C., 2020. Benzophenone-3 promotion of mammary tumorigenesis is diet-dependent. Oncotarget 11, 4465–4478. https://doi.org/10.18632/oncotarget.27831

Keppeler, F.W., Montaña, C.G., Winemiller, K.O., 2020. The relationship between trophic level and body size in fishes depends on functional traits. Ecological Monographs, e01415. https://doi.org/10.1002/ecm.1415

Kidd, K., Clayden, M., Jardine, T., 2011. Bioaccumulation and Biomagnification of Mercury through Food Webs. Environmental Chemistry and Toxicology of Mercury 453–499. https://doi.org/10.1002/9781118146644

Kim, J.-W., Chang, K.-H., Isobe, T., Tanabe, S., 2011a. Acute toxicity of benzotriazole ultraviolet stabilizers on freshwater crustacean (*Daphnia pulex*). The Journal of Toxicological Sciences 36, 247–251. https://doi.org/10.2131/jts.36.247

Kim, J.-W., Chang, K.-H., Prudente, M., Viet, P.H., Takahashi, S., Tanabe, S., Kunisue, T., Isobe, T., 2019. Occurrence of benzotriazole ultraviolet stabilizers (BUVSs) in human breast milk from three Asian countries. The Science of the Total Environment 655, 1081–1088. https://doi.org/10.1016/j.scitotenv.2018.11.298

Kim, J.-W., Isobe, T., Malarvannan, G., Sudaryanto, A., Chang, K.-H., Prudente, M, Tanabe, S., 2012. Contamination of benzotriazole ultraviolet stabilizers in house dust from the Philippines: Implications on human exposure. Science of the Total Environment 424, 174–181. https://doi.org/10.1016/j.scitotenv.2012.02.040

Kim, J.-W., Isobe, T., Ramaswamy, B.R., Chang, K.-H., Amano, A., Miller, T.M., Siringan, F.P., Tanabe, S., 2011b. Contamination and bioaccumulation of benzotriazole ultraviolet

stabilizers in fish from Manila Bay, the Philippines using an ultra-fast liquid chromatography–tandem mass spectrometry. Chemosphere 85, 751–758. https://doi.org/10.1016/j.chemosphere.2011.06.054

Kim, J.-W., Isobe, T., Tanoue, R., Chang, K.-H., Tanabe, S., 2015. Comprehensive Determination of Pharmaceuticals, Personal Care Products, Benzotriazole UV Stabilizers and Organophosphorus Flame Retardants in Environmental Water Samples Using SPE Coupled with UHPLC-MS/MS. Current Analytical Chemistry 11, 138–149. https://doi.org/10.2174/1573411011102150223141925

Kim, S.H., Lim, Y., Hwang, E., Yim, Y.-H., 2016. Development of an ID ICP-MS reference method for the determination of Cd, Hg and Pb in a cosmetic powder certified reference material. Analytical Methods 8, 796–804. https://doi.org/10.1039/c5ay02040a

Kockler, J., Oelgemöller, M., Robertson, S., Glass, B.D., 2012. Photostability of sunscreens. Journal of Photochemistry and Photobiology C: Photochemistry Reviews 13, 91–110. https://doi.org/10.1016/j.jphotochemrev.2011.12.001

Kortei, N. K., Heymann, M. E., Essuman, E. K., Kpodo, F. M., Akonor, P. T., Lokpo, S. Y., Boadi, N. O., Ayim-Akonor, M., & Tettey, C. ,2020. Health risk assessment and levels of toxic metals in fishes (*Oreochromis noliticus* and *Clarias anguillaris*) from Ankobrah and Pra basins: Impact of illegal mining activities on food safety. Toxicology Reports, 7, 360-369. https://doi.org/10.1016/j.toxrep.2020.02.011

Langford, K.H., Reid, M.J., Fjeld, E., Øxnevad, S., Thomas, K.V., 2015. Environmental occurrence and risk of organic UV filters and stabilizers in multiple matrices in Norway. Environment International 80, 1–7. https://doi.org/10.1016/j.envint.2015.03.012

Laske, S.M., Burke, S.M., Carey, M.P., Swanson, H.K., Zimmerman, C.E., 2023. Investigating effects of climate-induced changes in water temperature and diet on mercury concentrations in an Arctic freshwater forage fish. Environmental Research 218, 114851. https://doi.org/10.1016/j.envres.2022.114851

Lavoie, R.A., Hebert, C.E., Rail, J.-F., Braune, B.M., Yumvihoze, E., Hill, L.G., Lean, D.R.S., 2010. Trophic structure and mercury distribution in a Gulf of St. Lawrence (Canada) food web using stable isotope analysis. Science of the Total Environment 408, 5529–5539. https://doi.org/10.1016/j.scitotenv.2010.07.053

Legrand, M., Feeley, M., Tikhonov, C., Schoen, D., Li-Muller, A., 2010. Methylmercury Blood Guidance Values for Canada. Canadian Journal of Public Health 101, 28–31. https://doi.org/10.1007/bf03405557

Li, Y., Gillespie, Brenda,W., Shedden, K., Gillespie, John,A., 2019. Profile Likelihood Estimation of the Correlation Coefficient in the Presence of Left, Right or Interval Censoring and Missing Data. The R Journal 10, 159. https://doi.org/10.32614/rj-2018-040

Liang, X., Li, J., Martyniuk, C.J., Wang, J., Mao, Y., Lu, H., Zha, J., 2017. Benzotriazole ultraviolet stabilizers alter the expression of the thyroid hormone pathway in zebrafish (*Danio rerio*) embryos. Chemosphere 182, 22–30. https://doi.org/10.1016/j.chemosphere.2017.05.015

Liu, R., Ruan, T., Wang, T., Song, S., Guo, F., Jiang, G., 2014. Determination of nine benzotriazole UV stabilizers in environmental water samples by automated on-line solid phase extraction coupled with high-performance liquid chromatography–tandem mass spectrometry. Talanta 120, 158–166. https://doi.org/10.1016/j.talanta.2013.10.041

Lu, Z., De Silva, A.O., McGoldrick, D.J., Zhou, W., Peart, T.E., Cook, C., Tetreault, G.R., Martin, P.A., de Solla, S.R., 2018. Substituted diphenylamine antioxidants and benzotriazole UV stabilizers in aquatic organisms in the great lakes of North America: terrestrial exposure and biodilution. Environmental Science & Technology 52, 1280–1289. https://doi.org/10.1021/acs.est.7b05214

Lu, Z., De Silva, A.O., Peart, T.E., Cook, C.J., Tetreault, G.R., 2017a. Tissue Distribution of Substituted Diphenylamine Antioxidants and Benzotriazole Ultraviolet Stabilizers in White Sucker (*Catostomus commersonii*) from an Urban Creek in Canada. Environmental Science & Technology Letters 4, 433–438. https://doi.org/10.1021/acs.estlett.7b00355

Lu, Z., De Silva, A.O., Peart, T.E., Cook, C.J., Tetreault, G.R., Servos, M.R., Muir, D.C.G., 2016a. Distribution, Partitioning and Bioaccumulation of Substituted Diphenylamine Antioxidants and Benzotriazole UV Stabilizers in an Urban Creek in Canada. Environmental Science & Technology 50, 9089–9097. https://doi.org/10.1021/acs.est.6b01796

Lu, Z., De Silva, A.O., Zhou, W., Tetreault, G.R., de Solla, S.R., Fair, P.A., Houde, M., Bossart, G., Muir, D.C.G., 2019. Substituted diphenylamine antioxidants and benzotriazole UV stabilizers in blood plasma of fish, turtles, birds and dolphins from North America. Science of The Total Environment 647, 182–190. https://doi.org/10.1016/j.scitotenv.2018.07.405

Lu, Z., Peart, T.E., Cook, C.J., De Silva, A.O., 2016b. Simultaneous determination of substituted diphenylamine antioxidants and benzotriazole ultra violet stabilizers in blood plasma and fish homogenates by ultra-high performance liquid chromatography–electrospray tandem mass spectrometry. Journal of Chromatography A 1461, 51–58. https://doi.org/10.1016/j.chroma.2016.07.027

Lu, Z., Smyth, S.A., Peart, T.E., De Silva, A.O., 2017b. Occurrence and fate of substituted diphenylamine antioxidants and benzotriazole UV stabilizers in various Canadian

wastewater treatment processes. Water Research 124, 158–166. https://doi.org/10.1016/j.watres.2017.07.055

Lye, E., Legrand, M., Clarke, J., Probert, A., 2013. Blood Total Mercury Concentrations in the Canadian Population: Canadian Health Measures Survey Cycle 1, 2007–2009. Canadian Journal of Public Health 104, e246–e251. https://doi.org/10.17269/cjph.104.3772

Maghazaji, H.I., 1974. Psychiatric aspects of methylmercury poisoning. Journal of Neurology, Neurosurgery & Psychiatry 37, 954–958. https://doi.org/10.1136/jnnp.37.8.954

Mao, F., He, Y., Gin, K.Y.-H., 2019. Occurrence and fate of benzophenone-type UV filters in aquatic environments: a review. Environmental Science: Water Research & Technology 5, 209–223. https://doi.org/10.1039/c8ew00539g

Marrugo-Negrete, J., Vargas-Licona, S., Ruiz-Guzmán, J.A., Marrugo-Madrid, S., Bravo, A.G., Díez, S., 2020. Human health risk of methylmercury from fish consumption at the largest floodplain in Colombia. Environmental Research 182, 109050. https://doi.org/10.1016/j.envres.2019.109050

McGregor, A.J., Mason, H.J., 1991. Occupational Mercury Vapour Exposure and Testicular, Pituitary and Thyroid Endocrine Function. Human & Experimental Toxicology 10, 199–203. https://doi.org/10.1177/096032719101000309 Mikkelsen, S.H., 2015. Survey and health assessment of UV filters. Survey of chemical substances in consumer products No. 142, 2015, The Danish Environmental Protection Agency Strandgade 29 1401 Copenhagen K Denmark www.mst.dk/english.

Miller, E.J., Vanarsdale, A., Keeler, G.J., Chalmers, A., Poissant, L., Kamman, N.C., Brulotte, R.L., 2005. Estimation and Mapping of Wet and Dry Mercury Deposition Across Northeastern North America. Ecotoxicology 14, 53–70. https://doi.org/10.1007/s10646-004-6259-9

Molins-Delgado, D., Mar, del, Valeta-Juan, G., Pleguezuelos-Hernández, V., Damià Barceló, M. Silvia Díaz-Cruz, 2018. Determination of UV filters in human breast milk using turbulent flow chromatography and babies' daily intake estimation. Environmental Research 161, 532–539. https://doi.org/10.1016/j.envres.2017.11.033

Molins-Delgado, D., Muñoz, R., Nogueira, S., Alonso, M.B., Torres, J.P., Malm, O., Ziolli, R.L., Hauser-Davis, R.A., Eljarrat, E., Barceló, D., Díaz-Cruz, M.S., 2018. Occurrence of organic UV filters and metabolites in lebranche mullet (*Mugil liza*) from Brazil. Science of The Total Environment 618, 451–459. https://doi.org/10.1016/j.scitotenv.2017.11.033

Montesdeoca-Esponda, S., Sosa-Ferrera, Z., Kabir, A., Furton, K.G., Santana-Rodríguez, J.J., 2015. Fabric phase sorptive extraction followed by UHPLC-MS/MS for the analysis of

benzotriazole UV stabilizers in sewage samples. Analytical and Bioanalytical Chemistry 407, 8137–8150. https://doi.org/10.1007/s00216-015-8990-x

Moualek, F., Belanger, D., Babin, M., Parent, G.J., Ponton, D.E., Amyot, M., Senay, C., Robert, D., Lu, Z., 2023. Spatial distribution and speciation of mercury in a recovering deepwater redfish (Sebastes mentella) population from St. Lawrence Estuary and Gulf, Canada. Environmental Pollution 337, 122604. https://doi.org/10.1016/j.envpol.2023.122604

Nagayoshi, H., Kakimoto, K., Takagi, S., Konishi, Y., Kajimura, K., Matsuda, T., 2014. Benzotriazole Ultraviolet Stabilizers Show Potent Activities as Human Aryl Hydrocarbon Receptor Ligands. Environmental Science & Technology 49, 578–587. https://doi.org/10.1021/es503926w

Nakata, H., Murata, S., Filatreau, J., 2009. Occurrence and Concentrations of Benzotriazole UV Stabilizers in Marine Organisms and Sediments from the Ariake Sea, Japan. Environmental Science & Technology 43, 6920–6926. https://doi.org/10.1021/es900939j

Nogara, P.A., Oliveira, C.S., Schmitz, G.L., Piquini, P.C., Farina, M., Aschner, M., Rocha, J.B.T., 2019. Methylmercury's chemistry: From the environment to the mammalian brain. Biochimica et Biophysica Acta (BBA) - General Subjects 1863, 129284. https://doi.org/10.1016/j.bbagen.2019.01.006

Puga, S., Pereira, P., Pinto-Ribeiro, F., O'Driscoll, N.J., Mann, E., Barata, M., Pousão-Ferreira, P., Canário, J., Almeida, A., Pacheco, M., 2016. Unveiling the neurotoxicity of methylmercury in fish (Diplodus sargus) through a regional morphometric analysis of brain and swimming behavior assessment. Aquatic Toxicology (Amsterdam, Netherlands) 180, 320–333. https://doi.org/10.1016/j.aquatox.2016.10.014

Pêche et Ocean Canada (MPO), 2020. L'estuaire et le golfe du Saint-Laurent. MPO, https://www.qc.dfo-mpo.gc.ca/fr/lestuaire-et-le-golfe-du-saint-laurent.

Peng, X., Fan, Y., Jin, J., Xiong, S., Liu, J., Tang, C., 2017a. Bioaccumulation and biomagnification of ultraviolet absorbents in marine wildlife of the Pearl River Estuarine, South China Sea. Environmental Pollution 225, 55–65. https://doi.org/10.1016/j.envpol.2017.03.035

Peng, X., Jin, J., Wang, C., Ou, W., Tang, C., 2015. Multi-target determination of organic ultraviolet absorbents in organism tissues by ultrasonic assisted extraction and ultra-high performance liquid chromatography-tandem mass spectrometry. Journal of Chromatography. A 1384, 97–106. https://doi.org/10.1016/j.chroma.2015.01.051

Peng, X., Xiong, S., Ou, W., Wang, Z., Tan, J., Jin, J., Tang, C., Liu, J., Fan, Y., 2017b. Persistence, temporal and spatial profiles of ultraviolet absorbents and phenolic personal care products in

riverine and estuarine sediment of the Pearl River catchment, China. Journal of Hazardous Materials 323, 139–146. https://doi.org/10.1016/j.jhazmat.2016.05.020

Peng, X., Zhu, Z., Xiong, S., Fan, Y., Chen, G., Tang, C., 2020. Tissue Distribution, Growth Dilution, and Species-Specific Bioaccumulation of Organic Ultraviolet Absorbents in Wildlife Freshwater Fish in the Pearl River Catchment, China. Environmental Toxicology and Chemistry 39, 343–351. https://doi.org/10.1002/etc.4616

Pinheiro, M.D.O., Simmons, D.B.D., Villella, M., Tetreault, G.R., Muir, D.C.G., McMaster, M.E., Hewitt, L.M., Parrott, J.L., Park, B.J., Brown, S.B., Sherry, J.P., 2020. Brown bullhead at the St. Lawrence River (Cornwall) Area of Concern: health and endocrine status in the context of tissue concentrations of PCBs and mercury. Environmental Monitoring and Assessment 192, 404. https://doi.org/10.1007/s10661-020-08355-6

Planque, B., Kristinsson, K., Astakhov, A., Bernreuther, M., Bethke, E., Drevetnyak, K., Nedreaas, K., Reinert, J., Rolskiy, A., Sigurðsson, T., Stransky, C., 2013. Monitoring beaked redfish (*Sebastes mentella*) in the North Atlantic, current challenges and future prospects. agris.fao.org. URL https://agris.fao.org/agris-search/search.do?recordID=US202100184501 (accessed 4.20.23).

Raissy, M., Ansari, M., 2013. Health risk assessment of mercury and arsenic associated with consumption of fish from the Persian Gulf. Environmental Monitoring and Assessment 186, 1235–1240. https://doi.org/10.1007/s10661-013-3452-4

Ramirez-Llodra, E., Tyler, P.A., Baker, M.C., Bergstad, O.A., Clark, M.R., Escobar, E., Levin, L.A., Menot, L., Rowden, A.A., Smith, C.R., Van Dover, C.L., 2011. Man and the Last Great Wilderness: Human Impact on the Deep Sea. PLoS ONE 6, e22588. https://doi.org/10.1371/journal.pone.0022588

Ramos, S., Homem, V., Alves, A., Santos, L., 2016. A review of organic UV-filters in wastewater treatment plants. Environment International 86, 24–44. https://doi.org/10.1016/j.envint.2015.10.004

Rantetampang, A., Mallongi, A., 2014. Environmental risks assessment of total mercury accumulation at Sentani Lake Papua, Indonesia. International Journal of Scientific & Technology Research 3, 157–163.

Regnell, O., Tunlid, A., Ewald, G., Sangfors, O., 1996. Methyl mercury production in freshwater microcosms affected by dissolved oxygen levels: role of cobalamin and microbial community composition. Canadian Journal of Fisheries and Aquatic Sciences 53, 1535–1545. https://doi.org/10.1139/f96-086

Rice, K.M., Walker, E.M., Wu, M., Gillette, C., Blough, E.R., 2014. Environmental Mercury and Its Toxic Effects. Journal of Preventive Medicine & Public Health 47, 74–83. https://doi.org/10.3961/jpmph.2014.47.2.74

Romero-Romero, S., García-Ordiales, E., Roqueñí, N., Acuña, J.L., 2022. Increase in mercury and methylmercury levels with depth in a fish assemblage. Chemosphere 292, 133–445. https://doi.org/10.1016/j.chemosphere.2021.133445

Ruan, T., Liu, R., Fu, Q., Wang, T., Wang, Y., Song, S., Wang, P., Teng, M., Jiang, G., 2012. Concentrations and Composition Profiles of Benzotriazole UV Stabilizers in Municipal Sewage Sludge in China. Environmental Science & Technology 46, 2071–2079. https://doi.org/10.1021/es203376x

Rustam, H., Hamdi, T., 1974. Methyl mercury poisoning in Iraq. A neurological study. Brain: A Journal of Neurology 97, 500–510.

Santander Ballestín, S., Luesma Bartolomé, M.J., 2023. Toxicity of Different Chemical Components in Sun Cream Filters and Their Impact on Human Health: A Review. Applied Sciences 13, 712. https://doi.org/10.3390/app13020712

Savenkoff, C., Savard, L., Morin, B., Chabot, D., 2006. Main prey and predators of northern shrimp (Pandalus borealis) in the northern Gulf of St. Lawrence during the mid-1980s, mid-1990s, and early 2000s. Canadian Technical Report of Fisheries and Aquatic Sciences 2639, 2639,28.

Schreurs, R.H.M.M., 2004. Interaction of Polycyclic Musks and UV Filters with the Estrogen Receptor (ER), Androgen Receptor (AR), and Progesterone Receptor (PR) in Reporter Gene Bioassays. Toxicological Sciences 83, 264–272. https://doi.org/10.1093/toxsci/kfi035

Selin, N.E., 2009. Global Biogeochemical Cycling of Mercury: A Review. Annual Review of Environment and Resources 34, 43–63. https://doi.org/10.1146/annurev.environ.051308.084314

Senay, C., Gauthier, J., Bourdages, H., Brassard, C., Duplisea, D., Ouellette-Plante, J., 2021a. Redfish (*Sebastes mentella* and *S. fasciatus*) stocks status in Unit 1 in 2017. Canadian Science Advisory Secretariat Ottawa, ON.

Senay, C., Gauthier, J., Bourdages, H., Brassard, C., Duplisea, D., Ouellette-Plante, J., 2019. Redfish (*Sebastes mentella* and *S. fasciatus*) Stocks Status in Unit 1 in 2017. Canadian Science Advisory Secretariat Ottawa, ON.

Senay, C., Ouellette-Plante, J., Bourdages, H., Bermingham, T., Gauthier, J., Parent, G., Chabot, D., Duplisea, D., 2019. Canadian Science Advisory Secretariat (CSAS) Unit 1 Redfish (*Sebastes mentella* and *S. fasciatus*) stock status in 2019 and updated information on population structure, biology, ecology, and current fishery closures.

Senay, C., Ouellette-Plante, J., Bourdages, H., Bermingham, T., Parent, G., Chabot, D., Duplisea, D., 2021b. Unit 1 redfish (*Sebastes mentella* and *S. fasciatus*) stock status in 2019 and updated information on population structure, biology, ecology, and current fishery closures. Canadian Science Advisory Secretariat Ottawa, ON.

Senay, C., Rousseau, S., Brûlé, C., Chavarria, C., Isabel, L., Parent, G.J., Chabot, D., and Duplisea, D. 2023. Unit 1 Redfish (*Sebastes mentella* and *S. fasciatus*) stock status in 2021. Fisheries and Oceans Canada, Canadian Science Advisory Secretariat Research Document 2023/036. xi+125.

Simoneau, M., Lucotte, M., Garceau, S., Laliberté, D., 2005. Fish growth rates modulate mercury concentrations in walleye (*Sander vitreus*) from eastern Canadian lakes. Environmental Research 98, 73–82. https://doi.org/10.1016/j.envres.2004.08.002

Sofoulaki, K., Kalantzi, I., Machias, A., Pergantis, S.A., Tsapakis, M., 2019. Metals in sardine and anchovy from Greek coastal areas: Public health risk and nutritional benefits assessment. Food and Chemical Toxicology 123, 113–124. https://doi.org/10.1016/j.fct.2018.10.053

Statistics Canada. 2015. Mean height, weight, body mass index (BMI) and prevalence of obesity, by collection method and sex, household population aged 18 to 79, Canada, 2008, 2007 to 2009, and 2005. (https://www150.statcan.gc.ca/n1/pub/82-003-x/2011003/article/11533/tbl/tbl1-eng.htm; accessed June 12, 2023)

Statistics Canada. 2023. Food available in Canada, Table 32-10-0054-01.

Stoeckelhuber, M., Scherer, M., Peschel, O., Leibold, E., Bracher, F., Scherer, G., Pluym, N., 2020. Human metabolism and urinary excretion kinetics of the UV filter Uvinul A plus® after a single oral or dermal dosage. International Journal of Hygiene and Environmental Health 227, 113509. https://doi.org/10.1016/j.ijheh.2020.113509

Sun, Y., Lu, G., Zhang, P., Wang, Y., Ling, X., Xue, Q., Yan, Z., Liu, J., 2022. Natural colloids at environmentally relevant concentrations affect the absorption and removal of benzophenone-3 in zebrafish. Environmental Pollution 310, 119860. https://doi.org/10.1016/j.envpol.2022.119860

Suzuki, T., Kitamura, S., Khota, R., Sugihara, K., Fujimoto, N., Ohta, S., 2005. Estrogenic and antiandrogenic activities of 17 benzophenone derivatives used as UV stabilizers and

sunscreens. Toxicology and Applied Pharmacology 203, 9–17. https://doi.org/10.1016/j.taap.2004.07.005

Tang, Z., Zhong, F., Cheng, J., Nie, Z., Han, X., Han, Y., Yang, Y., 2019. Concentrations and tissue-specific distributions of organic ultraviolet absorbents in wild fish from a large subtropical lake in China. Science of the Total Environment 647, 1305–1313. https://doi.org/10.1016/j.scitotenv.2018.08.117

Teunen, L., Belpaire, C., De Boeck, G., Blust, R., Bervoets, L., 2021. Mercury accumulation in muscle and liver tissue and human health risk assessment of two resident freshwater fish species in Flanders (Belgium): a multilocation approach. Environmental Science and Pollution Research 29, 7853–7865. https://doi.org/10.1007/s11356-021-16215-0

Tomy, G.T., Budakowski, W., Halldorson, T., Helm, P.A., Stern, G.A., Friesen, K., Pepper, K., Tittlemier, S.A., Fisk, A.T., 2004. Fluorinated Organic Compounds in Eastern Arctic Marine Food Web. Environmental Science & Technology 38, 6475–6481. https://doi.org/10.1021/es049620g

Tsui, M.M.P., Leung, H.W., Wai, T.-C., Yamashita, N., Taniyasu, S., Liu, W., Lam, P.K.S., Murphy, M.B., 2014. Occurrence, distribution and ecological risk assessment of multiple classes of UV filters in surface waters from different countries. Water Research 67, 55–65. https://doi.org/10.1016/j.watres.2014.09.013

UNEP/WHO, 2008. Guidance for identifying populations at risk from mercury. www.who.int. URL https://www.who.int/publications/m/item/guidance-for-identifying-populations-at-risk-from-mercury-exposure (accessed on April 13, 2023).

United Nations Environment Programme (UNEP), 2023. Recommendation by the Persistent Organic Pollutants Review Committee to list UV-328 in Annex A to the Convention and draft text of the proposed amendment. UNEP/POPS/COP.11/14.

United States Environmental Protection Agency (US EPA), 2006. Phenolic Benzotriazole Association/ Phenolic Benzotriazole. URL.http://www.epa. gov/HPV/pubs/summaries/phenbenz/c13266tp.pdf

United States Environmental Protection Agency (US EPA), 2016. U.S. Environmental Protection Agency. URL http://iaspub.epa.gov/%20oppthpv/quicksearch.display?pChem=100708

United States Environmental Protection Agency (US EPA). 2001. Methylmercury (MeHg); CASRN 22967-92-6 (https://iris.epa.gov/static/pdfs/0073_summary.pdf; accessed June 12, 2023)

United States Environmental Protection Agency (US EPA). 2009. Screening-level hazard characterization, sponsored chemicals, Phenolic Benzotriazoles Category, 2-(2'-Hydroxy-5'-methylphenyl) benzotriazole (CASRN 2440-22-4), 2-(2'-Hydroxy-5'-octylphenyl) benzotriazole (CASRN 3147-75-9), 2-(2'-Hydroxy-3',5'-di-t-amylphenyl) benzotriazole (CASRN 25973-55-1), 2-(2H-Benzotriazol-2-yl)-4,6-bis(1-methyl-1-phenylethyl) phenol (CASRN 70321-86-7).

United States Environmental Protection Agency (US EPA). 2016. Definition and procedure for the determination of the method detection limit, revision 2.

Valle-Sistac, J., Molins-Delgado, D., Díaz, M., Ibáñez, L., Barceló, D., Silvia Díaz-Cruz, M., 2016. Determination of parabens and benzophenone-type UV filters in human placenta. First description of the existence of benzyl paraben and benzophenone-4. Environment International 88, 243–249. https://doi.org/10.1016/j.envint.2015.12.034

Villar, E., Cabrol, L., Heimbürger-Boavida, L., 2020. Widespread microbial mercury methylation genes in the global ocean. Environmental Microbiology Reports 12, 277–287. https://doi.org/10.1111/1758-2229.12829

Wada, H., Cristol, D.A., McNabb, F.M.A., Hopkins, W.A., 2009. Suppressed Adrenocortical Responses and Thyroid Hormone Levels in Birds near a Mercury-Contaminated River. Environmental Science & Technology 43, 6031–6038. https://doi.org/10.1021/es803707f

Wang, J., Pan, L., Wu, S., Lu, L., Xu, Y., Zhu, Y., Guo, M., Zhuang, S., 2016. Recent Advances on Endocrine Disrupting Effects of UV Filters. International Journal of Environmental Research and Public Health 13. https://doi.org/10.3390/ijerph13080782

Wang, L., Asimakopoulos, A.G., Kannan, K., 2015. Accumulation of 19 environmental phenolic and xenobiotic heterocyclic aromatic compounds in human adipose tissue. Environment International 78, 45–50. https://doi.org/10.1016/j.envint.2015.02.015

Wang, R., Wong, M.-H., Wang, W.-X., 2011. Coupling of methylmercury uptake with respiration and water pumping in freshwater tilapia *Oreochromis niloticus*. Environmental Toxicology and Chemistry 30, 2142–2147. https://doi.org/10.1002/etc.604

Wang, W., Lee, I.-S., Oh, J.-E., 2022. Specific-accumulation and trophic transfer of UV filters and stabilizers in marine food web. Science of the Total Environment 825, 154079. https://doi.org/10.1016/j.scitotenv.2022.154079

Ward, D.M., Nislow, K.H., Chen, C.Y., Folt, C.L., 2010. Rapid, efficient growth reduces mercury concentrations in stream-dwelling Atlantic Salmon. Transactions of the American Fisheries Society 139, 1–10. https://doi.org/10.1577/t09-032.1

WHO, 2020. 10 chemicals of public health concern (https://www.who.int/news-room/photo-story/photo-story-detail/10-chemicals-of-public-health-concern; accessed April 13, 2023).

Wick, A., Jacobs, B., Kunkel, U., Heininger, P., Ternes, T.A., 2016. Benzotriazole UV stabilizers in sediments, suspended particulate matter and fish of German rivers: New insights into occurrence, time trends and persistency. Environmental Pollution 212, 401–412. https://doi.org/10.1016/j.envpol.2016.01.024

Wolfe, M.F., Schwarzbach, S., Sulaiman, R.A., 1998. Effects of mercury on wildlife: A comprehensive review. Environmental Toxicology and Chemistry 17, 146–160. https://doi.org/10.1002/etc.5620170203

Wong, S.L., Lye, E.J.D., 2008. Lead, mercury and cadmium levels in Canadians. Health Reports 19, 31–36.

Yamanaga, H., 1983. Quantitative analysis of tremor in Minamata disease. The Tohoku Journal of Experimental Medicine 141, 13–22. https://doi.org/10.1620/tjem.141.13

Yamano, T., Shimizu, M., Noda, T., 2001. Relative Elicitation Potencies of Seven Chemical Allergens in the Guinea Pig Maximization Test. Journal of Health Science 47, 123–128. https://doi.org/10.1248/jhs.47.123

Yang, H., Lu, G., Yan, Z., Liu, J., Dong, H., Bao, X., Zhang, X., Sun, Y., 2020. Residues, bioaccumulation, and trophic transfer of pharmaceuticals and personal care products in highly urbanized rivers affected by water diversion. Journal of Hazardous Materials 391, 122245. https://doi.org/10.1016/j.jhazmat.2020.122245

Yorifuji, T., Tsuda, T., Takao, S., Harada, M., 2008. Long-Term Exposure to Methylmercury and Neurologic Signs in Minamata and Neighboring Communities. Epidemiology 19, 3–9. https://doi.org/10.1097/ede.0b013e31815c09d2

Zhang, S., Wang, Z., Chen, J., Xie, Q., Zhu, M., Han, W., 2021. Tissue-specific accumulation, biotransformation, and physiologically based toxicokinetic modeling of benzotriazole ultraviolet stabilizers in Zebrafish (*Danio rerio*). Environmental Science & Technology 55, 11874–11884. https://doi.org/10.1021/acs.est.1c02861

Zhang, Z., Sverko, E., Smyth, S.A., Marvin, C.H., 2016. Determination of substituted diphenylamines in environmental samples. Analytical and Bioanalytical Chemistry 408, 7945–7954. https://doi.org/10.1007/s00216-016-9881-5

Zhang, Z., Yang, H., Wu, G., Li, Z., Song, T., Li, X.Q., 2011. Probing the difference between BH3 groove of Mcl-1 and Bcl-2 protein: Implications for dual inhibitors design. European

Journal of Medicinal Chemistry 46, 3909–3916. https://doi.org/10.1016/j.ejmech.2011.05.062

Zheng, N., Wang, S., Dong, W., Hua, X., Li, Y., Song, X., Chu, Q., Hou, S., Li, Y., 2019. The toxicological effects of mercury exposure in marine fish. Bulletin of Environmental Contamination and Toxicology 102, 714–720. https://doi.org/10.1007/s00128-019-02593-2

Zhuang, S., Lv, X., Pan, L., Lu, L., Ge, Z., Wang, J., Wang, J., Liu, J., Liu, W., Zhang, C., 2017. Benzotriazole UV 328 and UV-P showed distinct antiandrogenic activity upon human CYP3A4-mediated biotransformation. Environnemental Pollution 220, 616–624. https://doi.org/10.1016/j.envpol.2016.10.011